The University of Maine
DigitalCommons@UMaine

Electronic Theses and Dissertations | Fogler Library

Spring 5-14-2016

Modeling and Measurement of Evaporation from Frequently Tilled Sandy Soils

Nicholas R. Lawson
University of Maine - Main, Nicholas_Lawson@umit.maine.edu

Follow this and additional works at: http://digitalcommons.library.umaine.edu/etd


Part of the Computer-Aided Engineering and Design Commons, Energy Systems Commons, and the Soil Science Commons

Recommended Citation
Lawson, Nicholas R., "Modeling and Measurement of Evaporation from Frequently Tilled Sandy Soils" (2016). *Electronic Theses and Dissertations*. 2439.
http://digitalcommons.library.umaine.edu/etd/2439

This Open-Access Thesis is brought to you for free and open access by DigitalCommons@UMaine. It has been accepted for inclusion in Electronic Theses and Dissertations by an authorized administrator of DigitalCommons@UMaine.

MODELING AND MEASUREMENT OF EVAPORATION FROM FREQUENTLY TILLED SANDY SOILS

By

Nicholas Lawson

B.S. University of Maine, 2014

A THESIS

Submitted in Partial Fulfillment of the

Requirements for the Degree of

Master of Science

(in Mechanical Engineering)

The Graduate School

The University of Maine

May 2016

Advisory Committee:

Michael Peterson, Professor of Mechanical Engineering, Advisor

Senthil Vel, Professor of Mechanical Engineering

Zhihe Jin, Associate Professor of Mechanical Engineering

Anil Kizhakkepurakkal, Assistant Professor of Forest Operations

THESIS ACCEPTANCE STATEMENT

On behalf of the Graduate Committee for Nicholas Lawson I affirm that this manuscript is the final and accepted thesis. Signatures of all committee members are on file with the Graduate School at the University of Maine, 42 Stodder Hall, Orono, Maine.

Dr. Michael Peterson, Professor of Mechanical Engineering Date

LIBRARY RIGHTS STATEMENT

In presenting this thesis in partial fulfillment of the requirements for an advanced degree at the University of Maine, I agree that the Library shall make it freely available for inspection. I further agree that permission for "fair use" copying of this thesis for scholarly purposes may be granted by the Librarian. It is understood that any copying or publication of this thesis for financial gain shall not be allowed without my written permission.

Signature:

Date:

MODELING AND MEASUREMENT OF EVAPORATION FROM FREQUENTLY TILLED SANDY SOILS

By Nicholas Lawson

Thesis Advisor: Dr. Michael Peterson

An Abstract of the Thesis Presented
in Partial Fulfillment of the Requirements for the
Degree of Master of Science
(in Mechanical Engineering)
May 2016

Moisture observation and control is the single largest factor that controls the mechanical properties of sand based surfaces used for thoroughbred horse racing. Currently the moisture content is estimated based on the experience and expertise of the superintendent and water is added as needed based on experience. While extensive modelling has been done on moisture loss from a range of soils with crop covers in agronomy, currently no method exists to estimate the evaporation from a surface that is tilled many times a day and remains in a partially compacted state. This thesis develops an evaporation model based on real time weather data which also factors in track maintenance. The model is based on the Penman-Monteith evapotranspiration model for crops. The effect of transpiration of agricultural crops is eliminated from the model and a correction is developed for the effect of harrowing of the track which is done during breaks in training as well as between races. Calculated moisture contents are compared to moisture contents measured at four racetracks in a range of climates encountered in North American racing. Reasonable agreement between the measured moisture content and the calculated moisture content is achieved through the use of corrected terms.

ACKNOWLEDGEMENTS

I would like to thank my committee members, Dr. Michael Peterson, Dr. Senthil Vel, Dr. Zhihe Jin, and Dr. Anil Kizhakkepurakkal for their guidance. This work would not be possible without the insight, editing and limitless patience of Dr. Peterson. I would also like to thank my family for their constant support.

Support for the experimental portion of this work was provided by Biologically Applied Engineering LLC in Orono Maine. Additional support was supplied by Keeneland Association, Inc., the Racing Surfaces Testing Laboratory and the University of Maine.

TABLE OF CONTENTS

LIST OF TABLES

LIST OF FIGURES

SYMBOLS AND ABBREVIATIONS

γ	Psychrometric constant
b	Used in the calculation of the seasonal correction for solar time
C_d	Curve fitting constant
C_n	Curve fitting constant
DM	Day of the month
d_r	Squared inverse relative distance factor for the earth-sun
dT	Difference in temperature between the thermocouples
dz	Difference in height between the thermocouples
e_a	Average vapor pressure over the period
e_s	Maximum vapor pressure over the period
G	Ground heat flux
G_{sc}	Solar constant, 4.92MJ/m^2hr
H	Height of the water in the soil
H_d	Height of the soil at the track
J	Number of days into the year
k	Thermal conductivity of the dirt
L_m	Longitude of the solar radiation measurement site, in degrees
L_z	Longitude of the center of the local time zone, in degrees
M	Number of the month
m_p	Mass percentage of water in the soil
P	Average pressure of the time step
q	Heat flux density
R	Net solar radiation
R_a	Total solar radiation with no atmosphere
rcd	Dimensionless cloudiness factor
R_{nl}	Net long wave radiation out
R_{ns}	Net shortwave radiation in
R_{so}	Clear sky radiation,
s	Slope of the saturation vapor pressure curve
S_c	Seasonal correction for solar time, in hours
T	Air temperature
t	Time at the midpoint of the period, in hours

T_{Kavg}	Average temperature at 2 m in K
t_n	Number of hours in the time step
U_2	Wind speed at 2 m above the ground
U_z	Wind speed at the height of the wind measurement
VPD	Vapor Pressure Deficit.
X	Factor used to calculate ω_s
Y	Used to calculate β
Yr	Number of the year
z	Measurement height above ground level
Z	Measurement elevation above mean sea level
α	Albedo of dirt
β	Angle of the sun at the middle of the time step
δ	Solar declination
θ	Volumetric water content of the soil
λ	Latent heat of vaporization of water
ρ_b	Bulk density of the soil
ρ_w	Density of the water
σ	Stefan Boltzmann constant
ω	Solar time angle at the midpoint of the period
ω_1	Solar time angle at the beginning of the time step
ω_2	Solar time angle at the end of the time step
ω_s	Solar time angle at sunset

1. INTRODUCTION AND BACKGROUND

1.1 Introduction

While thoroughbred horse racing is not a sport with a growing fan base, it remains an important economic activity in the United States along with the associated equine industry. The supporting industry for horses and associated service industries represent over $102 Billion a year in spending as recently as 2005, with racing alone generating $26.1 billion per year of spending, not including gambling (Deloitte Consulting for the American Horse council, 2005). Like many sports, safety is a growing concern for all participants in racing. From both an ethical and a business perspective it is important to protect both the horse and rider. High profile injuries as well as a recognition of the risk associated with the sport led to the creation of the Jockey Club Welfare and Safety Summit along with other initiatives such as the creation of the Equine Injury Database in 2008 (Jocky Club, n.d.) as well as racetrack accreditation for safety and integrity created by the National Thoroughbred Racing Association (National Thoroughbred Racing Asociation, n.d.). In all of these efforts racing surfaces have been only one aspect of the discussion, along with medication, training, breeding and even logistics on the track and padding of the gates. Injury to both horses and riders is both complex and multifactorial (Hitchens, Hill, & Stover, 2013; Mohammed, Hill, & Lowe, 1991; Welsh et al., 2013).

While racing surfaces are only one aspect of safety and likely not even the most important issue, it is arguably one of the few features that are associated with risk for all horses and riders on a track on a particular day. Therefore to enhance safety, understanding the importance of different aspects of the racing surface design is critical. Safety concerns in horse racing are often focused on surfaces and other variables at the track surface-hoof interface (Peterson, Roepstorff, Thomason, Mahaffey, & McIlwraith,

2011). Thoroughbred racing in the United States takes place mostly on tracks which are referred to as dirt (combination of sand, silt, and clay). Over 1,250,000 'starts' from 2009 through 2014 are tracked in the Equine Injury database (Jocky Club, n.d.). The balance of the starts during this period occurred on turf and synthetic with 205,000 and 195,000 respectively. Previous research has demonstrated that surface characteristics including cushion depth (Mahaffey, Peterson, & Roepstorff, 2013), composition (Mahaffey, Peterson, & McIlwraith, 2012), temperature in synthetic tracks (Peterson, Reiser, Kou, Radford, & McIlwraith, 2010), and the effects of maintenance (Peterson & McIlwraith, 2008) all influence the properties of a surface. However, throughout prior research one factor has consistently been shown to have the biggest influence on the mechanical properties of dirt and turf racing surfaces, namely moisture.

The idea that moisture has a large impact on the mechanical properties of soil is intuitive to anyone who has walked along a beach. The dry sand far from the water is loose and offers little support, while closer to the water it is much firmer. The effect of the interaction of moisture and sand is complex and is related to a number of factors in the sand (Kindle, 1936). Systematic research in agriculture (Haine, 1930) and in geotechnical applications (Palmer, Barber, & Krynine, 1937) has consistently included the effects of moisture as a primary effect along with the composition of the soil. While the interaction of soil and water is complex, the current application with racetracks, along with applications in sports fields, is somewhat unique. Because of the relatively small size and critical nature of the facilities, the surfaces used are not natural, but instead a site is excavated and then appropriate fill material is chosen which meets the performance requirements and is consistent over the entire racing surface. While water flowing across

the track from precipitation and movement of the material during operation and maintenance can segregate the material or lead to a change in the percentage of fine material, the general composition of a racing surface is maintained at a consistent composition. Therefore, the effects of moisture content become the dominant factor in the performance of either dirt or a turf racing surface with the primary-secondary effects associated with changes in the material which impact the interaction of the surface material and water. Interaction of water with synthetic surfaces is complex and may change over time, therefore it is not considered in this analysis.

Racetracks have both spatial and temporal variations in moisture content. Spatially, moisture content changes around the length, as well as across the track. These changes may occur due to changes in the material, for example a washing out of the fine material to the inside lower side of the track may result in a dryer areas, or in areas where organic material may accumulate moisture may be retained leading to a wetter surface. Most commonly however, spatial variation is caused by the problems with the application of water to the surface either with a sprinkler on turf or with a water truck on a dirt surface. The effect of spatial variation is perhaps most important for the safety of horse and rider due to the problems associated with an inconsistent surface. However, the temporal variation in moisture content should be addressed first since it can create risks associated with the surface for every horse racing or training on the track. Some trainers believe that horses can adapt to a certain surface over time, and temporal changes in the surface impede that adaption. However, both issues must be addressed in order to provide the safest possible surface for racing.

Temporal changes can occur rapidly; the track can dry quickly during the day due to hot dry weather, or become saturated quickly by rain. Just as challenging for maintenance of the track is the slower overnight or daily changes that may differ based on factors such as wind, temperature and humidity. These sort of changes may lead, for example, to a dry looking top surface with saturated material below a thin top layer. The dynamics of the hoof of a 450 kg load dynamically loading the surface at 15 m/s depend not only on the top surface of the track but on layers as deep as 0.3 m (Peterson et al., 2011). Kickback of material into the horses and riders following behind may be influenced by a drying top surface (Hayler, 2011; Pricci, 2013). Therefore it is important to not only monitor the moisture content of the track at any given time but also recognize that the rate of drying of the surface may impact the perception of the track by riders and fans.

To address these needs, an evaporation model focusing on temporal changes would allow water to be added in a way that could provide the most consistent surface possible for the safety of the horse and rider. While this model is based on existing models used in agriculture to estimate the watering needs for crops, the models requires several distinctive characteristics. Not only must the model accommodate the weather, irrigation and rain which is similar to agriculture, but also the race track surface is heavily trafficked by both maintenance equipment and horses. The model is also distinct from existing evaporation models used in agriculture since the surface is bare of crops and the maintenance is altered based on the weather. Finally, it is common for a racetrack to be completely harrowed twelve or more times in one afternoon on a race day. This level of maintenance is different from that seen in agriculture. Civil engineering models of water

are primarily related to maximizing the compaction of the surface, a goal which is not shared with horse racing. Therefore it is important to understand the factors which differ for horse racing as well as determine which terms in the existing models can be altered to accommodate the differences in the application.

1.2 Background Literature

Prior work related to the effect of moisture on the surfaces used for horse racing is relatively limited. The literature that is available is clearly tied to the goals of the present study. Literature related to the loss of moisture content from farmland is much more extensive, but is not immediately applicable to the current work.

1.2.1 Composition and Moisture in Racing Surfaces

Dirt horse racetracks are composed of sand, silt, and clay(Mahaffey, 2012). The clay and moisture content of the track strongly influence the mechanical properties of the track (Al-Shayea, 2001). The racetracks involved utilized different construction techniques, such as shallow sand, false base, or false base with pad, shown in Figure 1. All dirt horse racetrack surfaces have an upper cushion layer, which decelerates the horses' hooves. Shallow sand tracks have a hard base layer immediately below the cushion. False base and false base with pad both utilize a hard-packed base of cushion material, with more loosely packed pad between the cushion and base on the false base with pad. The pad or false base with pad tracks is regularly harrowed and conditioned to maintain a consistent pad depth and level of compaction. Regardless of the design, moisture content of dirt tracks plays a major role in the physical properties of the track (Ratzlaff, Hyde, Hutton, Rathgeber, & Balch, 1997).

The base of the track is chosen based on the way the track is intended to be used; a track with a winter race meet will tend to have a crushed limestone base, and tracks with summer race meets will tend to have a clay base . Crushed stone allows the track to drain vertically. Clay bases do not allow vertical drainage which limits moisture losses and allows maintenance personnel to more easily maintain a consistent moisture content, even with high evaporation rates on hot summer days.

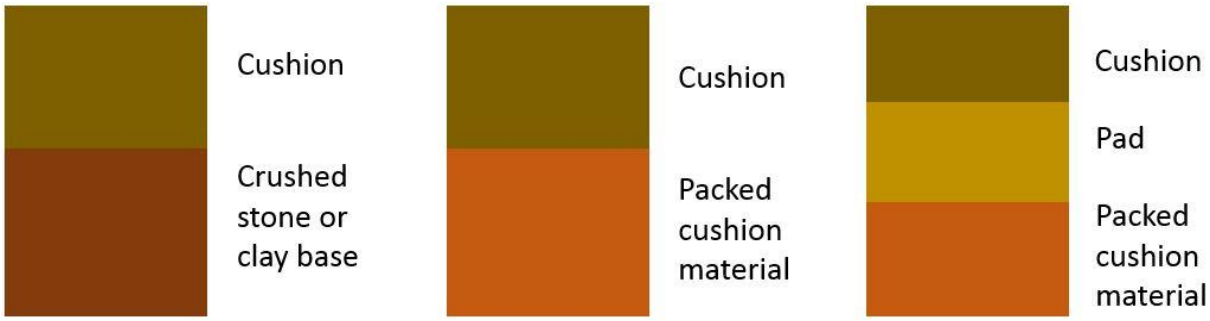

Figure 1: Examples of the layers of different types of track construction. Left to right, the track types are shallow sand, false base, false base with pad.

1.2.2 Evaporation Modelling

Both the Food and Agriculture Organization of the United Nations and the American Society of Civil Engineers recommend using the Penman-Monteith (PM) equation for evapotranspiration (Allen, Pereira, Raes, & Smith, 1998; Walter et al., 2005). The PM equation was designed to use weather and crop data to calculate evapotranspiration from farmland. Agronomists monitor moisture content in order to maximize crop yields without using excessive amounts of water (Evett, 2007). They use volumetric water content (VWC) instead of mass percent because they are primarily interested in knowing how much water is available to the plant. In farming, fields are not typically harrowed during the time that farmers are interested in evaporation. Farmers

also need to account for transpiration, which does not occur on a horse racetrack. Transpiration is the use of water by plants. Overall water loss from land is primarily due to transpiration (Jasechko et al., 2013). Crops shield the soil they grow in from the wind and sun, reducing the evaporation directly from the soil.

While the agronomic evaporation models provide valuable insight into the evaporation rates, they cannot be directly applied to dirt horse racetracks. This application is different in the timing and frequency of harrowing, the frequency of watering, and lack of transpiration from dirt racetracks. Also, the impermeable clay base of some tracks prevents percolation that would occur on some fields. Modifications to the Penman-Monteith (PM) evaporation model are required to account for these differences.

1.2.3 Evaporation Equation

Allen (1998) discussed the Penman-Monteith equation, and details the terms including calculations for solar radiation from other weather measurements (Allen et al., 1998). The equation is presented for use with both daily and hourly time steps. The equation is also discussed in regards to how different environmental conditions can affect the evapotranspiration rates.

Walter (2005) discusses the Penman-Monteith equation and modifies it to remove dependence on stomatal resistance (Walter et al., 2005). Removing the dependence on stomatal resistance is essential to using the equation to calculate the evaporation from racetrack surfaces, where there are no plants. The equation was presented with coefficients which were useful as an initial simplex for the Nelder Mead optimization.

1.2.4 Moisture Content Monitoring

In order to ensure the accuracy of the modified program, the moisture content of the soil was monitored. Evett (2007) discusses the conversion between volumetric and mass percent water content (Evett, 2007). The paper gives background on different methods of measuring moisture content of soils, including Time Domain Reflectometry (TDR). Time Domain Reflectometry is useful for measuring moisture content of the racetracks because of the good response time and accuracy of the probe. Evett also documents how increasing moisture measurement volume, either by increasing sample size or by taking additional samples, will decrease the variance of the results.

1.2.5 Dynamic Soil Properties

Al-Shayea (2001) explores how moisture content impacts the mechanical properties of soils. The soils tested are similar to those used on dirt horse racetracks (Al-Shayea, 2001). Triaxial testing shows the influence of moisture content on the stress-strain relationships of sandy soils with clay contents similar to those of horse racetracks. Horse racetracks are typically between 10-20% clay by mass, which is within the range of clay contents that was tested. Experiments on soils with varying clay contents indicate that the clay content also impacts the shear strength of the material.

Mahaffey (2012) discusses how variations in the racetrack surface effects the loads experienced by horses (Mahaffey, 2012). The experiments with track samples of different moisture contents demonstrates that moisture content has a significant impact on the mechanical properties of the track material. The moisture contents used for the experiments were 14, 16, and 18% mass percent, which are values that would be expected on racetracks. The biomechanical surface tester used in the tests simulates the

leading forelimb of a thoroughbred racehorse at a gallop, which ensures that the impact of material nonlinearities are mitigated as much as possible.

Ratzlaff (1997) examines how moisture content impacts the properties of the track that impact racehorses (Ratzlaff et al., 1997). The horse hooves were instrumented to measure vertical forces experienced by each hoof as they galloped on a track straight-away. Horses were split into different groups based on the speeds they were traveling during the tests, and the moisture content of the track was varied over a range of values that would be expected in an actual race. The tests show that moisture content impacts the forces experienced by the racehorse while galloping.

2. MATERIALS AND METHODS

2.1 Study Locations and Materials

Four racetracks were considered for the development of this model. The racetracks were chosen to represent a range of climates and seasons, and are some of the premier racetracks and race meets in North America. The horse racetracks used for the development of the model were Saratoga, Santa Anita, Keeneland, and Fair Grounds. Saratoga in New York has a humid continental climate. Santa Anita is in southern California and has a Mediterranean climate with little annual rainfall, averaging only 45.5 cm per year. The climates of Keeneland in Kentucky and Fair Grounds in Louisiana represent the northern and southern portions of the North American humid subtropical zone. Over the period of data collection all of the tracks except Santa Anita experienced periods of rainfall, as well as dry periods. The rainfall ranged from light (.254mm/hr) to heavy (23.622mm/hr). The various climate and weather conditions were used to ensure the accuracy of the model over a broad range of climates.

The tracks were all constructed based on the climate of the region. Saratoga and Keeneland both have crushed limestone bases because of the frequent heavy rains they experience. Santa Anita was designed with a crushed stone base, with a 16” pad because of the low annual rainfall, and the warm climate. Fair Grounds has a clay and concrete base, with built in drainage.

2.1.1 Composition of the Main Track

2.1.1.1 Composition of Materials

The cushion of the main dirt racetracks are composed of varying proportions of sand, silt, and clay. In some cases fiber is also used. Turf tracks have a normal growing medium for the turf although there is an emphasis on the shear strength which is critical to the durability of a surface which must support the traffic of horses and riders at full gallop. The modelling of evaporation from a turf racing surface is not significantly different than any other turf surface and thus can be managed in a similar manner.

The particle size distributions vary between dirt racetracks which can result in different mechanical properties. Often the mixture of sand particles is chosen to obtain mechanical properties which are similar to other tracks while using local materials. The differences in particle size and shape helps to compensate for track material that have different mineralogical compositions as well as the need to select materials which will perform well in the local climatic conditions. Those differences impact shear strength, bulk density, as well as how the materials react when they at different moisture contents (Ratzlaff et al., 1997; Zhang, Zhao, Horn, & Baumgartl, 2001).

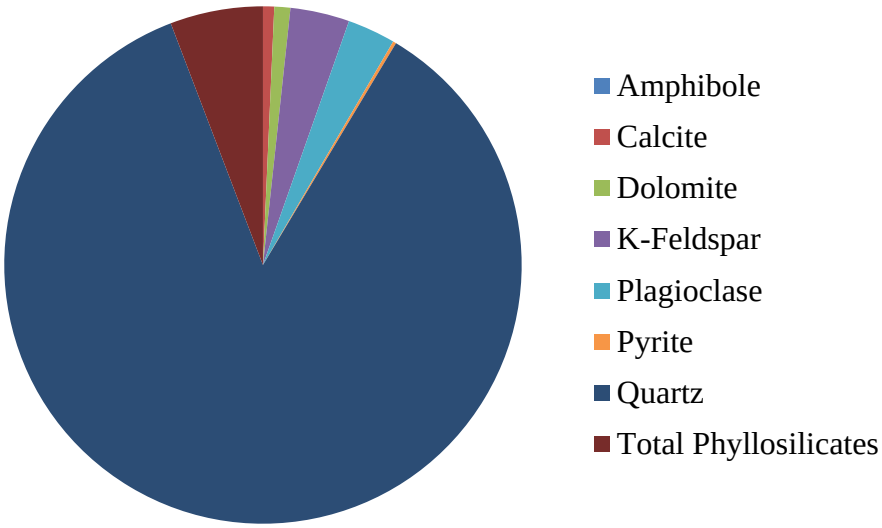

Figure 2: Chart showing mineralogical makeup of Keeneland.

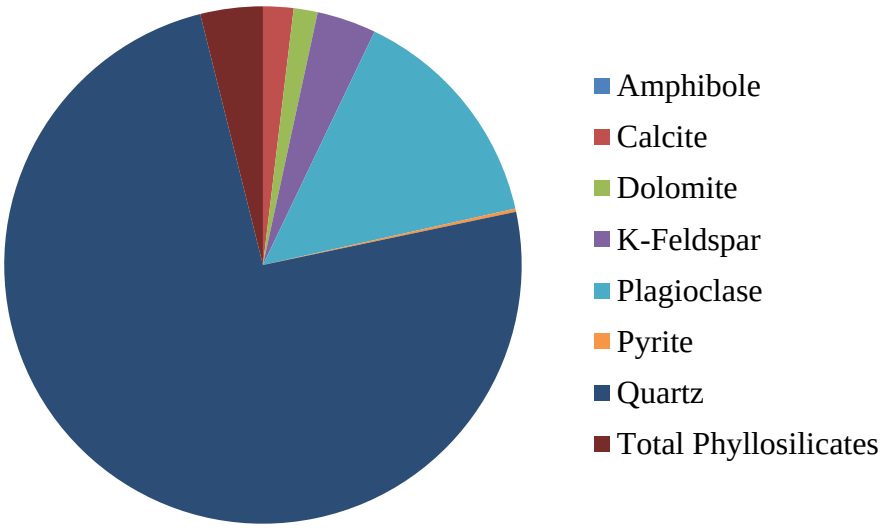

Figure 3: Chart showing mineralogical makeup of Fair Grounds.

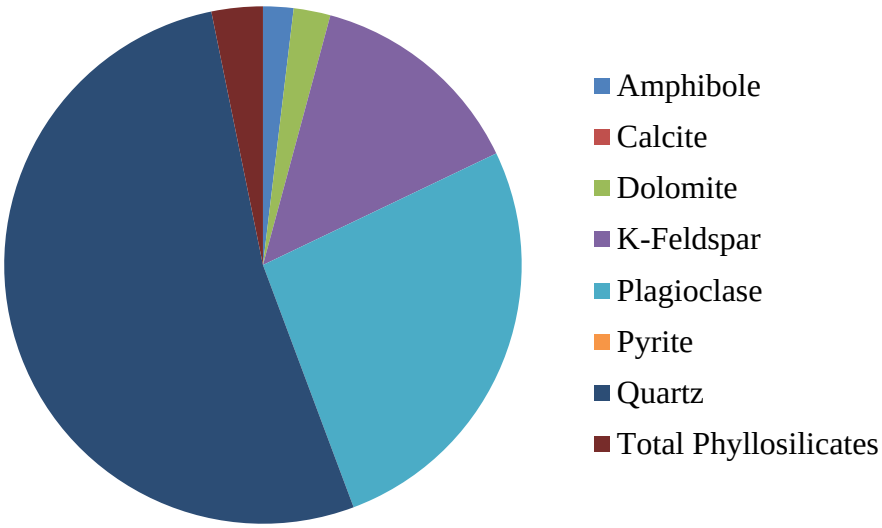

Figure 4: Chart showing mineralogical makeup of Saratoga.

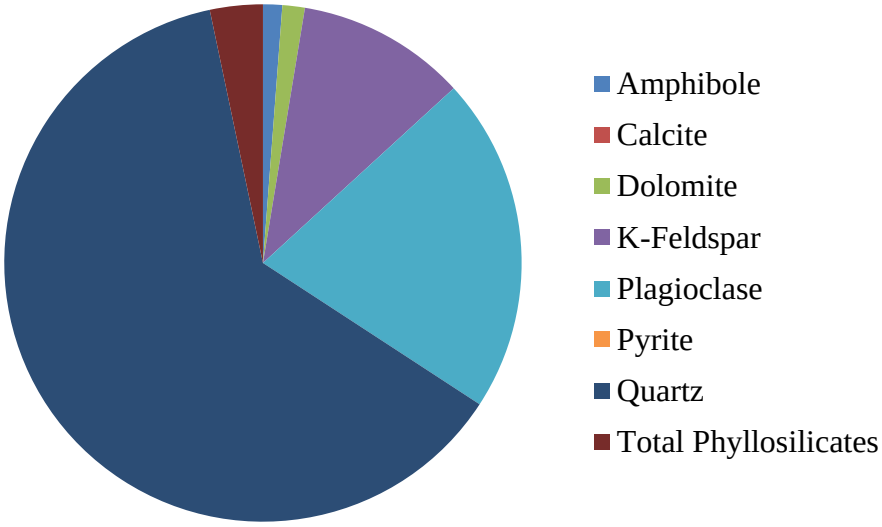

Figure 5: Chart showing mineralogical makeup of Santa Anita.

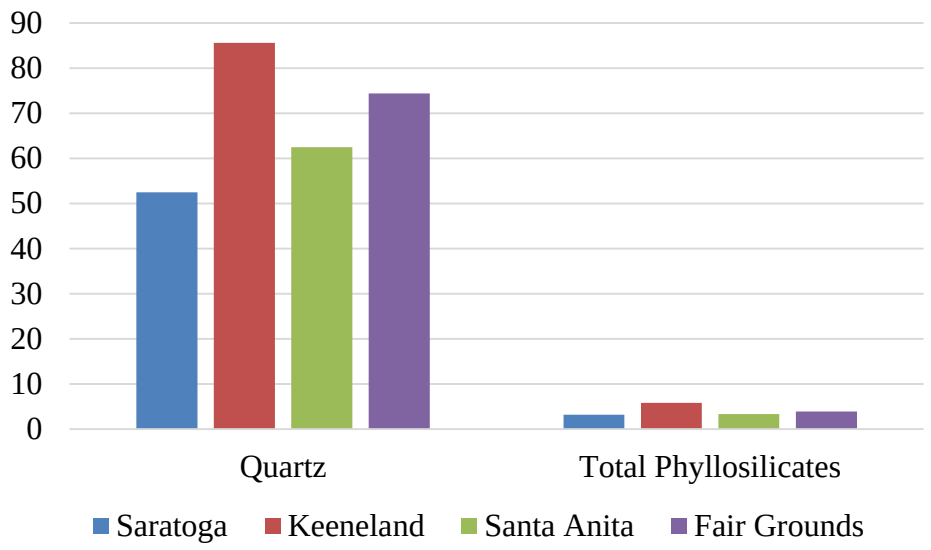

Figure 6: Chart showing quartz content vs phyllosilicates for each of the tracks.

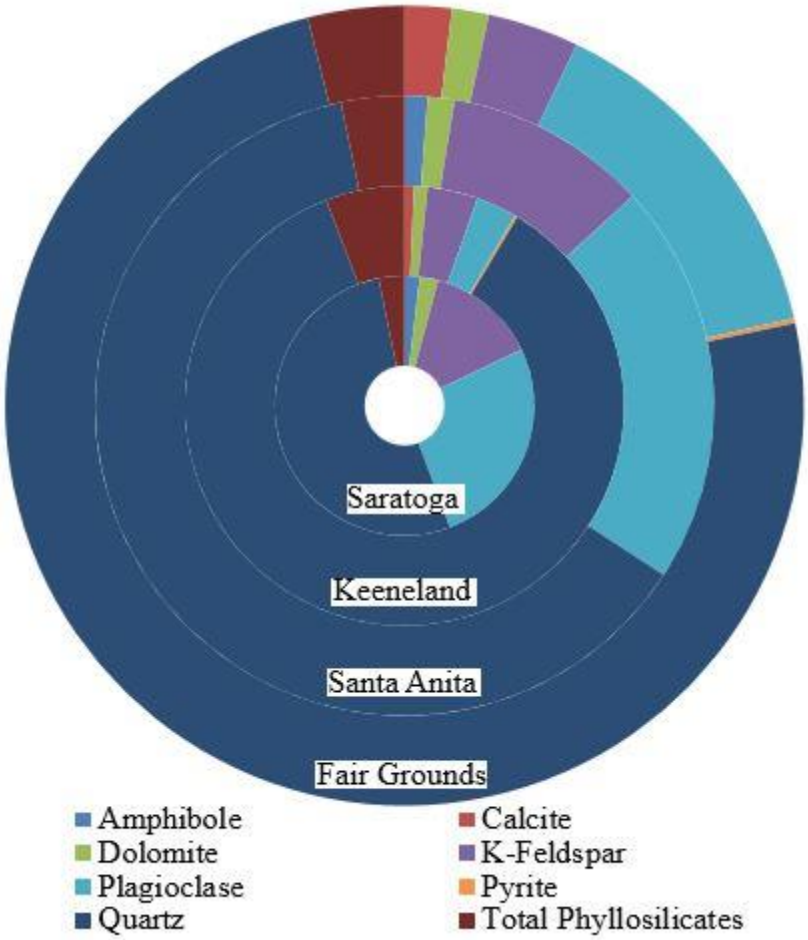

Figure 7: Comparing mineralogical makeup of each of the tracks for the study.

Figure 6 and Figure 7 show that each of the tracks have significantly different mineralogical makeups. Saratoga has a lower quartz content than any of the other tracks, and a relatively low phyllosilicate content. Keeneland has the highest quartz content, as well as the highest content of phyllosilicates. Santa Anita, Fair Grounds, and Saratoga all have relatively high concentrations of plagioclase.

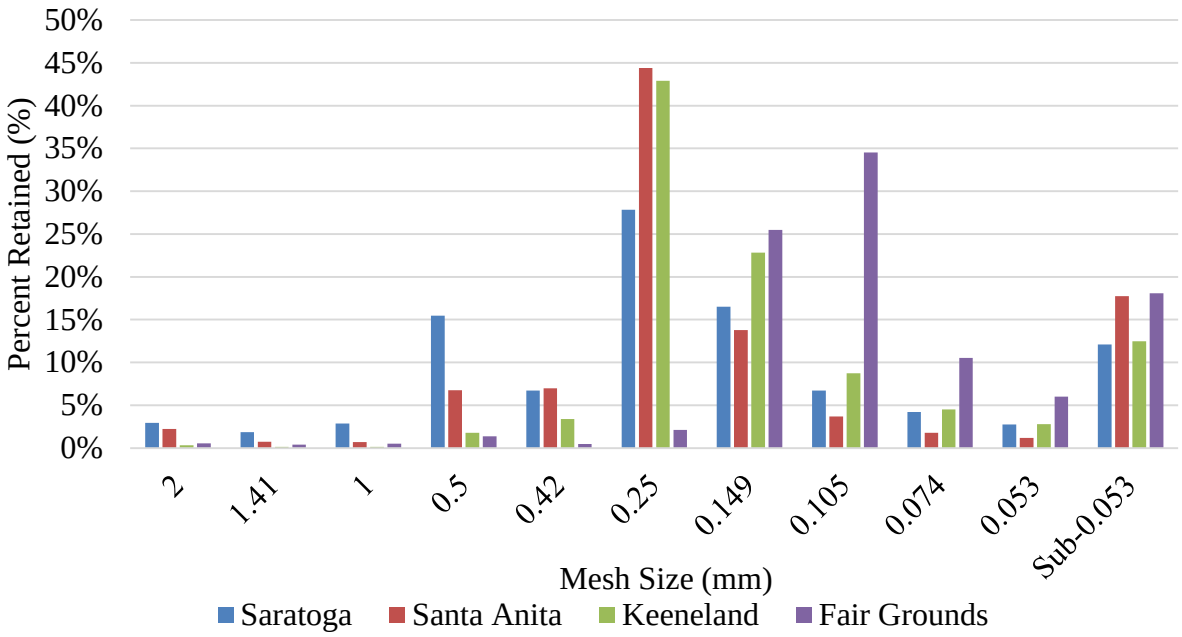

Figure 8: Particle size distribution as measured by sieve separation.

Figure 8 shows how the particle size distributions vary between tracks, as measured in accordance with ASTM D422 (ASTM, 2007). Results from Saratoga show that it has more than twice as much coarse sand (0.5-1mm) as any of the other tracks. Results from Fair Grounds show that it has significantly higher concentration of very fine sand (0.125-0.0625mm) than the other tracks.

2.1.1.2 Material Response to Moisture Content

Differences in track composition lead to differences in mechanical properties, such as bulk density, and shear strength. The differences in composition also impact how the materials properties change at different moisture contents.

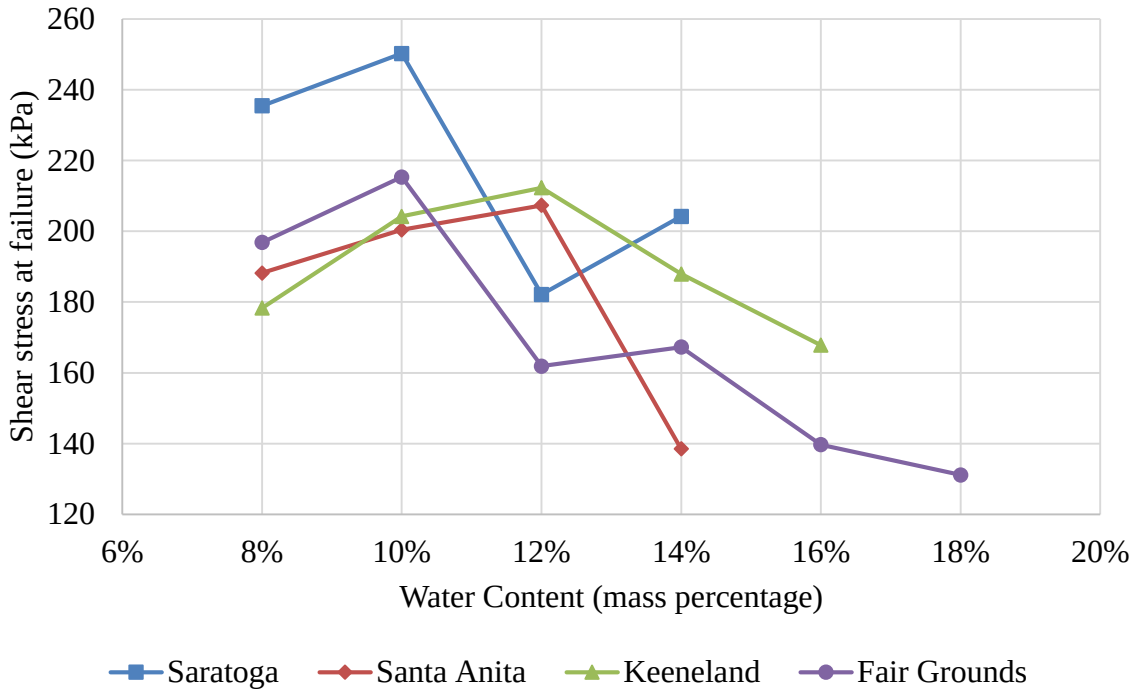

Figure 9: Maximum shear stress at failure of triaxial test specimen plotted against water content. Higher moisture content tests for Saratoga, Santa Anita and Keeneland were too saturated for accurate testing.

Triaxial data from ASTM D4767 gives maximum shear stress (ASTM, 2004). Figure 9 shows how relatively minor changes in moisture content can have an large impact on shear strength (Ratzlaff et al. (1997). These results are significant because the moisture contents over which the shear strength changes rapidly are within the range of fluctuation of the moisture content at a horse racetrack on any given day. This behavior is documented by Zhang, Zhao, Horn, & Baumgartl (2001).

Bulk density, measured in accordance with ASTM D698, is required to convert between volumetric water content (VWC) and mass percent water content (ASTM, 2007; Evett, 2007). Figure 10 shows how bulk density is different between tracks, and varies with moisture content. Saratoga has a significantly higher bulk density than the other tracks.

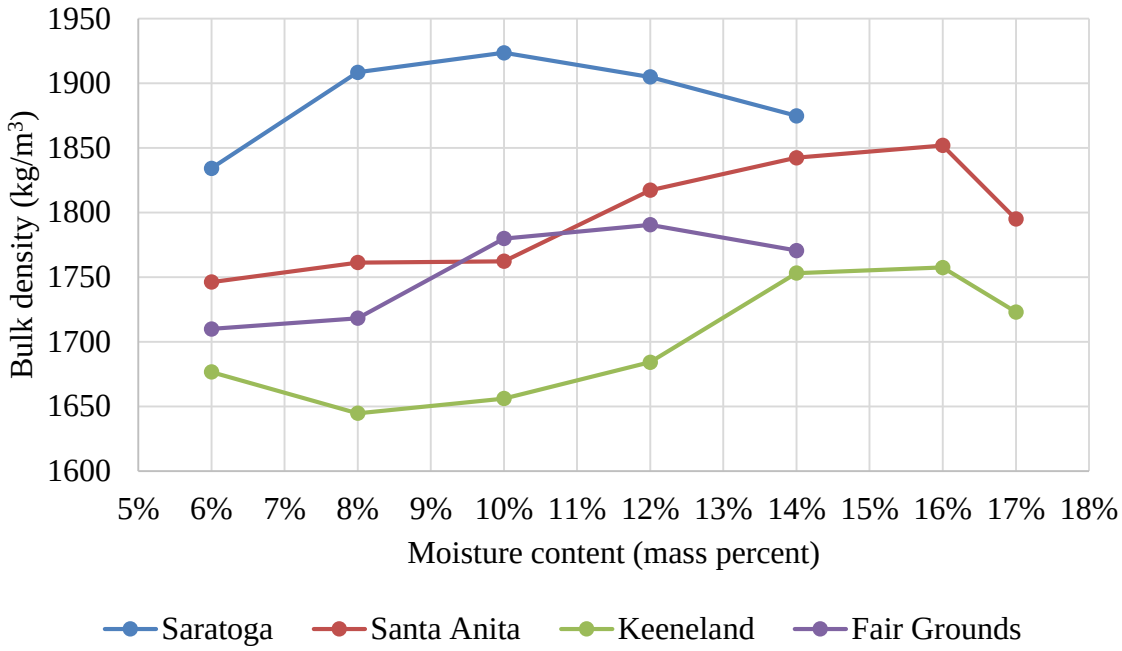

Figure 10: Maximum bulk density of track material plotted against moisture content. Higher moisture contents tests on Saratoga and Fair Grounds were too saturated for accurate testing.

2.1.2 Dirt Race Track Maintenance

Track maintenance equipment and nomenclature varies from track to track, but tracks use the same basic pieces of equipment. In order to maintain a consistent cushion for racing, tracks are harrowed or conditioned before and after training and racing, as well as between races. In order to protect the track from rain, and in some cases to minimize evaporation overnight, tracks are compacted and 'sealed' with weighted rollers or large steel plates. Tracks are also watered with trucks, and often mixing tools are used periodically to maintain consistency.

Track maintenance is performed for morning training, as well as for racing, which is held in the afternoon or evening. There are typically between 1 and 3 training breaks, occurring every 1-2 hours. There are between 8 and 12 races a day which are spaced

apart approximately every half hour. Assuming the tracks are not saturated with water from rain, they are harrowed during each of the training breaks, and in between the races. That maintenance schedule leads to tracks being harrowed or conditioned up to 17 times per day. When the track has been harrowed or conditioned, there is significantly more surface area for water to evaporate from, which increases evaporation. See equation 4 for how surface condition impacts evaporation. During periods of drying, harrows and conditioners also mix drier top layers of dirt with the underlying dirt, which is at a higher moisture content (Yamanaka & Yonetani, 1999). That mixing leads to higher moisture content dirt in contact with the air, increasing evaporation.

There are two main types of harrows. Drag harrows, Figure 11, are load controlled and conditioners, shown in Figure 12, are depth controlled. Load controlled harrows cut to a depth in the track based on the weight and design of the harrow, as well as the hardness of the track material. A harrow with enough load can cut all the way to the base material, which is useful for some track types. A depth controlled conditioner, as well as some types of diamond harrows, ride on a set of wheels, which can be raised or lowered relative to the cutting teeth with hydraulic cylinders. This allows them to cut to a consistent depth. Depth controlled harrows are used by tracks which maintain a hardpan between the cushion and base, to ensure that the cushion is maintained to a consistent depth.

Figure 11: Load controlled harrow showing multiple rows of harrow teeth.

Figure 12: Conditioner with two sets of harrow teeth and the compacting wheels. Some versions of the conditioner are also known as a roller harrow.

During periods of rain or at night the track is smoothed and compacted, or 'sealed' using rollers, plates, or floats (Figure 13). They are sealed both to decrease evaporation, and to prevent material from washing away in heavy rain. The smaller surface area that results from the track being 'plated' or sealed causes lower rates of evaporation. The lower evaporation rates from the sealed tracks are utilized by

maintenance personnel, who seal the track in the evening to maintain the moisture content for the next day. This allows them to avoid adding extra water in the morning. During rain storms, the harder packed surface causes increased runoff, and decreases the chance for track material to be washed away.

The maintenance of racetracks has developed over time and only recently has been documented. Some tracks now maintain extensive data relating to the track surface condition and additions of water using the Maintenance Quality System (MQS), which is detailed in Appendix D. Data on the time and type of track equipment that is used, including water trucks, and other information is entered by maintenance personnel at each of the tracks considered. For this research, these data are used in the calculations to determine if the track was harrowed or sealed at any given time. Appropriate coefficients for that surface condition are then used in equations 1, 4, 13, and 15.

Figure 13: Plate (float) with raised backrake.

In order to replace water lost by evaporation, water trucks, ranging from 11.4-22.8 m^3 add water to the track. Figure 14 shows a water truck with 22.8 m^3 capacity, and the

boom arm retracted. Many tracks use water trucks with boom arms to prevent the track from becoming compacted near the rail, where the majority of racing occurs. The booms are also useful to help maximize the coverage of the track, and keep the water addition more consistent than other styles of water truck. The alternative to boom trucks are fan spray trucks, which spray water in a fan shaped arc behind them. The fan spray trucks typically apply water less evenly than the boom trucks. Another issues with the fan spray trucks is that they cannot spray water the same distance as the boom trucks, which requires them to drive in the racing lanes used by the horses, causing uneven compaction.

Figure 14: 22.8 m^3 capacity water truck with boom arm retracted.

2.2 Evaporation Model

2.2.1 Use of Penman-Monteith Equation

In section 2.1.1, the large impact of moisture content on the mechanical properties was described. Unlike many other variables such as track composition, moisture content can change rapidly as a result of rainy, hot, dry, or windy weather. The goal of this thesis is to provide a reliable method to determine whether or not the track requires additional

water. The basis for this model is the Penman-Monteith (PM) equation which is used to calculate evaporation. If implemented to provide near real time data, the program could enable the track personnel to make better informed decisions about when and how much water needs to be added to the track. In addition to helping to determine when water must be added to the tracks, the programs output could be used to decide when the track has recovered enough from recent rain to begin using pieces of maintenance equipment that require a lower moisture content to be effective.

The PM equation was chosen as the basis for calculations because it is the standard evaporation equation used by the American Society of Civil Engineers and the Food and Agriculture Organization of the United Nations (Allen et al., 1998; Walter et al., 2005). Evaporation models are used to help farmers estimate the total loss of moisture from a crop in order to irrigate more precisely. The PM equation uses weather data to calculate evaporation with an hourly time step. To apply these models to the surface of a dirt racetrack the transpiration losses are eliminated from the calculations and the losses which result from frequent maintenance of the surface are added.

2.2.2 Penman-Monteith Equation Application

In order to calculate evaporation from racetracks, modifications to the Penman-Monteith (PM) equation are needed. The PM equation was initially developed for calculating evapotranspiration from cropland, so it includes both evaporation from the soil and moisture loss from the plant leaves (transpiration). The modifications of Walter et al. (2005) are used so that the calculations do not depend on the stomatal resistance of the plants, which is not needed for use on horse racetracks. Terms are also added to account for the varying surface condition of the track.

Input data for the calculations include the use of maintenance equipment, application of water and weather conditions. The weather data required for the PM equation is supplied by weather stations located at the tracks. The weather stations include sensors to monitor all of the variables required by the PM equation as well as additional sensors such as flux plates that allow the accuracy of simplifications of the model to be assessed.

Track maintenance is documented by track personnel, who record the type and timing of maintenance equipment. There are three main types of maintenance equipment used at the tracks, harrows, plates, and water trucks. Harrows 'fluff' and mix the surface, they are used to maintain a consistent cushion for racing. Plates are used to protect the track from rain, by compacting and 'sealing' the surface. Plates are also used after the days racing is finished to minimize overnight evaporation losses. The final major piece of maintenance equipment, the water truck, is used to maintain a relatively constant moisture content in the track material. Track maintenance personnel determine when to add water to the track based on visual cues and past experience.

In order to establish the accuracy of the model and to reset the program on a daily basis, moisture measurements are made at the track. The measurements are taken at a range of locations around the track, to avoid being impacted by local variations in moisture content. It would be impractical for maintenance personnel to take moisture measurements between races, but measuring the moisture content once per day allows the program to be reset to the correct moisture content each day. The daily reset would prevent errors from accumulating over time, and help ensure accuracy over the race card, when maintaining a consistent moisture content is most critical.

The standard unmodified PM equation calculates ET_0, evapotranspiration in mm, from

$$ET_0 = \frac{\frac{s(R_n\text{-}G)}{\lambda} + \gamma \frac{C_n}{T+273} U_2 VPD}{s+\gamma(1+C_d U_2)} \quad (1)$$

The PM equation can be broken down into three terms, the energy balance term, the temperature and relative humidity term, and the aerodynamic effects term. The energy balance term is

$$\frac{s(R_n\text{-}G)}{\lambda} \quad (2)$$

where s is the slope of the saturation vapor pressure curve ($kPa°C^{-1}$), R_n is the net solar radiation ($MJm^{-2}h^{-1}$), G is the ground heat flux ($MJm^{-2}h^{-1}$), and λ is the latent heat of vaporization of water ($MJ\ kg^{-1}$).

The temperature and relative humidity term is

$$\gamma \frac{C_n}{T+273} U_2 VPD \quad (3)$$

where γ is the psychrometric constant ($kPa°C^{-1}$), C_n is a curve fitting constant, T is the average air temperature (°C), U_2 is the wind speed at 2m above the ground (ms^{-1}), and VPD is the Vapor Pressure Deficit (kPa).

The third term is the aerodynamic effects term is

$$s+\gamma(1+C_d U_2) \qquad 4$$

where C_d is a curve fitting constant that accounts for changes in surface condition.

The energy balance is used along with the latent heat of vaporization of water, and the slope of the saturation vapor pressure curve. The purpose of the energy balance term is to determine evaporation caused by energy absorbed by the top surface of soil. The amount of energy absorbed by the soil is the difference between net solar radiation and ground flux. A portion of that energy is absorbed by water as it evaporates, which can be calculated by using the latent heat of vaporization.

The temperature and relative humidity are used to increase evaporation in some conditions and decrease it in other conditions. The vapor pressure deficit goes to zero as the relative humidity approaches 100%, and increases as the relative humidity decreases, which results in decreased evaporation rates in humid conditions. The vapor pressure deficit is also highly temperature dependent, which causes decreased evaporation in cold conditions. The psychrometric constant is used to account for the partial pressure of water in the air. The wind speed is included because higher wind speeds increase mixing of the air above the surface of the ground, which impacts evaporation.

The aerodynamic effects term accounts for changes in track condition, as well as wind speed. The denominator curve fitting constant is multiplied directly by wind speed, which is why it is used to account for changing surface condition. The aerodynamic term is in the denominator, so increasing its value decreases evaporation rates.

The energy balance term, equation 2, accounts for changes in incoming and outgoing energy, both the incident solar radiation from the sun and the ground flux lost to

the ground. The temperature and relative humidity term, equation 3, factors in temperature and humidity, as well as wind speed, a curve fitting constant, and the psychrometric constant. The aerodynamic effects term, equation 4, includes the slope of the saturation vapor pressure curve, the psychrometric constant, the denominator curve fitting constant, and the wind speed.

The slope of the vapor pressure curve s, can be calculated from the temperature, T, using either

$$s=0.04145e^{.06088T} \quad (5)$$

or more accurately by using

$$s=\frac{2503e^{\frac{17.27T}{(T+237.3)}}}{(T+237.3)^2} \quad (6)$$

Net solar radiation, R_n, needs to account for outgoing long wave radiation, so net radiation is calculated as

$$R_n = R_{ns} - R_{nl} \quad (7)$$

where R_{ns} is net incident shortwave radiation ($MJm^{-2}h^{-1}$) and R_{nl} is net radiated long wave radiation ($MJm^{-2}h^{-1}$).

Details of solar radiation calculations are shown in Appendix K.

Ground flux, G, can be measured directly or it can be estimated from net solar radiation if measurements are unavailable as

$$G = .1R_n \quad (8)$$

For daytime calculations, or for night time calculations as

$$G = .5R_n \quad (9)$$

At tracks which did not have ground flux data available, equations 8 and 9 are used to calculate it. The estimation does not account for the typical overnight negative values of flux when the ground is warmer than the air, but it does provide a reasonable daily net value of the flux.

The vapor pressure deficit, VPD, can be calculated as the difference between the maximum and actual average vapor pressures of the time step with

$$\mathrm{VPD} = 0.6108e^{\frac{17.27T}{T+237.3}} - \frac{RH}{100}0.6108e^{\frac{17.27T}{T+237.3}} \quad (10)$$

where RH is the relative humidity (%).

The psychrometric constant γ , is calculated from

$$\gamma = 0.000665P \quad (11)$$

where P is the average atmospheric pressure for the time step (kPa).

The wind speed in the calculation is from 2m above the ground. The wind speed profile varies with height, but it is possible to convert from the measurement height to the 2m height using

$$U_2 = \frac{U_z 4.87}{\ln(67.8z\text{-}5.42)} \qquad 12$$

where U_z is the wind speed at measurement height z (ms^{-1}), and z is the height at which the wind is measured at (m).

2.2.3 Modifications to the Penman-Monteith Equation

In order to increase the accuracy of the evaporation calculations and to account for factors unique to horse racetracks, the Penman-Monteith equation was modified. Similar to the unmodified equation, the modified program uses weather station and maintenance data to calculate evaporation from each period. Calculated evaporation is then subtracted from the water added by rain or water trucks during the same period to get net water gain. The net water gain is then added to the moisture content that had been calculated in the previous period to get the current moisture content. If there is no water added, then evaporation causes to net water gain to be negative, and the moisture content of the track decreases.

Weather, moisture content and maintenance data are imported into the program from comma-separated value (CSV) or text files. Weather data are processed for use with

an hourly time step by totalling or averaging all variables as appropriate. All units are also converted by the program to the correct units for the PM equation. Moisture data are checked by the program for incomplete or invalid data sets, and each complete set is spatially averaged. Data relating to the water trucks are used to determine how much water has been added, as well as the time of the water addition. The water truck data are used alongside the rainfall data to determine the increase of the moisture content of the track as water is added. Maintenance data are also used to determine whether the surface has been harrowed or sealed. If there is no maintenance data for any time period, then the surface condition has not changed, and is left the same as the previous time step. The maintenance data allows the program to optimize differently between different track conditions.

The modified equation is shown in equation 13. It is similar to the standard PM equation, except that the numerator and denominator coefficients have become functions of track moisture content and track surface condition respectively.

The program calculates evaporation, E (mm), from

$$E = \frac{\frac{s(R-G)}{\lambda} + 2\gamma\left(C_n(m_p)\right)\left(\frac{1}{T+273}\right)(U)(VPD)}{s + \gamma(1 + (C_d(TC))U)} \quad (13)$$

where m_p is moisture content of the track (% mass water content), and TC is the track surface condition, which can be either harrowed or sealed.

The numerator coefficient, C_n, is a function of moisture content as

$$\mathrm{C_n} = \mathrm{abs}\left(\mathrm{x_4}\left(\mathrm{m_p} - \mathrm{abs}(\mathrm{x_1})\right)\right) + 1 \quad (14)$$

where x1 and x4 are the coefficients that are optimized. X_4 is bounded to be less than 10.

The numerator coefficient is used to increase evaporation when the track has an elevated moisture content, and decrease evaporation when there is a deficit of moisture in the track. If there is less water in the track, then it will evaporate more slowly than if there is an excess of moisture (Evett, 2007). At the logical extreme, soil with no moisture can have no evaporation. Measurements of track moisture content indicate that increased moisture content cause higher evaporation rates.

The denominator coefficient, C_d, is a function of the track condition as

$$C_d = (TC)X_2 + (1 - TC)X_3 \qquad 15$$

where TC can be either 1 or 0 based on track condition(open or sealed), X_2, and X_3 are the coefficients that are optimized. X_2, and X_3 are bounded to be less than 5, and greater than .05.

The denominator curve fitting coefficient is changed based on the maintenance equipment that the track uses. Harrows and backrakes open, and increase the surface area of the track, which increases evaporation. Plates and other implements decrease surface area, which decreases evaporation. Having a separate curve fitting constant for each surface condition allows the model to accurately calculate evaporation throughout the entire day.

The program was optimized by using a Nelder-Mead optimization function (MatLab function fminsearch) for C_n and C_d. See Appendix F for more details about the

optimization. The optimization program minimizes the RMS difference between each of the moisture contents measured by the moisture probe, and the calculated moisture content for that point in time. The program optimizes harrowed and sealed tracks differently. To account for the changing surface condition of the track in the code, the denominator calibration coefficient is changed based on whether the track has been harrowed or sealed so that it is optimized separately for each track condition. An example of a typical harrowed surface finish is shown in Figure 16, and a sealed surface is shown in Figure 15.

The optimization process begins with the calibration coefficients set to the same values as the standard PM equation. The algorithm runs the equation repeatedly while changing the coefficients in order to minimize the total root mean square difference for all of the points. Once the algorithm has reached the required tolerance, 1e-4, it stops looping and reports the values of the coefficients that minimize the program output. It is possible that the algorithm could optimize to a local minimum, instead of the global minimum. That risk is minimized by beginning with the values from the standard PM equation, which have been demonstrated to work for farmland (Allen et al., 1998).

In addition to the optimization, the program can reset the calculated moisture content to the measured moisture content every morning. The daily reset can help to test the accuracy of the program in the same time scale that matters to the maintenance personnel. The maintenance personnel measure the moisture content every morning, so the calculated moisture content is reset in the morning. The calculated moisture content is then compared to the measured moisture content measured in the evening to determine how well the calculations fit measurements over the duration of racing for each day. The

calculations are not reset to measurements made after racing because maintenance personnel typically do not measure the moisture content of the track after racing.

Saturation is taken into account by the program. After a certain amount of rain, the track becomes saturated, and all additional water runs off or percolates through the track without increasing the moisture content. Saturation is modelled by ignoring all rain that would increase the moisture content above the saturation point. A saturated track can be seen in Figure 15.

Figure 15: Standing water on a track that has been saturated by rainfall.

Figure 16: Surface finish of a harrowed track at a typical moisture content.

2.2.4 Weather Station

2.2.4.1 Weather Station Sensors

On site weather stations provided the weather data used for evaporation calculations. Various sensors provide the basic data required for the evaporation model described in section 2.2. Temperature, vapor pressure deficit (VPD), slope of the saturation vapor pressure curve, wind speed, the psychrometric constant, short wave solar radiation, and ground flux are all directly or indirectly obtained from the weather station. Table 1 details how the weather station sensors are used. Appendix E includes a complete list of weather station components used for each of these variables.

Table 1: Explanation of variables provided by weather station.

Measurement	Used to calculate	Explanation
Temperature (T)	VPD(T,RH),s(T) (Eqn. 5, 6, 3, 10)	Temperature is used directly, as well as in the calculation of the vapor pressure deficit, and the slope of the saturation vapor pressure curve
Wind Speed (U_z)	U(U_z) (Eqn. 3, 12)	Wind speed at a given height is used to estimate the wind speed at 2m
Humidity (RH)	VPD(T,RH) (Eqn. 5)	Humidity is used to calculate the vapor pressure deficit
Atmospheric Pressure (P)	γ(P) (Eqn. 11)	Atmospheric pressure is used to calculate the psychrometric constant
Solar Radiation (R_s)	R_n(R_s) (Eqn. 2, 8, 9, 20)	Short wave solar radiation is used to calculate the net solar radiation
Ground Flux (G)	G (Eqn. 2)	Ground flux can be directly measured for the equation
Ground Temperature Gradient (∇T)	G (Eqn. 18)	If ground flux data is unavailable, it can be calculated from the ground temperature gradient and moisture content
Soil Moisture Content (m_p)	G (Eqn. 18)	If ground flux data is unavailable, it can be calculated from the ground temperature gradient and moisture content

At all locations, a datalogger (Campbell Scientific model CR1000, Logan UT) was connected to the internet and uploaded data to a server. A figure showing how the sensors were oriented can be seen in Figure 17. The barometric pressure sensor (Setra model 278, Boxborough MA) was mounted in the NEMA enclosure with the datalogger, to shield it from the weather. The enclosure does not hermetically seal, so the pressure readings were not affected by placing the pressure sensor in the enclosure. The solar pyranometer (Apogee model SP-110, Logan UT) was mounted on the southernmost end of a crossbar to ensure that it was never in the shadow of the weather station. Care was taken to ensure that the solar radiation sensor was oriented vertically, by using a spirit level and levelling plate. The wind monitor (RM Young model 5103, Traverse City, MI)

was mounted on the northernmost end of the same crossbar. It was mounted as high as possible to help mitigate the impact of obstructions to the wind at the weather station site. The temperature and relative humidity sensor (Campbell Scientific mode CS215, Logan UT) was mounted inside a solar radiation shield to prevent readings of air temperature from being impacted by the solar radiation.

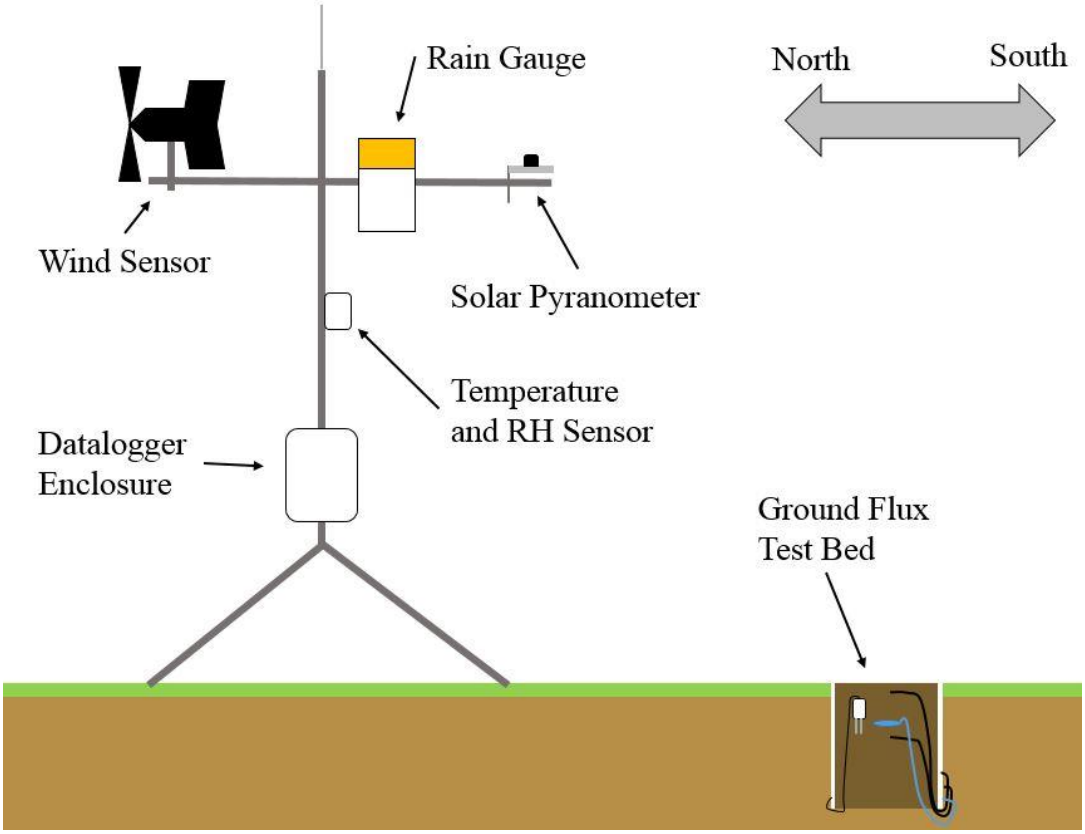

Figure 17: Campbell Scientific weather station showing relative sensor location.

At two of the installations (Keeneland and Fair Grounds), ground flux was measured using a test bed of track material set up near the track. Sensors installed in the test bed included a moisture probe (Campbell Scientific model CS655, Logan UT), and two burial thermocouples (Campbell Scientific 105E, Logan UT) to measure the thermal gradient. At Keeneland, there was also a ground flux sensor (Hukseflux model HFP01,

Manorville, NY). See Figure 18 for the relative location of each component. The upper thermocouple was buried 3.25 cm below the surface. The flux plate was 7.5 cm below the surface, level with the upper end of the prongs on the moisture probe. The lower thermocouple was buried 10 cm below the surface. Cables from the sensors were routed underground to avoid having the cables conduct heat to the sensors from the surface.

It would be possible to use either the flux plate, or a pair of the thermocouples with the soil moisture content probe to calculate the ground flux. If the thermocouples were the only source of flux data, knowing the vertical distance between the thermocouples would be essential to calculating the thermal gradient for use with Fourier's law. The thermal conductivity of each soil would need to be measured at several moisture contents to get an accurate measurement of flux. Calculation of ground flux from thermal gradients is shown in Appendix J.

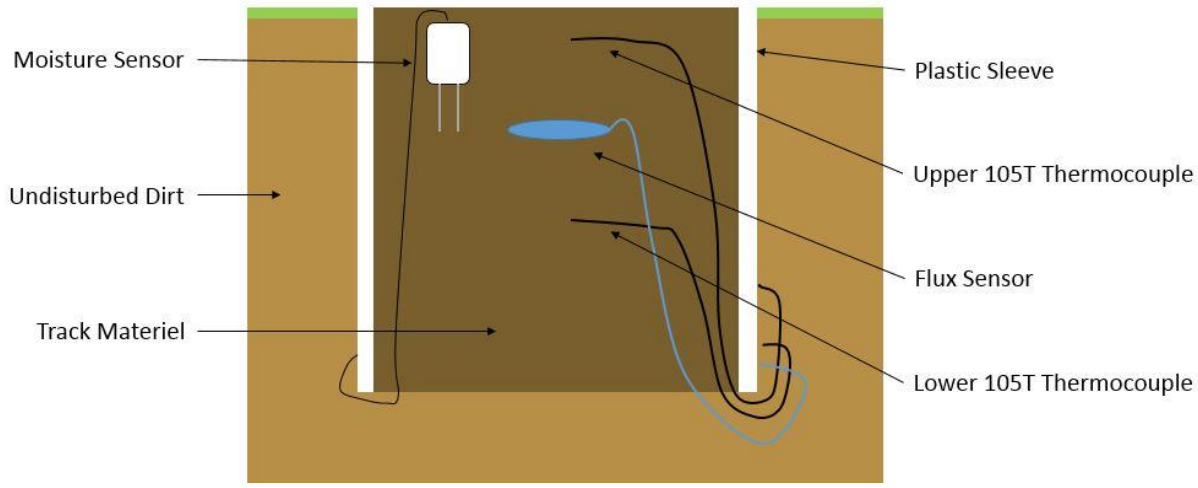

Figure 18: Layout of ground flux test bed.

2.2.4.2 Weather Station installation

The site that the weather station is installed at can have an impact on the quality of data it collects. Wind speed measurements taken from the lee of a tree, or rainfall measurements where the gauge is shadowed by a building will report lower values than the actual values on the track.

At Saratoga, the weather station was set up on the infield of the main track, shown in Figure 19. Data were collected between 8/14/14 and 9/2/14 at Saratoga.

Figure 19: Weather station location at Saratoga. Weather station was mounted on the infield of the main track.

The weather station at Keeneland was installed just outside the main track near the 5 furlong mark, shown in Figure 20. Data were collected between 9/29/14 and 10/26/14.

Figure 20: Weather station location at Keeneland. Weather station was installed outside the 5/8 chute.

At Fair grounds, the weather station was mounted to the side of the tote board, shown in Figure 21. Data were collected between 12/23/14 and 3/27/15 at Fair Grounds

Figure 21: Weather station location at Fair Grounds. Weather station was mounted on the side of the tote board, so that sensors are above the roof.

At Santa Anita, the weather station was installed on the inside rail of the west turn at Santa Anita, as shown in Figure 22. Data were collected between 3/5/14 and 3/15/14 at Santa Anita.

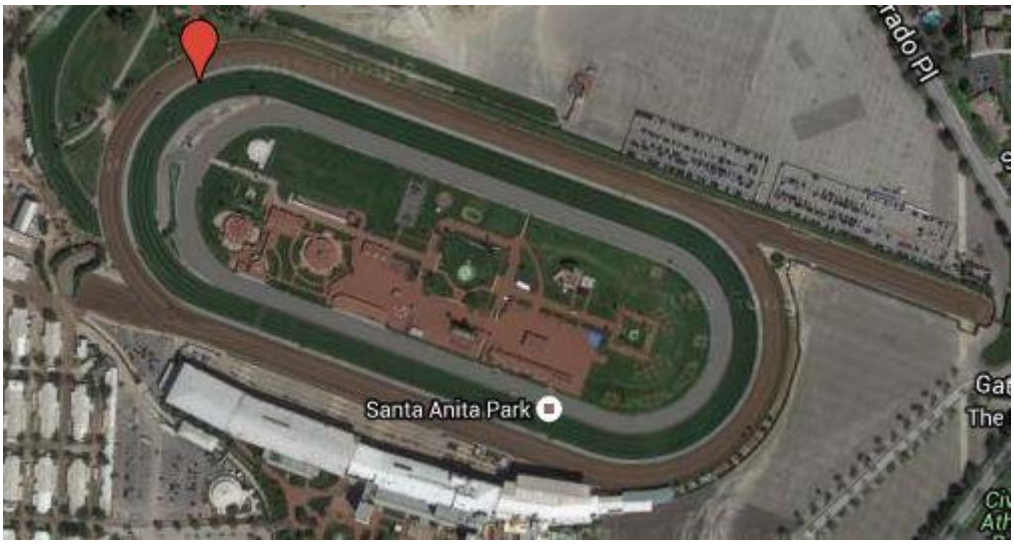

Figure 22: Weather station location at Santa Anita. Weather station is located on the inside rail, in the northern portion of the west turn.

2.2.5 Measurement of Surface Moisture Content

The moisture content of the track was measured with a time domain reflectometry probe (Spectrum Technologies model TDR300 Aurora, IL) at each of the tracks in order to validate the output from the evaporation model. See Appendix C for details on the moisture probe. Due to the focus on temporal changes over spatial changes, all moisture data was spatially averaged to produce a single moisture content for each set. The spatial averaging is important both to increase the accuracy of the measurement by increasing the number of points (Evett, 2007), as well as to ensure that moisture measurements are not effected by local variations in moisture content.

For comparison with the model, sets of moisture probe readings from around the entire length of the track were taken before and after racing, as well as a smaller sample

between races. The larger sets of data were taken at 1, 2 and 3 meters out from the rail, which covers the portion of the track most commonly for racing. At Keeneland, Saratoga and Santa Anita, the larger data sets were collected at 33 meter intervals, while Fair Grounds was sampled at 100 meter intervals. The smaller sets were taken between races in a 3 by 3 grid with a 1m spacing, for a total of 9 points in each set. Each of the smaller sets of data were taken in the same location each time, to ensure that spatial variations of the moisture content did not impact the results. Taking larger sets of data between races was not possible due to the timing of races and maintenance activity. Between all of the tracks, nearly 22,000 data points were taken in total.

Table 2: Shows the amount of moisture data collected from each track.

Track	Keeneland		Saratoga		Santa Anita	Fair Grounds
	Period 1	Period 2	Period 1	Period 2		
Spacing between points in large sets (m)	33	100	33	200	33	100
Number of points per large set	153	51	162	15	144	48
Number of large sets	46	27	23	58	18	62
Number of points per small set	9	N/A	9	N/A	9	N/A
Number of small sets	200	N/A	129	N/A	45	N/A
Range of dates data was taken	9/29/14-10/26/14	9/23/15-10/31/15	8/13/14-9/1/14	8/1/15-9/15/15	3/5/14-3/12/14	1/27/15-3/31/15
# of days	28	39	20	46	8	64

3. RESULTS

Data relating to track weather, maintenance and condition were collected from each track over 6 time periods. Maintenance data demonstrated how different pieces of maintenance equipment are used in different weather conditions, as well as the frequency of water trucks. Typical values and relationships from weather station data are shown. Temporal changes in measured moisture content are shown, as well as the variance of the moisture measurements. Results from the program are provided for both small (9 point) and large (144+ point) datasets. The data is shown with optimized constants and both with and without resetting the value to the measured moisture content on a daily basis. See Table 2 for more information on moisture datasets.

3.1 Maintenance Data

Track maintenance was monitored at each of the tracks considered for the development of the model. Typical equipment usage is shown, including implement usage based on track moisture content, and water truck utilization. The amount of time that different tracks spent harrowed 'open', and 'sealed' with plates is shown.

Figure 23 shows how different pieces of maintenance equipment are used in different weather conditions. On days 1 and 2, the track was at an appropriate moisture content for harrow (Figure 11), so the track was maintained as usual. Overnight rain on day 2 raised the moisture content, so plates (Figure 13) were used to maintain the track. A harrowed surface is generally preferred to a sealed surface for racing, so for races on the dirt maintenance personnel would backrake the track, and plate it during races held on the turf. Once they have finished maintaining the track for the day's racing, they switch to plates to protect the track from additional rain. On a sealed surface, the rain drains

horizontally due to crossfall of the track and does not soak into the track. On day 3, the track had begun to dry enough to stop using plates, and by the end of the day, it had dried enough to use harrows. On day 4, there was another, smaller, rainstorm which increased the track moisture content, so backrakes were used for the remainder of the day. By the morning of day 5, the track had dried out enough to use harrows again.

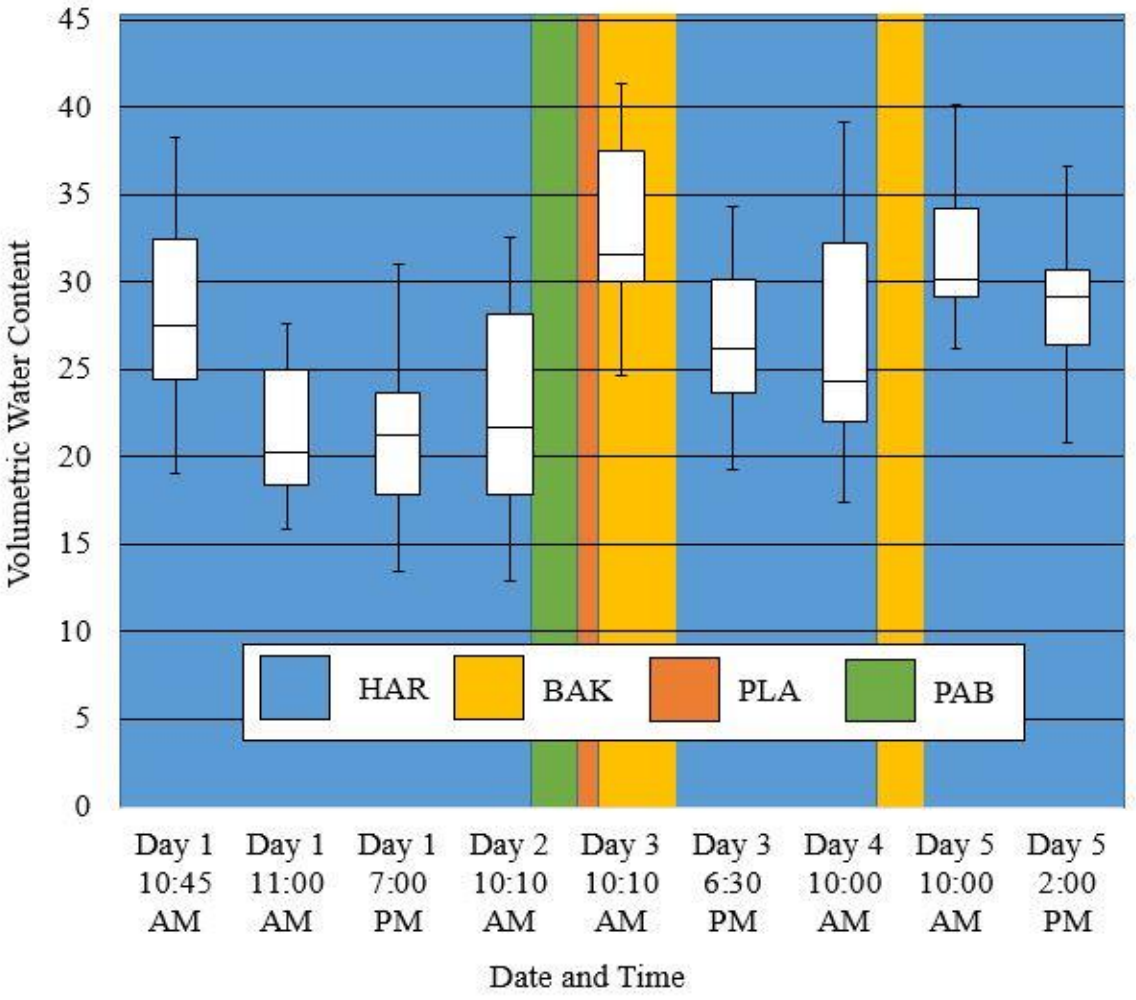

Figure 23: Impact of moisture content on maintenance practices. Harrows (HAR) are used at typical racing moisture contents to maintain the cushion. Backrakes (BAK) are used when the track is too wet for harrows, but can still maintain a cushion for racing. Plates (PLA) are used to protect the track from rain, and to maintain the track when it is too wet for backrakes or harrows. Plates and Backrakes (PAB) are used in conjunction with each other to maintain a cushion for races that are on the dirt track, and protect the track from rain when races are on the turf track.

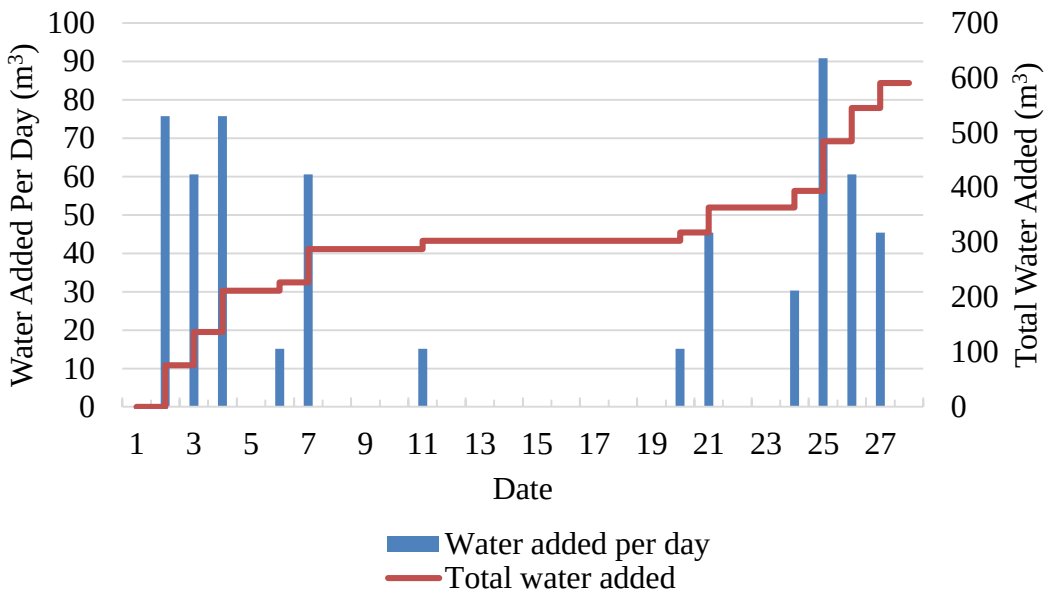

Figure 24: Date and number of trips made by water trucks at Keeneland over 28 days of the race meet.

Figure 24 shows the date and amount of water applied by water trucks at Keeneland. During the drier parts of the race meet the water trucks were used more, such as between day 2 and day 7. During the rainy parts of the meet, and while the track was drying from the rain, the water trucks were used less frequently, such as between day 8 and day 19.

Table 3 shows the time in hours that each of the tracks was harrowed, and the time it was sealed. Each of the tracks spent a similar percentage of the time open vs sealed. Santa Anita, which did not have any rain for the duration of data collection, was sealed for a smaller percentage of the time than the tracks which did experience rainfall.

Table 3: Amount of time different tracks spent harrowed or sealed.

Track	Time Harrowed (hr)	Time Sealed (hr)	Percentage Open (%)
Keeneland	305	362	45.7
Saratoga	188	264	41.6

Fair Grounds	594	725	45.0
Santa Anita	94	85	52.5

3.2 Weather Station Results

The results from all major components of the weather station were plotted to show relationships between variables. Soil temperature gradient is shown with solar radiation. Temperature, relative humidity, and wind speed are also plotted to illustrate typical values. Ground flux is shown, both measured with a flux plate as well as calculated from solar radiation. Cumulative rainfall and rate of rainfall from each track is also shown.

The amount of sunlight a track has on a given day impacts the air and soil temperatures for that day. Figure 25 and Figure 26 show the typical relationship between the soil-air temperature gradient, and solar radiation at Keeneland. Figure 25 shows conditions typical during sunny days, while Figure 26 shows typical cloudy conditions, which highlights the effect that solar radiation has in air and soil temperature.

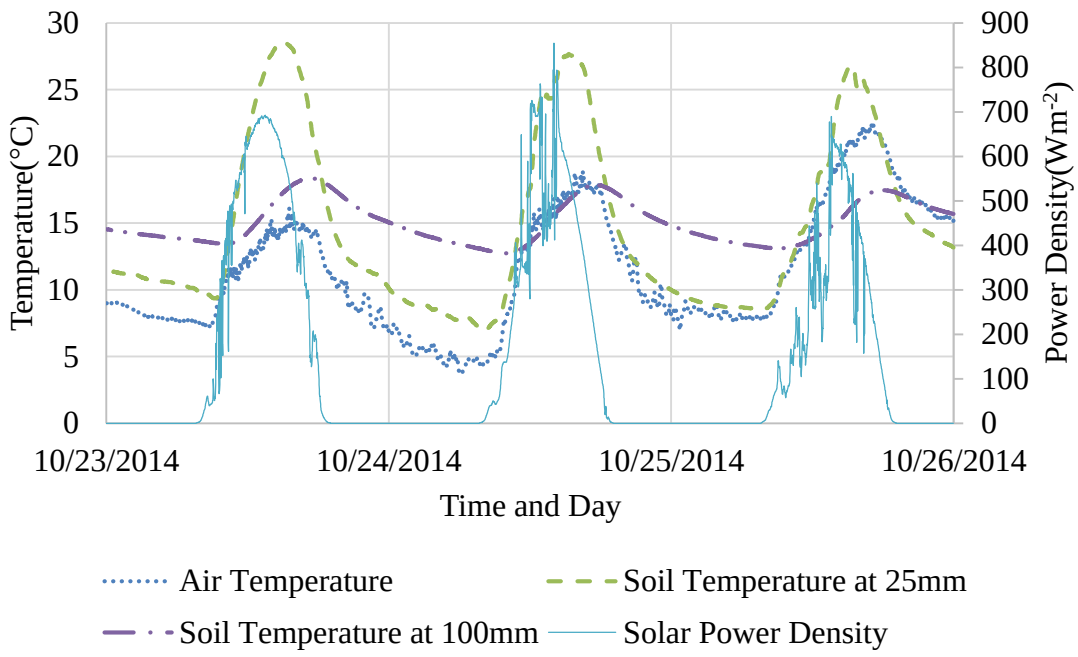

Figure 25: Temperature and solar radiation for typical sunny days at Keeneland

On a typical sunny day, solar radiation can add as much as 800Wm^{-2} to the track, raising air and soil temperatures. At 25mm below the surface the temperature increases to more than 25°C, higher than the ambient air temperature. This occurs on all three days. Air temperature peaked at 15°C, 17°C, and 22°C for the three days shown with a range of 12°C to 5°C below the soil temperature. There is a phase difference between the top soil temperature and the lower soil temperature, with the lower soil probe reaching a maximum temperature approximately 2.5 hours after the upper soil probe reached its peak temperature. The air temperature fluctuates more rapidly than either of the soil temperatures.

The overcast day shown in Figure 26 shows a smaller difference in soil temperature and air temperature. The average difference between the upper soil temperature and the air temperature is 1.97°C compared to the average difference from

the sunny days, of 3.28°C. The average power density of the solar radiation for the sample sunny period was 152.86W/m^2, while the average power from the cloudy period was less than half that, at 61.21W/m^2. The smaller temperatures and lower solar radiation power density on cloudy days contribute to lower values of evaporation from the track surface.

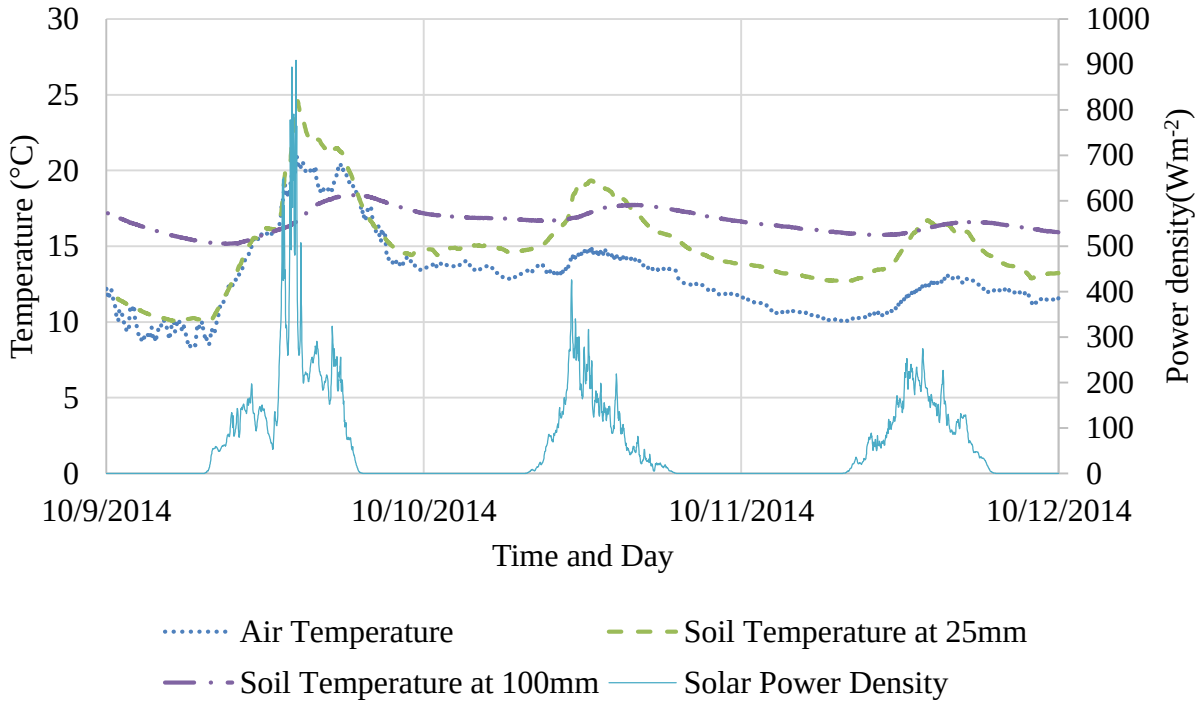

Figure 26: Temperature and solar radiation for typical overcast days at Keeneland.

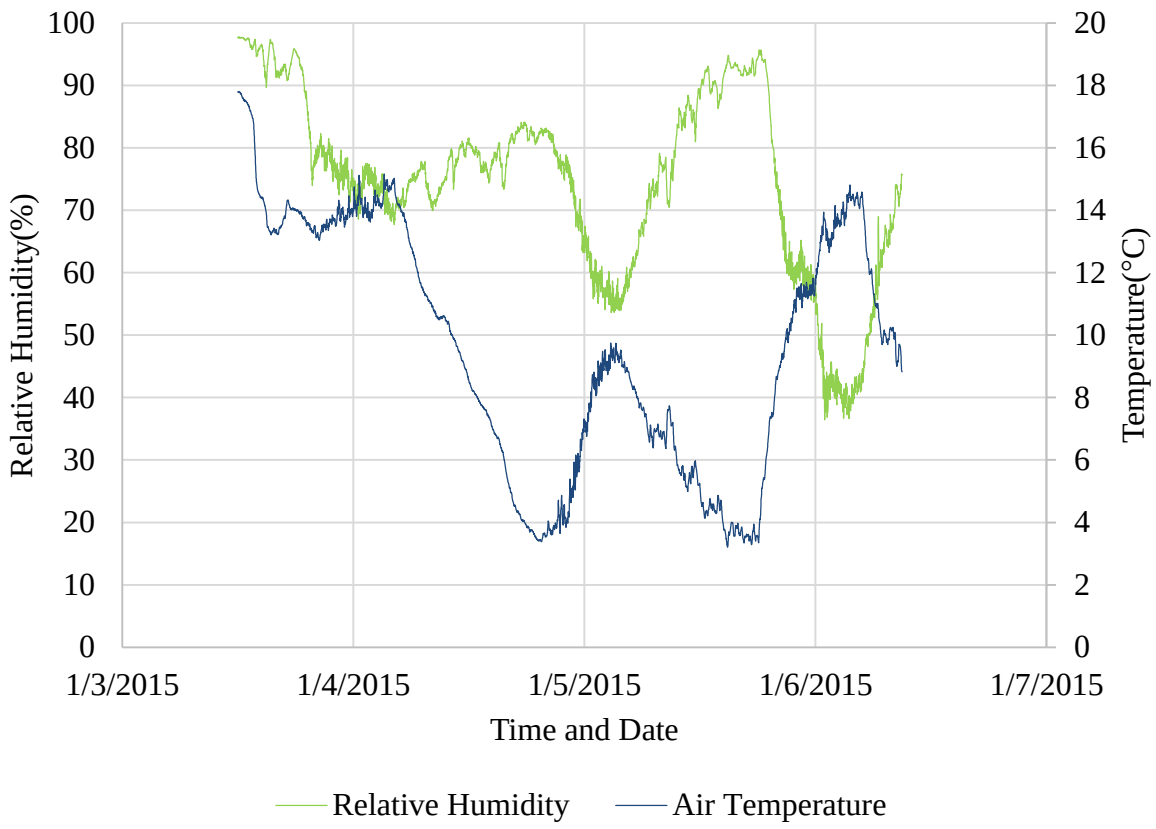

Figure 27: Relationship between air temperature and relative humidity at Fair Grounds.

Temperature and humidity also impact evaporation rates. Figure 27 shows temperature and relative humidity over a 3 day period at Fair Grounds. The temperature had a high of 17.8°C at 12pm on 1/4/15, and reached overnight low temperatures of 3.2 on the nights of 1/4/15 and 1/5/15. The relative humidity peaked at 97% in the early morning of 1/4/15, and reached a low value of 37% on 1/6/15. The air temperature and relative humidity curves tend to mirror each other, which is expected based on the relationship between temperature and relative humidity.

The ground flux represents the energy absorbed by the soil, which is not available for evaporation. Ground flux is used in equation 2. Ground flux can either be measured directly with flux plates, or estimated from solar radiation with equation 8.

Figure 28 shows the ground flux calculated from solar radiation at Keeneland, and Figure 29 shows measured ground flux over the same period at Keeneland. Cooler, overcast days, such as between 10/9/14-10/12/14, shown in Figure 26, result in low flux measurements from both the measurement and the calculation. Similarly, warmer sunny days result in higher flux measurements, such as between 10/23/14-10/26/14, shown in Figure 25. Figure 30 shows the difference between the direct measurements and the calculations from solar radiation. The average difference is -.018MJm^{-2}hr^{-1}, which is approximately a third of the typical maximum values. The error tends to be largest overnight, when solar radiation is 0, and the flux values are negative. There is also a small phase difference between the direct measurements and the solar radiation, which contributes to the error.

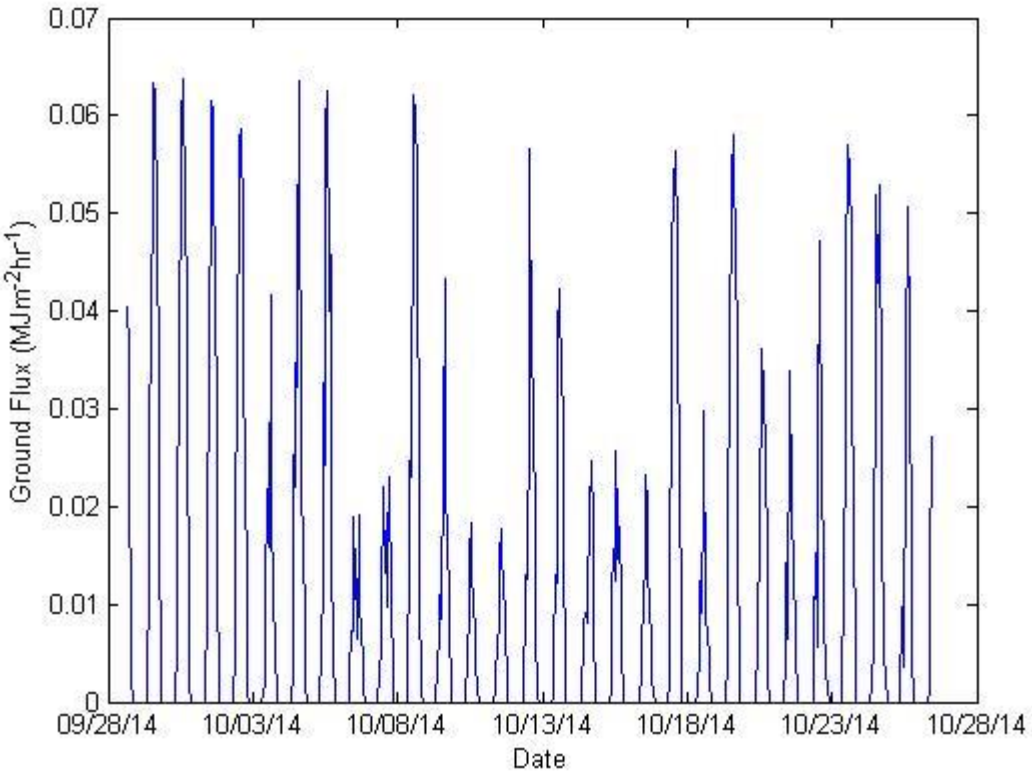

Figure 28: Ground flux data calculated from solar radiation at Keeneland.

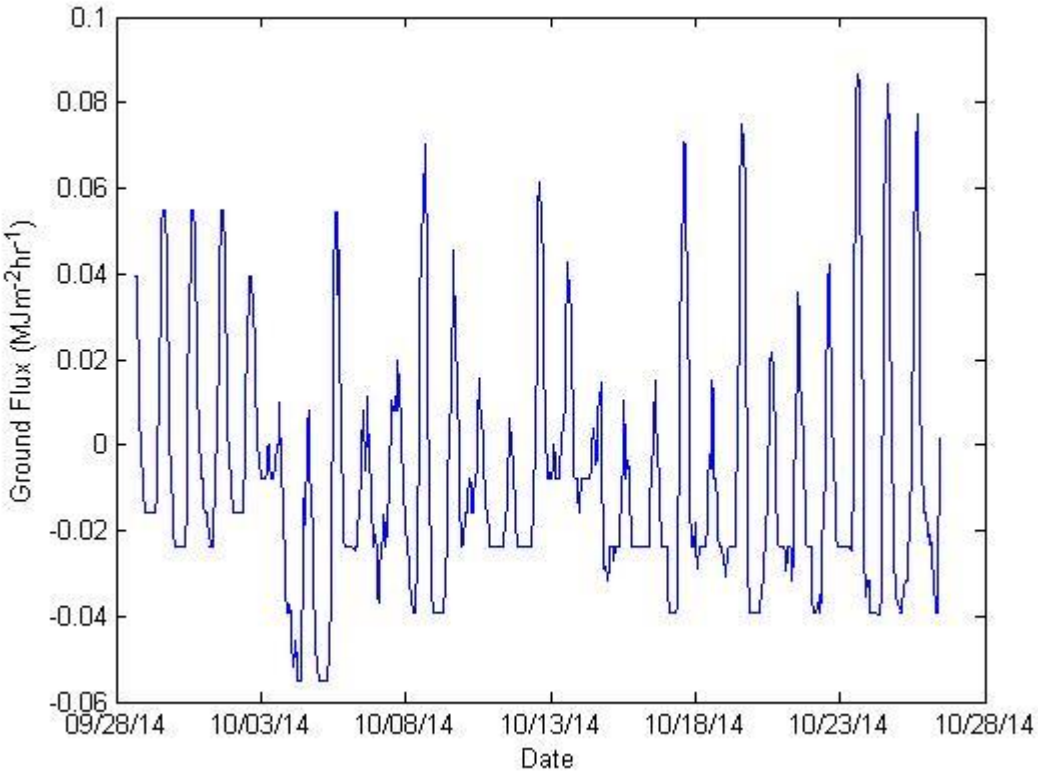

Figure 29: Ground flux measured by a flux plate at Keeneland.

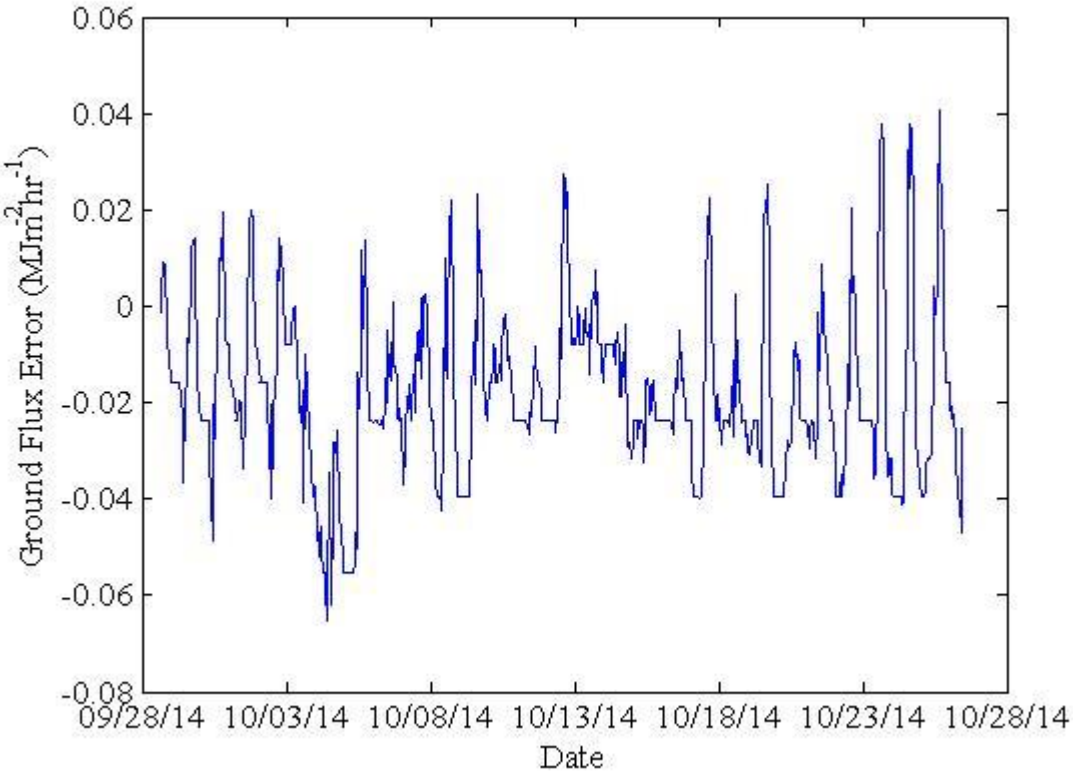

Figure 30: Difference between flux plate measurement and calculation from solar radiation.

The calculations from solar radiation tend to follow the relative magnitudes of the direct measurement. The calculations fail to account for overnight negative values which occur when the air is cooler than the ground. The overall average flux value from the solar radiation calculations is 10.1 kJ/m^{2}hr, while from the direct flux measurements, the average is -7.9 kJ/m^{2}hr. The average air temperature, 14.2 °C, is lower than the average soil temperature, 17.4°C, which supports the negative average flux value reported by the direct flux measurement.

Rain storms are capable of changing the moisture content of a racetrack more quickly than would be possible with only water trucks. Figure 31 shows the per-minute and cumulative rainfall at Keeneland. Over the 27 day period that the weather station

was set up at Keeneland, there was a total of 75.48mm of rain. The majority of the rain came from a series of rain events between 10/13/14 and 10/14/14. There were frequent smaller rain events, and several periods without any rain at all.

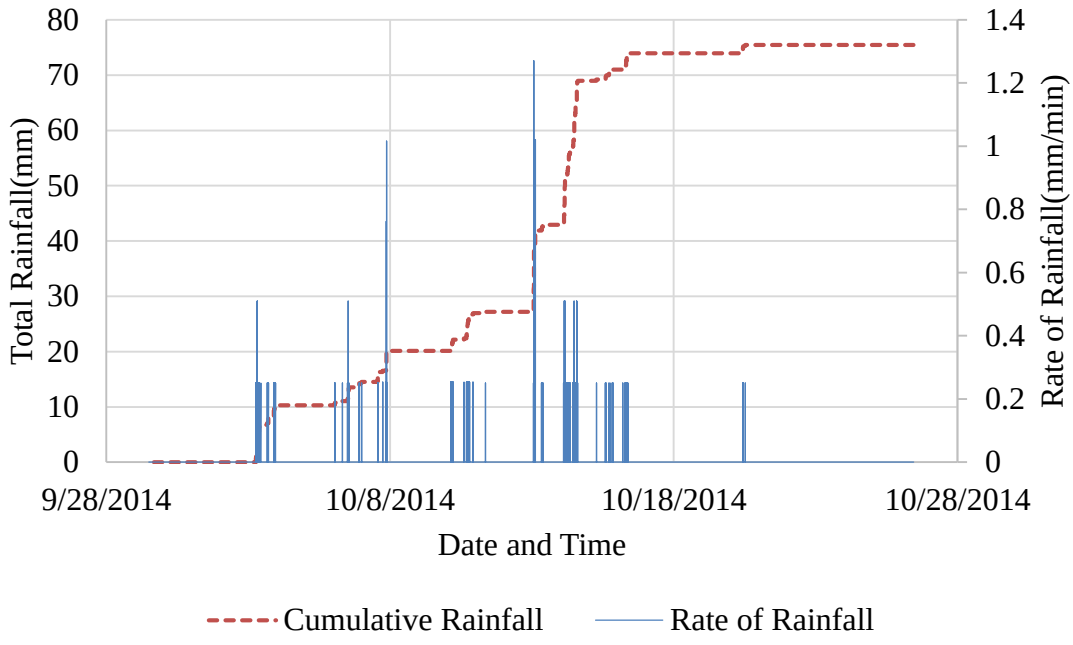

Figure 31: Total and rate of rainfall during data collection at Keeneland.

Figure 32 shows total rainfall from Saratoga during the period that data was collected. The station was collecting rain data over 19 days of the Saratoga race meet, for a total of 78.49mm of rain. The majority of the rain at Saratoga came during two large rain events, while at Keeneland the rain was more evenly spread out over the period of the testing.

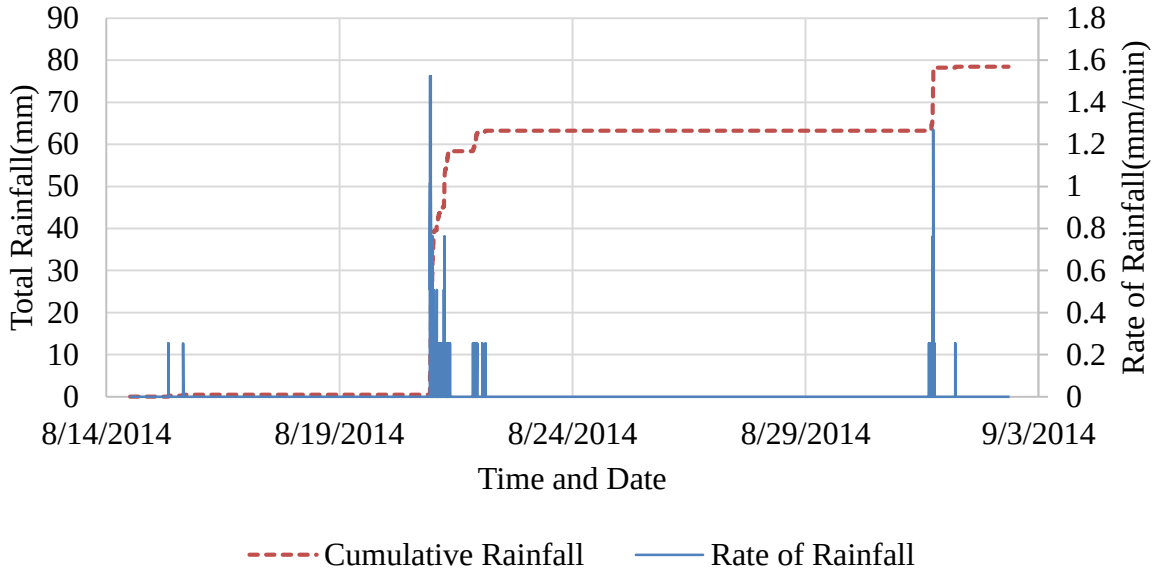

Figure 32: Total and rate of rainfall during data collection at Saratoga.

Figure 33 shows rate of rainfall, as well as cumulative rainfall at fairgrounds over 64 days that data was collected. There was a large rain event with 72.65mm of rain between 3/9/15 and 3/12/15, which accounts for over half the rain during the period of data collection.

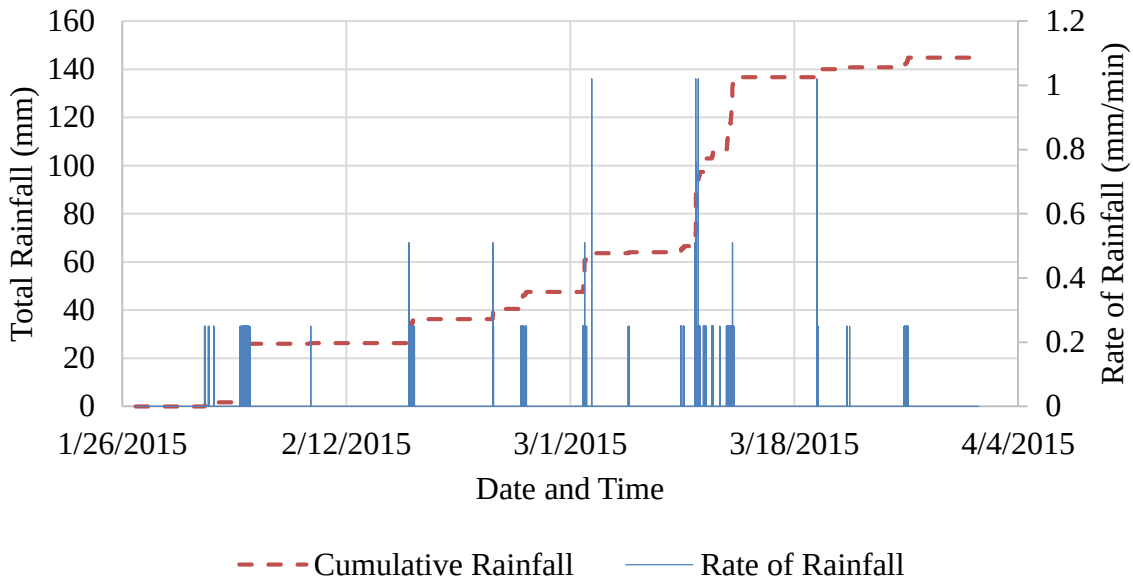

Figure 33: Total and rate of rainfall during data collection at Fair Grounds.

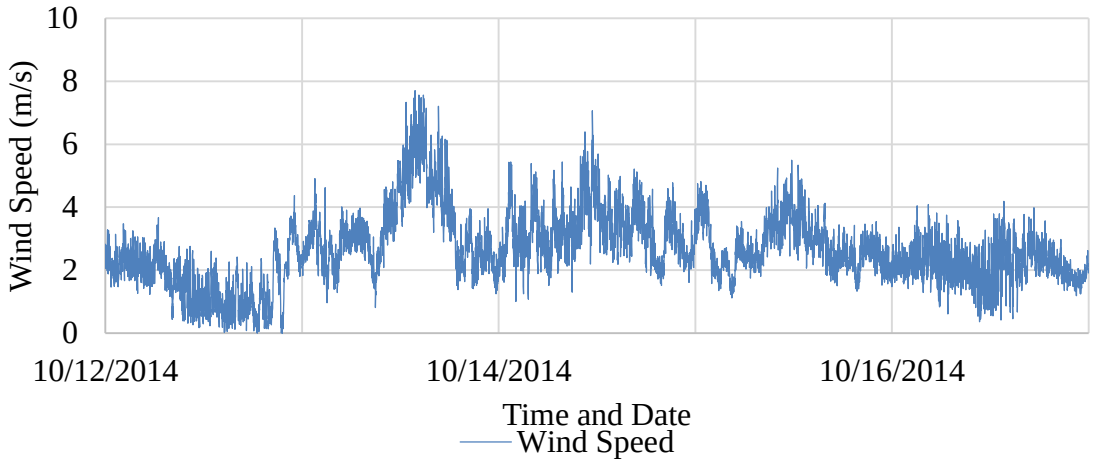

Figure 34: Wind speed measurements from Keeneland.

Wind speed factors into the evaporation rates at the track. Figure 34 shows wind speed measurements taken over 5 days at Keeneland. The average wind speed for that period was 2.65 m/s, and the standard deviation was 1.13 m/s.

3.3 Moisture Measurement Results

TDR probes were used to monitor temporal changes in moisture content at each of the tracks. Box plots are used to show changes in moisture content. Box plots show the median of the sample, as well as the 25^{th} and 75^{th} percentiles and any outliers (Grubbs, 1969). Figure 35 is a box plot showing the change in moisture content over time, as well as variability of moisture content on any given day at Santa Anita. There were no rain events at Santa Anita for the duration of data collection, so all increases in moisture content are due to water truck usage.

The median moisture content was fairly consistent over the duration of data collection. The median varied from 4 to 9% by mass. There were two discontinuities during data collection. One was on day 7, and the other was on day 14. The change on day 7 is a nearly 60% increase in the average moisture content over the previous measurement. The change on day 14 is a 30% decrease in moisture content from the previous measurement. The outliers and variance shown in the measurements are likely caused by spatial inconsistencies in the track.

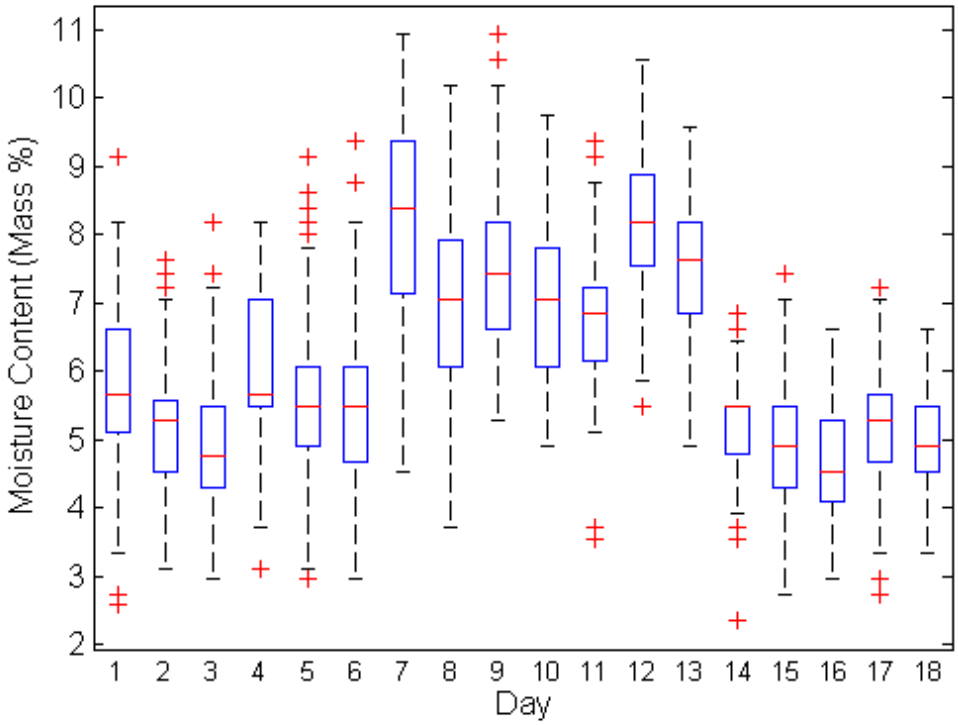

Figure 35: Box plot showing changes in moisture content at Santa Anita.

Figure 36 shows the change in moisture content from Keeneland over 25 measurements. The median of the moisture contents is between 10 and 15 percent by mass. The variation of the moisture content is twice as high during the first 12 measurements than during the final 13 measurements. The first 12 measurements are more consistent temporally than the last 13, with medians varying by 2% by mass, compared to a variance of 4% by mass for the later measurements.

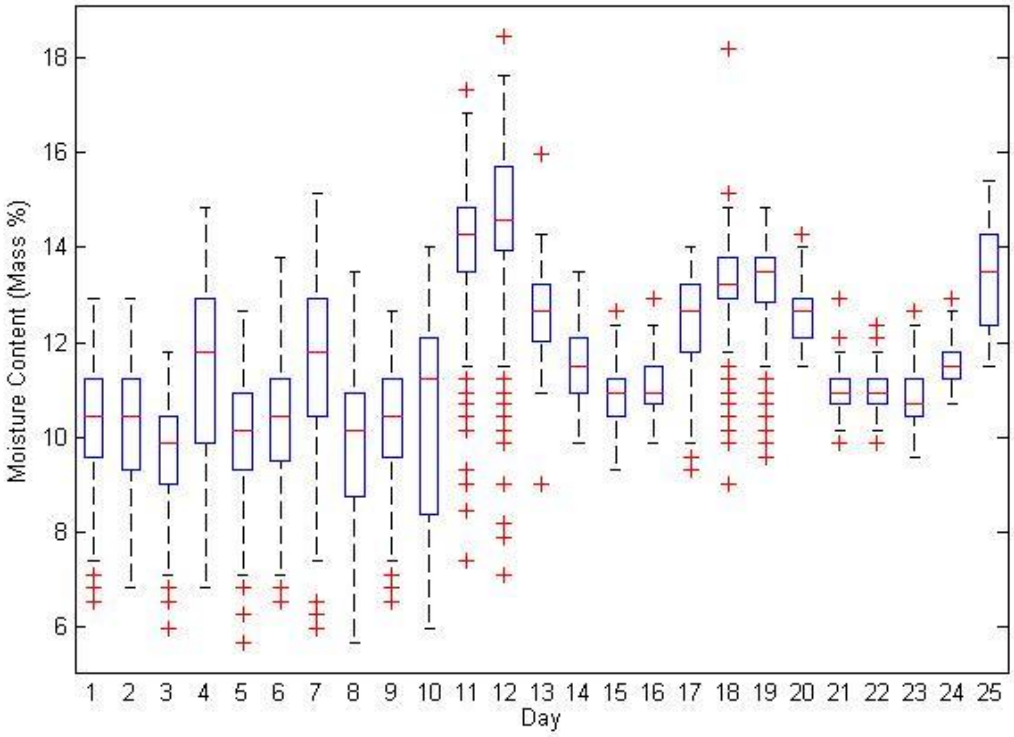

Figure 36: Change in moisture content for 25 daily measurements from Keeneland.

3.4 Program Results

The output of the program that implements the PM equation, equation 13 was compared to the measured moisture contents. The program was used with 3 different levels of optimization. The first, un-optimized, level was used to test the program with standard coefficients. The second level used the Nelder-Mead optimization method to optimize the program coefficients, and to improve agreement with measured results. The third level used optimization for the coefficients, as well as resetting the calculations to match the daily TDR readings. The third level is similar to how the program would be used by maintenance personnel.

3.4.1 Un-Optimized Results

Un-optimized calculations from the program use the standard coefficients from the PM equation. The un-optimized data is only shown to demonstrate the necessity of optimization. Additional un-optimized results are included in Appendix L for comparison. Figure 37 shows the measured moisture content of the Keeneland track over a 25 day period. Also plotted on Figure 37 is the moisture content calculated with the PM equation. Error bars are included to show uncertainty in the measured data. After the rain on day 7, the calculations underestimate the moisture content by 3% Mass Water Content (MWC). Between day 9 and 11, the error is less than 1% MWC for each measurement. After day 27, the calculations overshoot the measurements by at least 3% for the remainder of data collection.

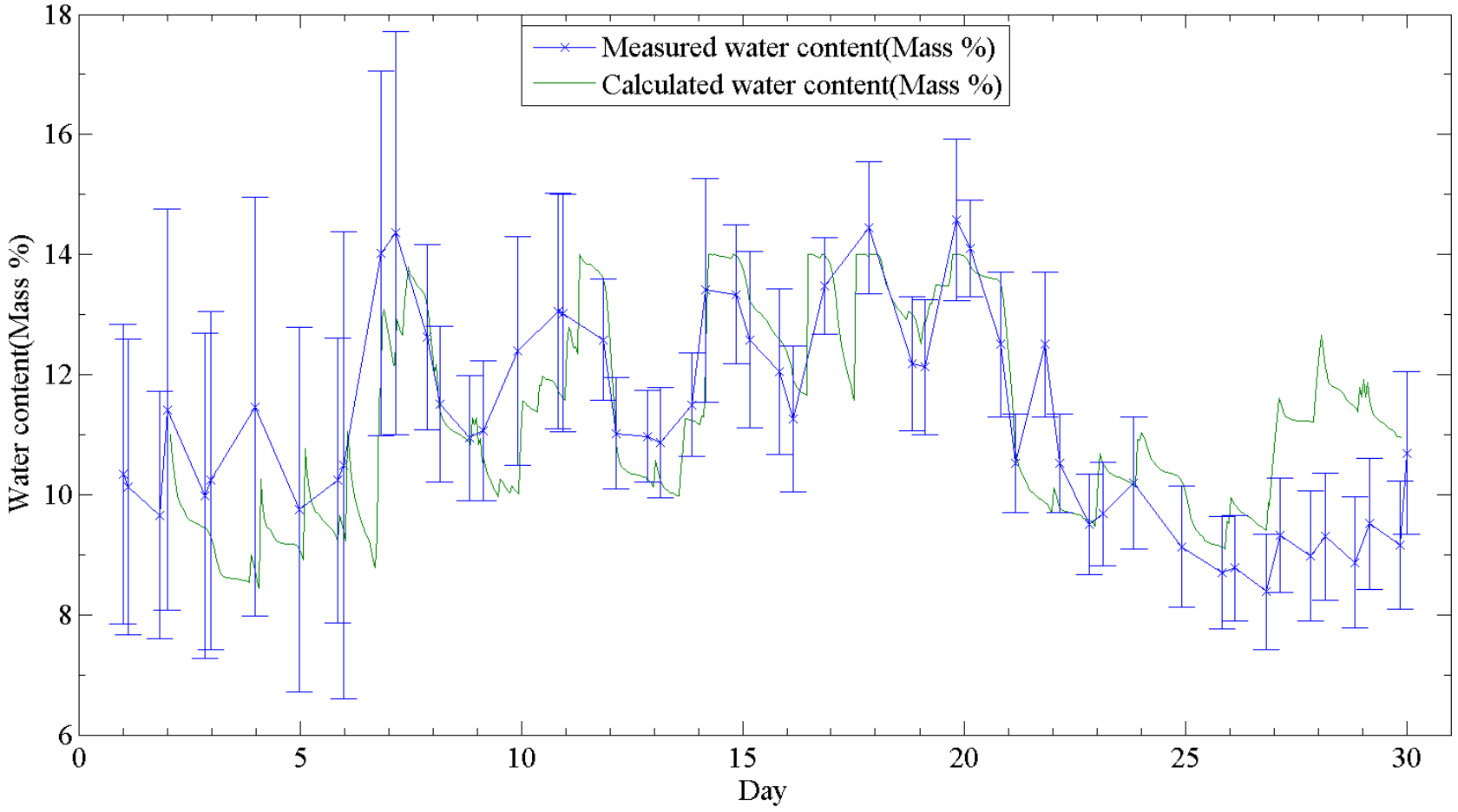

Figure 37: The moisture measured at Keeneland long data set showing calculated and measured moisture content.

3.4.2 Optimized Results

Optimization improves the fit of the calculations to the measured moisture content. The optimization is used to change the coefficients from the standard coefficients used by the PM equation, to coefficients that are more appropriate for a horse racetrack. Figure 38 shows the moisture content of Keeneland measured with a TDR probe, as well as plotted with the moisture content calculated with the modified PM equation. On day 4, the calculations overestimate the moisture content by 2% MWC. On day 5 and 6, the errors are smaller than .5% MWC. After rainfall on day 7, the calculations underestimate the moisture content by 1.5% MWC. As the track dries out, between day 8 and day 10, the moisture content is within .25% MWC of the measurements. Between day 12 and day 21, the error is less than .5% MWC for each measurement. After day 27, the calculations underestimate the moisture content by 2% MWC. Overall errors are quantified in section 3.4.4.

Figure 39 shows the measured moisture content of Keeneland, as well as plotted with the moisture content calculated with the optimized PM equation. Overall, the calculations follow the same trends as the measurements. On day 6, the measurements undershoot the calculations by 1.5% MWC. After day 20, the calculations tend to overshoot the measured values by 1% MWC.

Figure 40 shows the impact of rain on the calculated moisture content. The moisture content increases during periods of rain, as expected. Examples of the increases are visible on day 6, 14, 16, and 17. The moisture content also increases when there is no rainfall, indicating times that the program accounts for the water addition from water

trucks. Red boxes show where the moisture content increased due to water trucks. Rainfall is shown with optimized data without the daily correction, so that all sharp increases are due to water addition and not correction to measured values.

Also visible in Figure 40 is the program accounting for runoff after a certain moisture content has been reached. The track is sealed or floated prior to rainfall, as described in section 2.1.2. Sealing the track limits the permeability of the surface. Red circles highlight points where the track became saturated, and the program ignored additional rainfall that would have increased the moisture content beyond the saturation point. Saturation is both a function of the amount of rain, and the rate of rainfall.

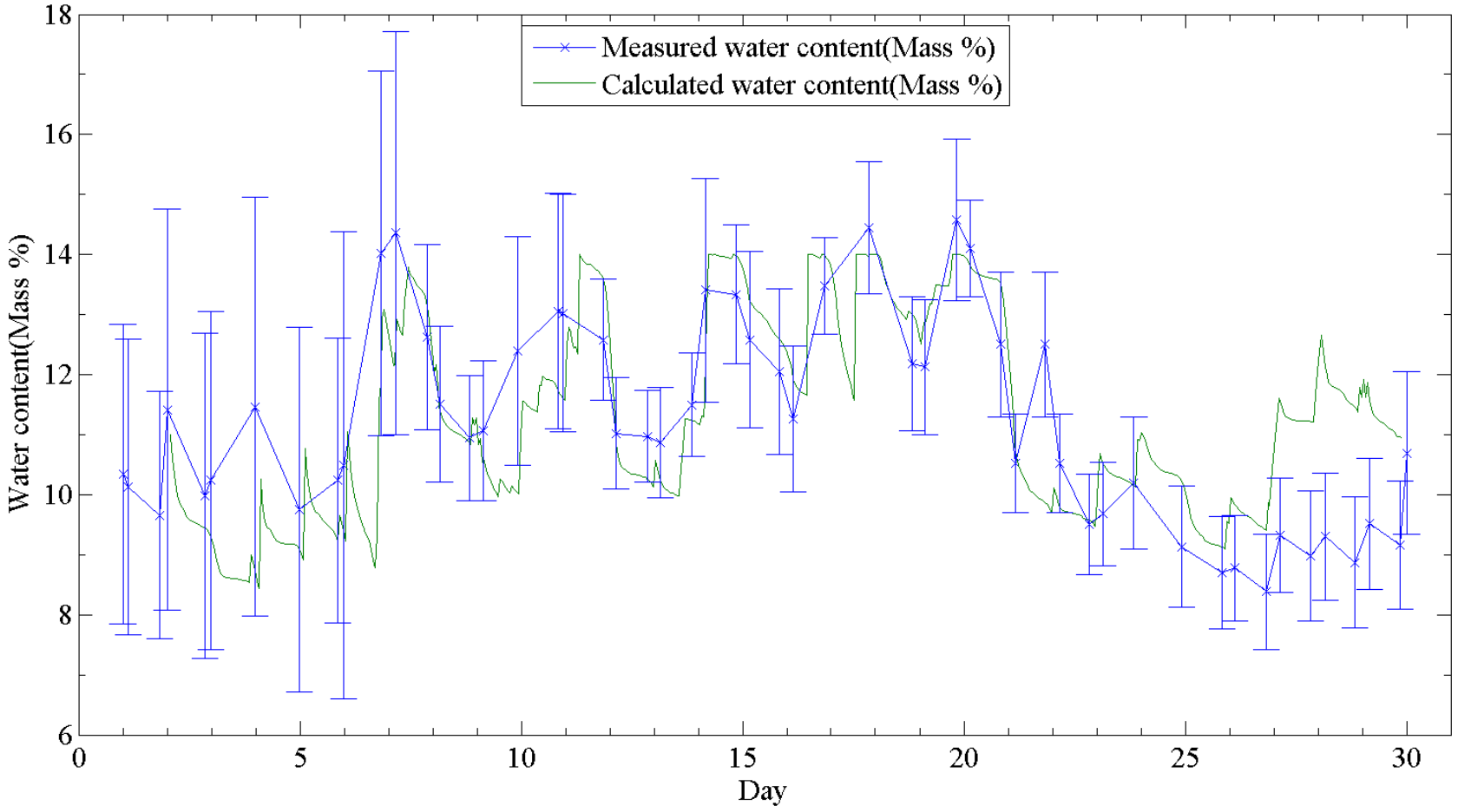

Figure 38: Keeneland calculations optimized for long data sets, with measurements

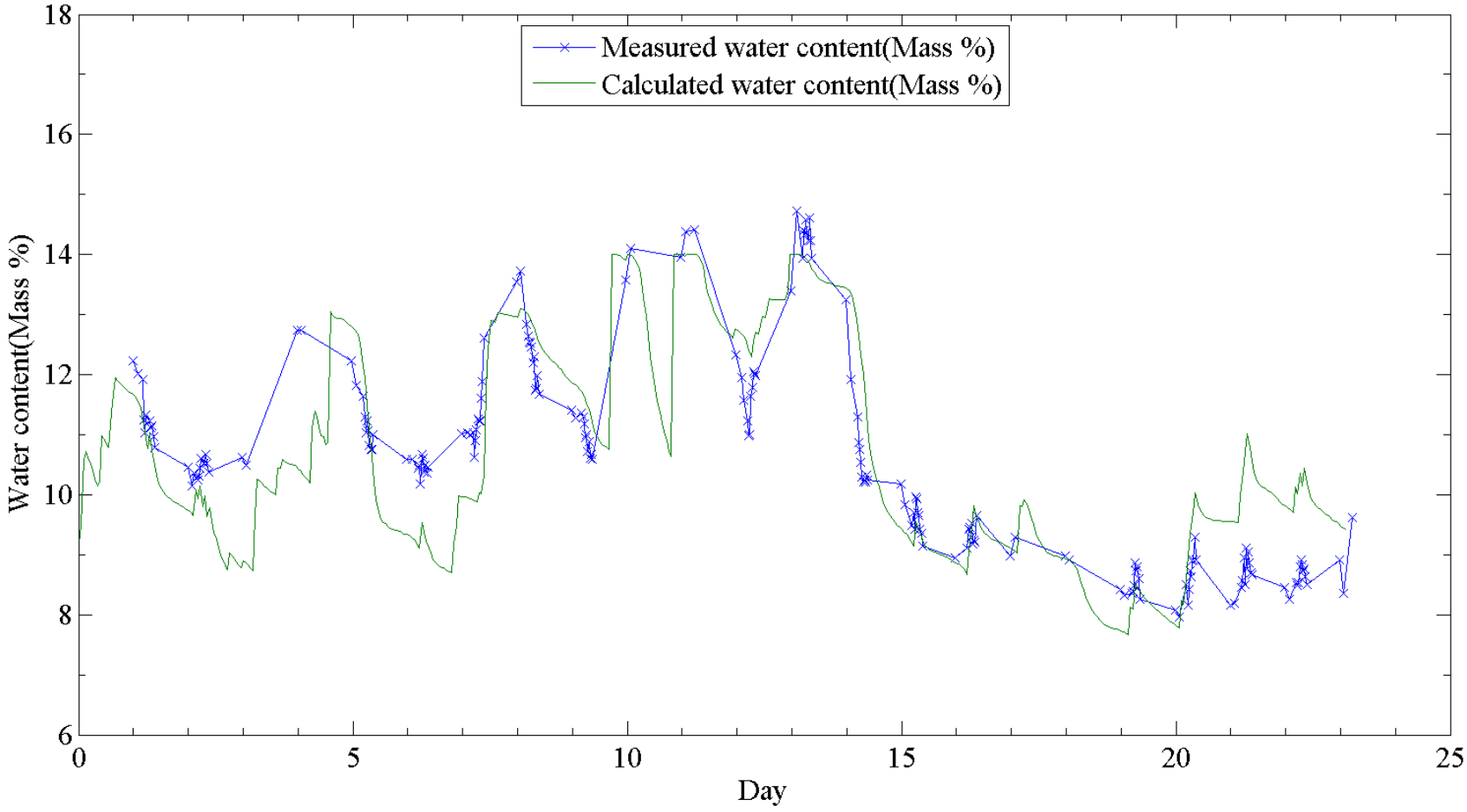

Figure 39: Keeneland optimized calculations for short data sets, with measured values.

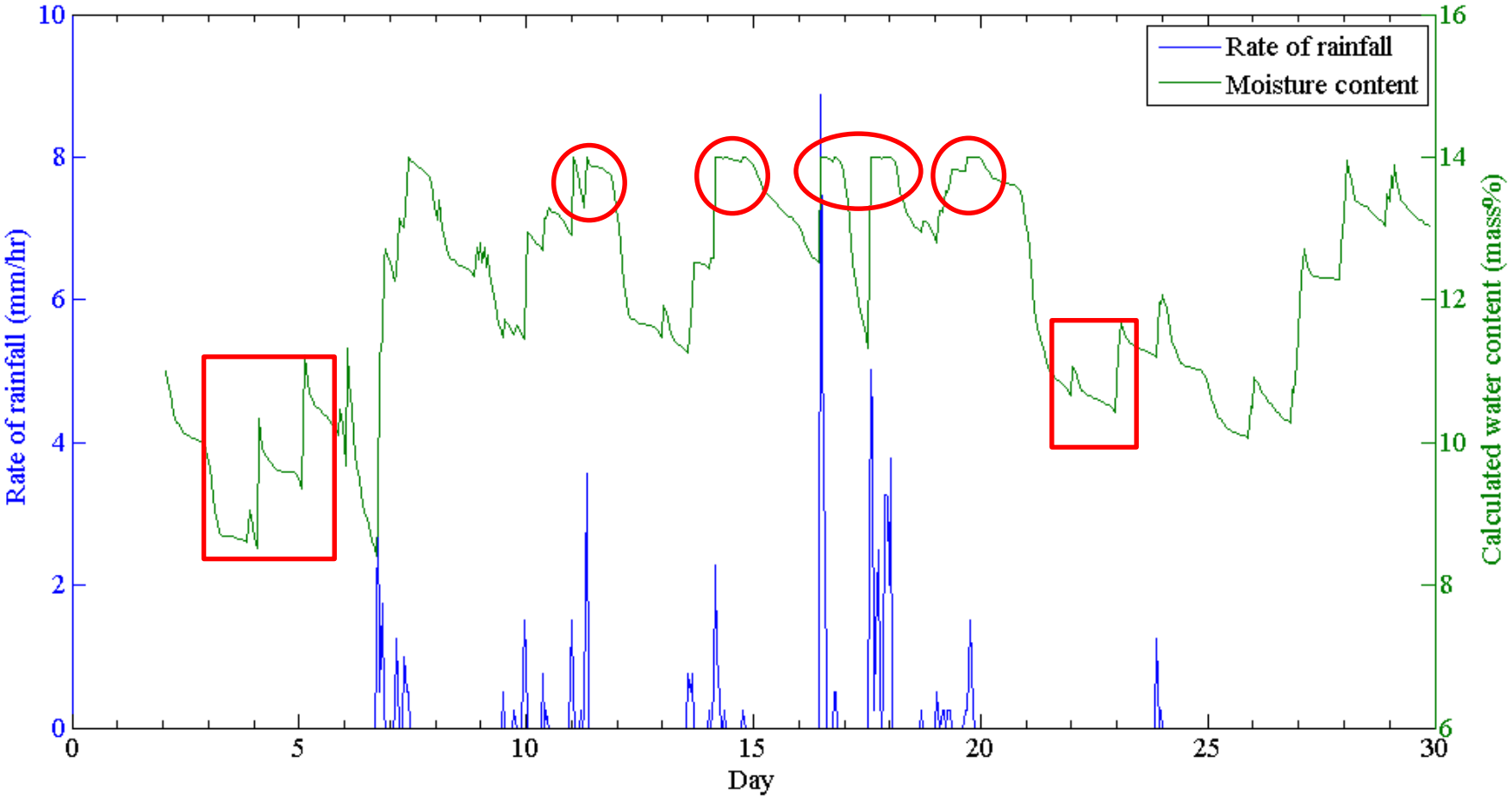

Figure 40: Calculated moisture content with rainfall at Keeneland.

3.4.3 Optimized results using daily experimental measurements

In order to further improve the accuracy of the calculated moisture content of the surface, the output of the model was corrected each day to match the measured moisture content. In practice, daily measurements of moisture are made so that the prediction only needs to be accurate over at most a 24 hour period. The daily correction prevents errors from accumulating over time.

Figure 41 shows the measured moisture content of Keeneland, with the optimized PM equation, reset to the experimental value each day. The sampling pattern is detailed in section 2.2.5. After the rain on day 10, and before the track had finished drying on day 11, the calculations overestimate the moisture content by 1.5% MWC. An example of the daily correction is visible on day 4, as the calculated value sharply drops to the measured value. Only TDR points taken before noon each day are used. Measurement for the purposes of this study were taken in the afternoon, but calculated value was not corrected for those measurements. This is the way measurements are taken at most tracks with data taken after training and before racing each day. An example of a measurement that did not cause the correction is visible on day 22. The calculations fit quite closely to the measured moisture values. Errors relating to the saturation of the track are visible on days 10 and 14. The error on day 10 is 1.5% MWC above the measured value.

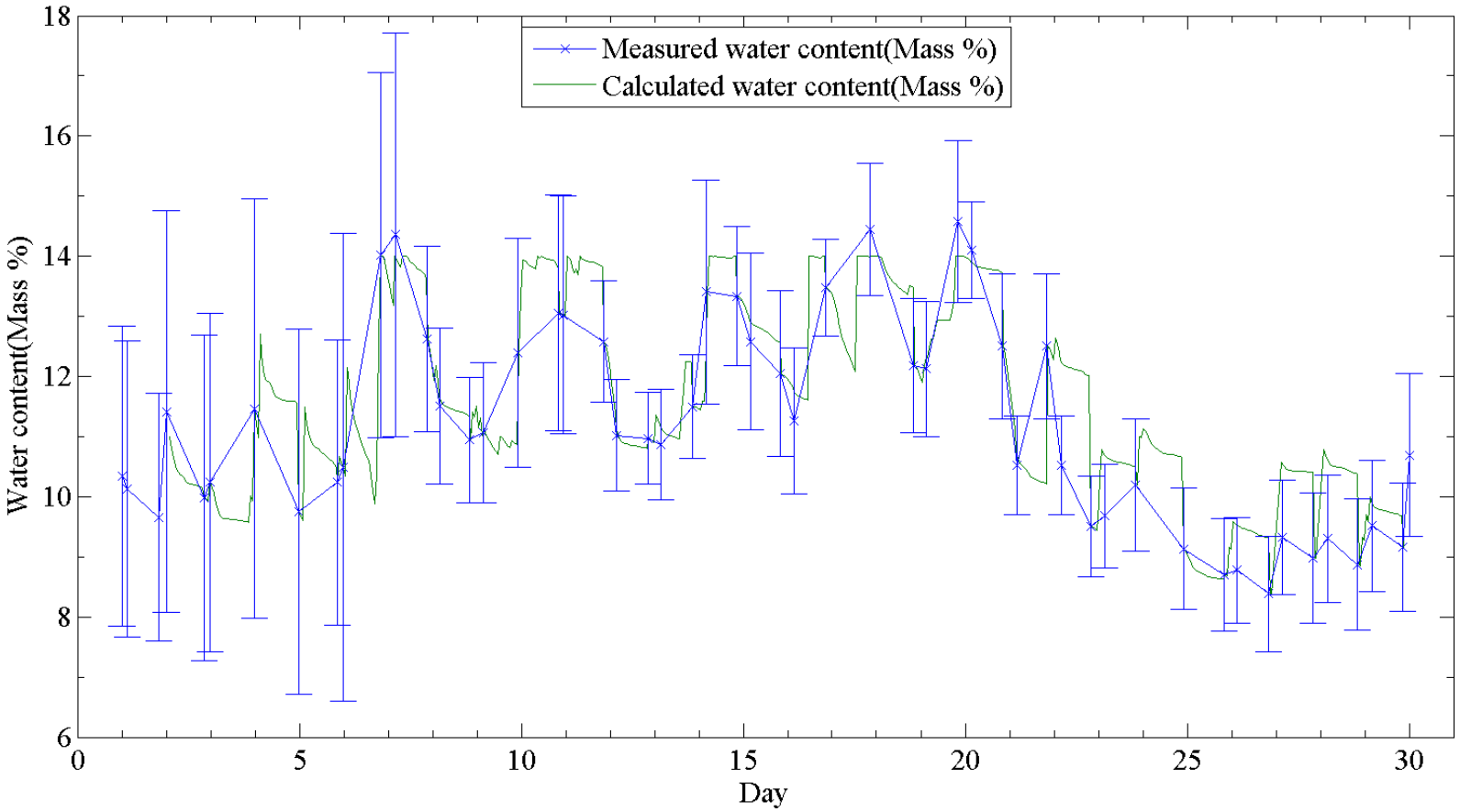

Figure 41: Optimized calculations for long Keeneland data sets with measured values, with daily resets.

Figure 42 shows the measured and calculated moisture content from the Keeneland main track during the second period of data collection. The calculations include the daily correction to the measured moisture content. The calculations follow the measurements during periods of rain, such as on day 4 or on day 21. For both of those storms, the difference between the program and the measured value was less than .5% MWC. The calculations also follow the measurements for periods of drying, such as on day 15 and on day 37. The error for both of those measurements was less than .25% MWC. On day 19, the calculations overestimated the moisture content by 1.5% MWC.

Figure 43 shows the measured and calculated moisture content of the Fair Grounds main track, including the daily correction. The sampling pattern for moisture measurements is detailed in section 2.2.5. The daily correction allow the calculations to follow the measurements, such as between day 15 and day 20, where the error is less than .5% MWC. The correction of errors in the calculation causes jumps in the calculated moisture content, when it is corrected to the measured value. A 3% MWC change caused by the difference between the program and the measured values is visible on day 39. A 5% MWC change is visible on day 48. These errors in the calculations are large compared to the other tracks.

Figure 44 shows optimized calculations from the Santa Anita main track, including daily correction, plotted with measured moisture values. On day 3, the model underestimates the moisture content by 2% MWC, and is not corrected due to the time of the measurement. Measurements taken after noon are ignored by the reset, because maintenance personnel typically only take measurements in the morning. Again, on day 5, the moisture content is underestimated by 1% MWC, and the value is reset to the

measured value. On day 6, the model also overestimates the moisture content, by 1% MWC. The underestimation is corrected to the measured value, and the subsequent 4 moisture measurements are within .2% MWC of the predicted values.

Figure 45 shows optimized results from the Saratoga main track during the first period of measurements. The calculations fit the measurements closely between day 1 and day 7. Between day 5 and day 6, the calculations underestimate the measured value by 1% MWC. After rain caused the moisture content to increase on day 7, the program overestimated the moisture content of the track. On day 9, the program overestimated the moisture content by 2% MWC. The overestimation was corrected to the measured value, which is the abrupt drop in moisture content. On day 16, the calculations underestimate the value by 3% MWC.

Figure 46 shows optimized results from the Saratoga main track during the second period of measurements. The calculations estimate an increase of the water content after the rain on day 10. The calculated value was corrected to the measured value on day 12, correcting an error of 4% MWC. On day 21, the calculations underestimated the impact of rain by 6% MWC, and the calculation is corrected to the measured value. After the track has dried out to the usual moisture content, on day 23, the program underestimates the moisture content by 1-2% MWC until day 27. From day 28 until the end of data measurement, the calculations accurately predict the moisture content in the morning, but underestimate the moisture content after racing has finished by 2% MWC.

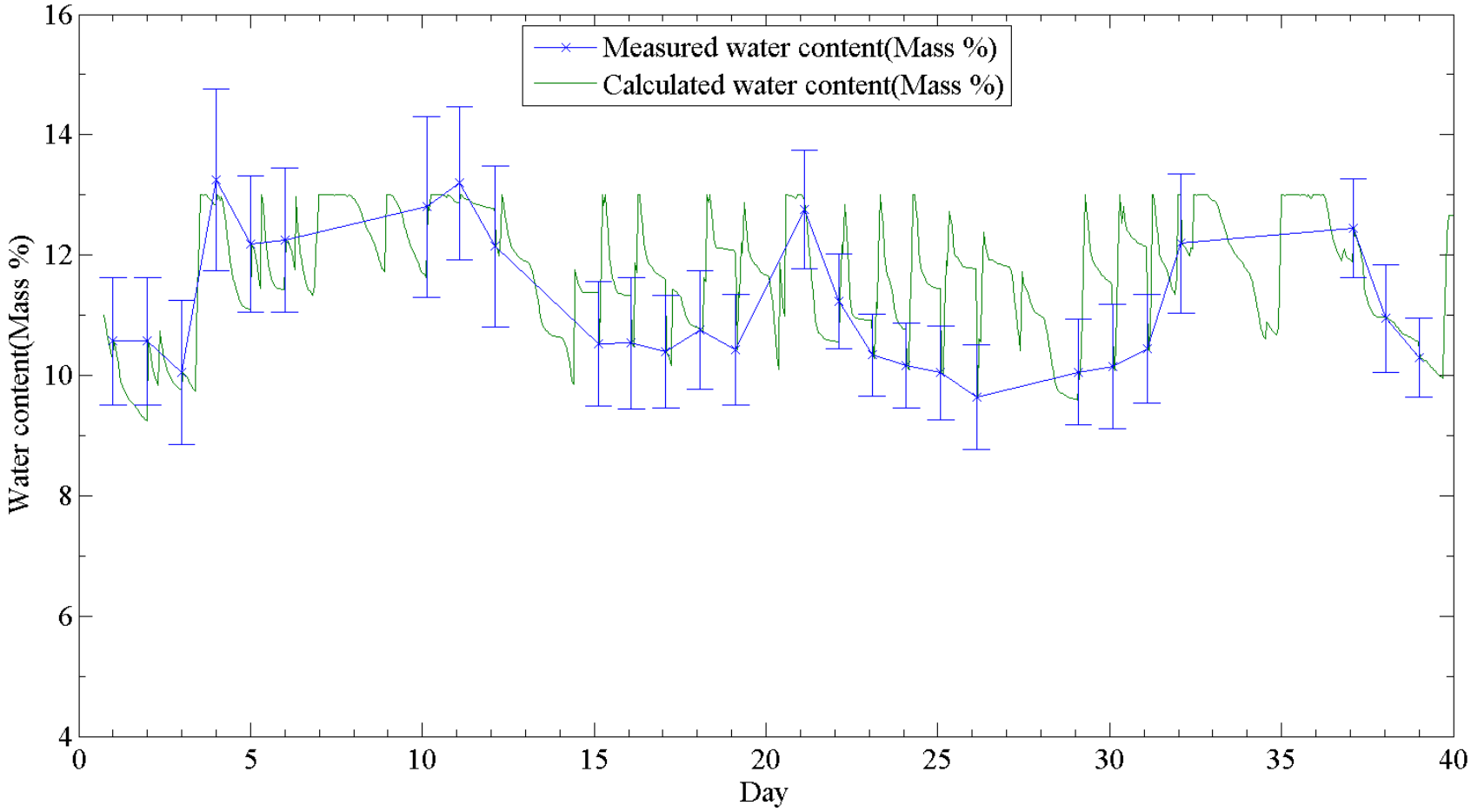

Figure 42: Optimized calculations for long Keeneland data sets from the second period of measurements. Measured values are also shown, and daily resets are used.

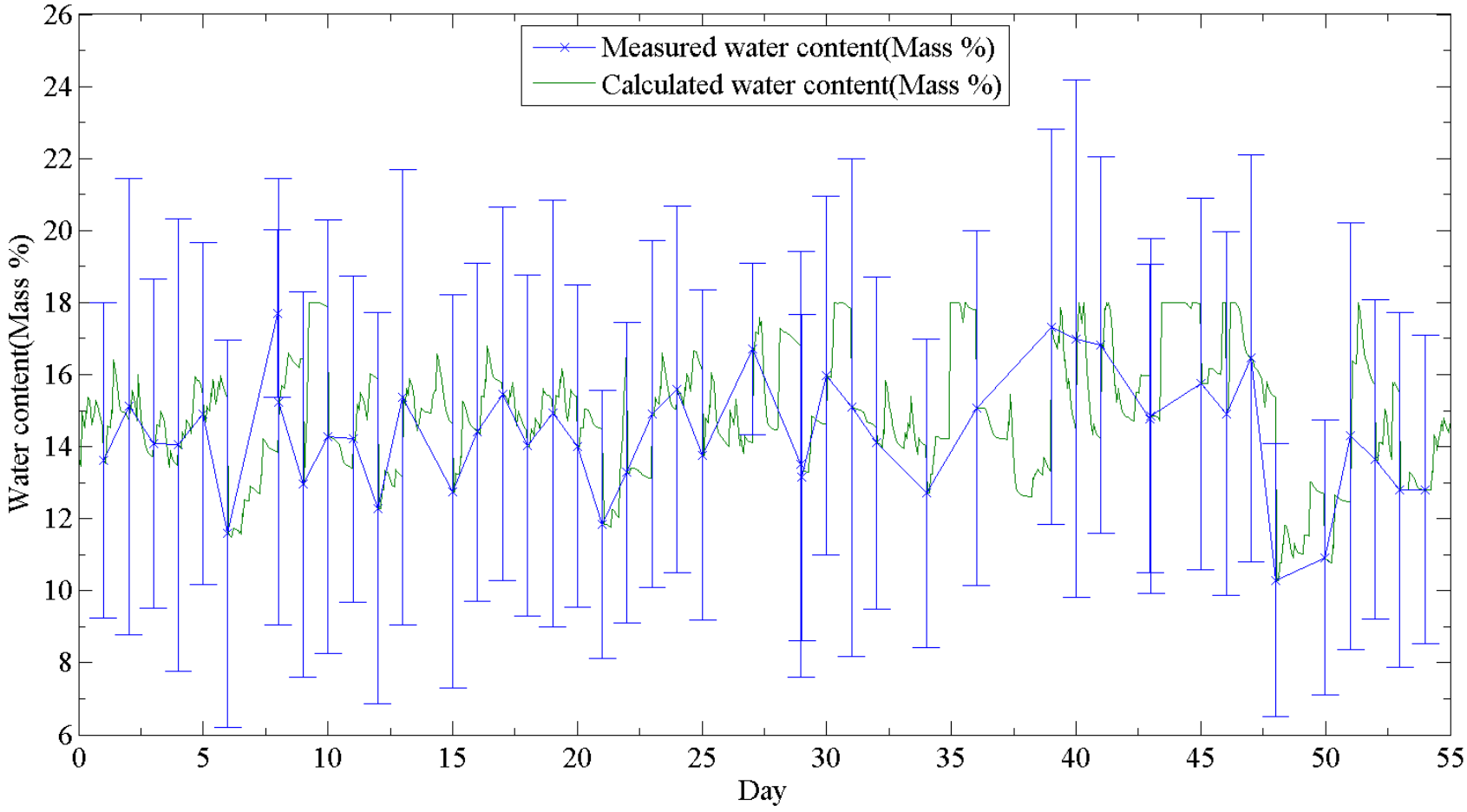

Figure 43: Optimized moisture calculations for Fair Grounds data with measured values, including daily reset.

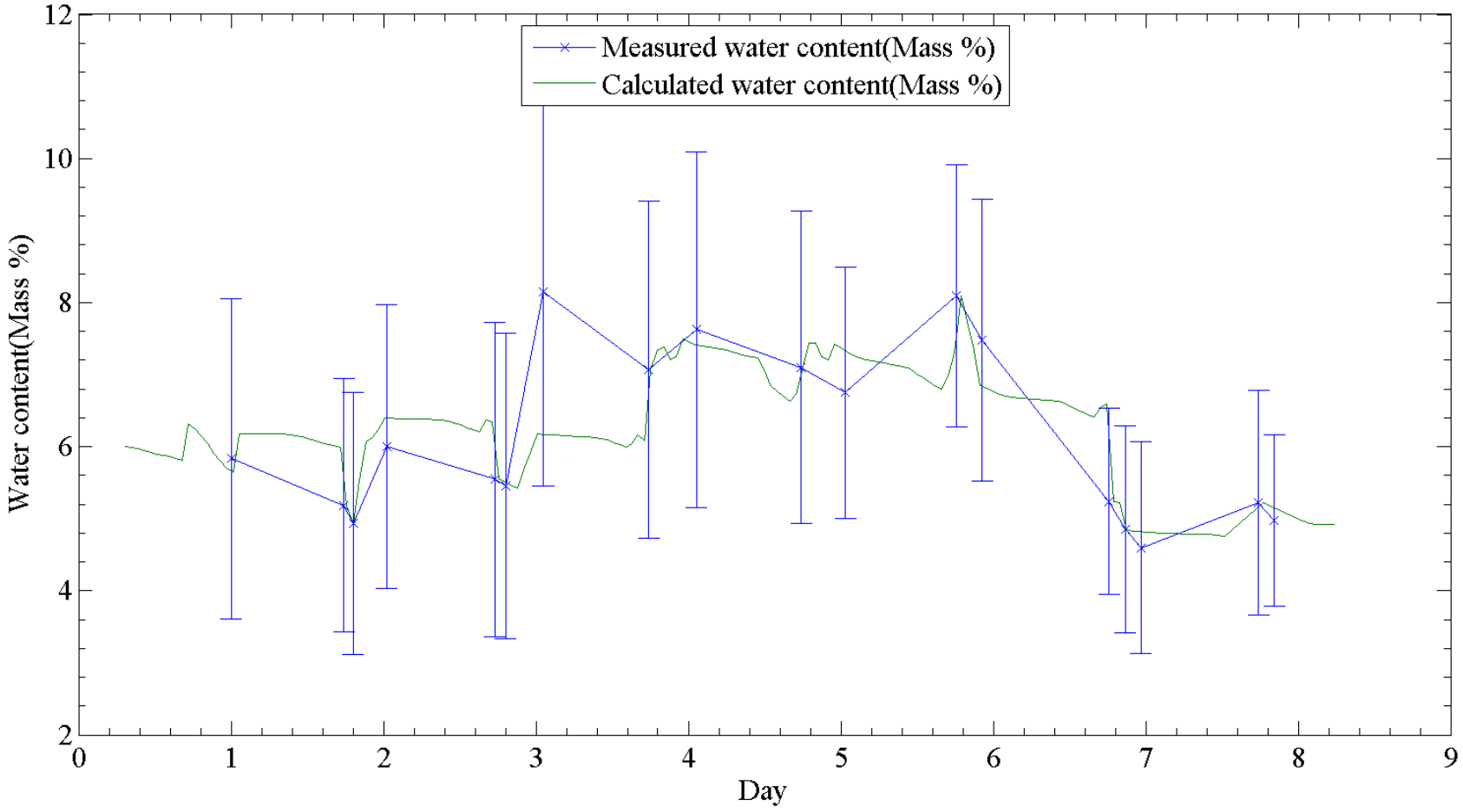

Figure 44: Optimized moisture calculations for Santa Anita long data sets with measured values, including daily resets.

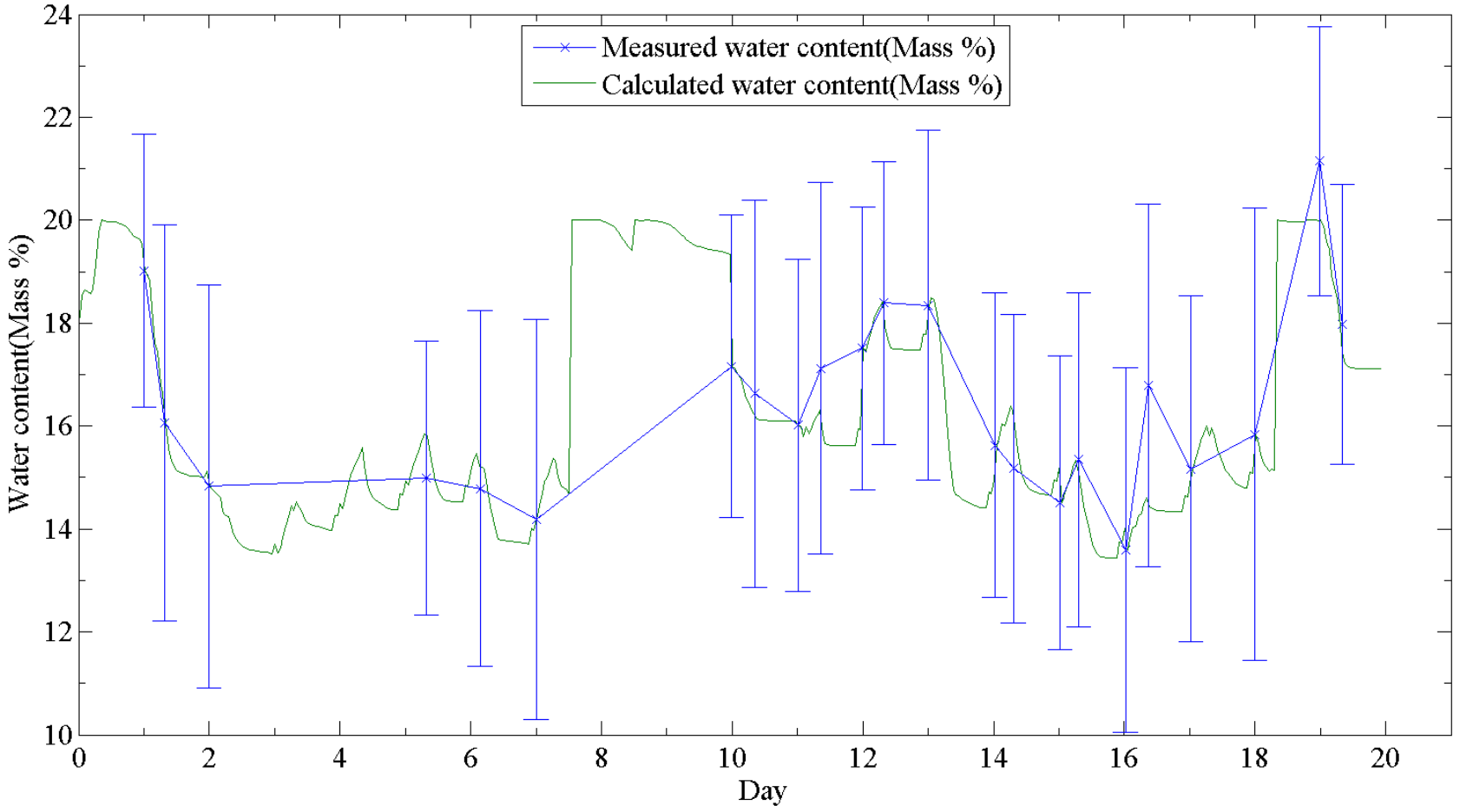

Figure 45: Optimized Saratoga long data sets from the first period of measurement plotted with measured values, including daily resets.

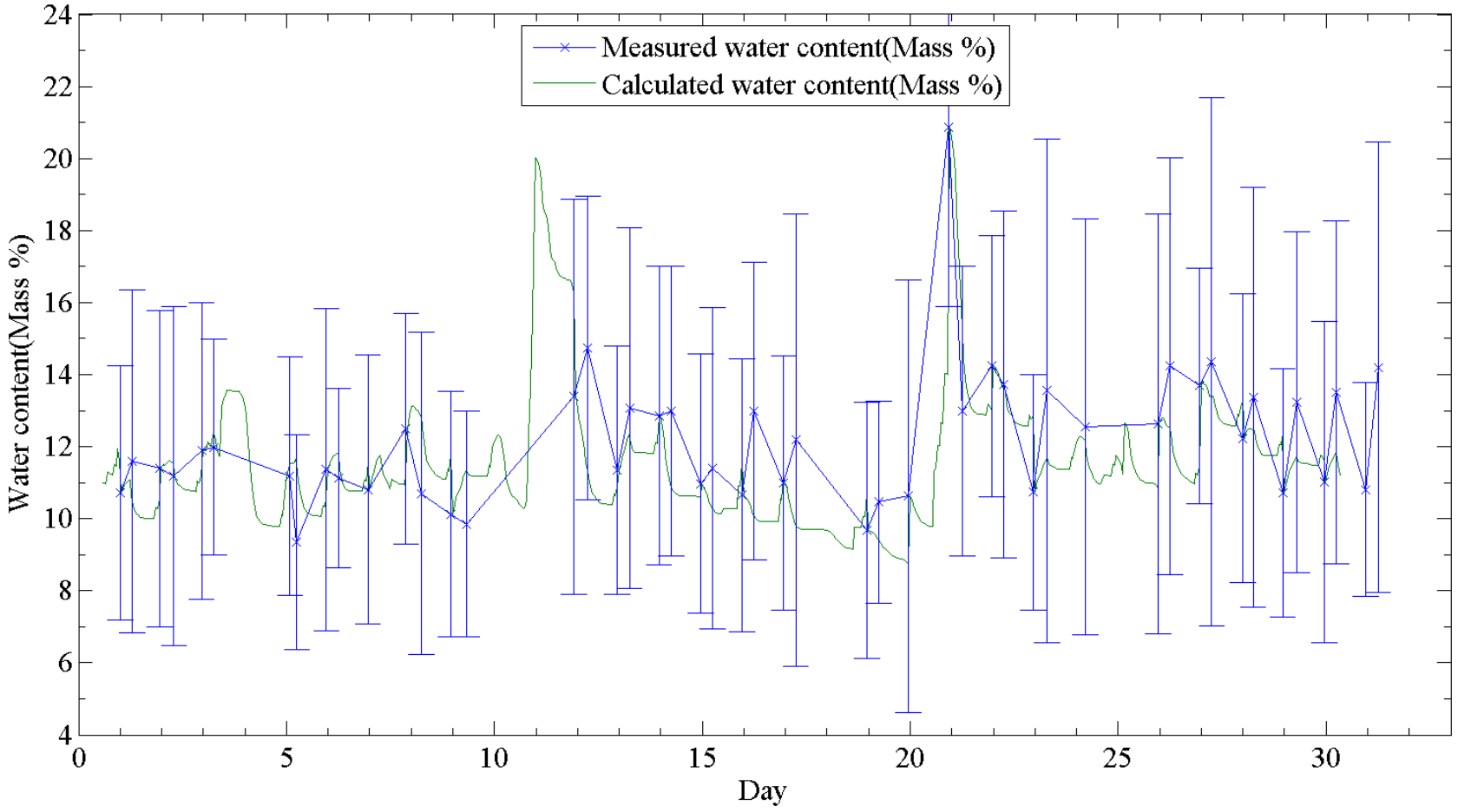

Figure 46: Optimized Saratoga long data sets from the second period of measurements plotted with measured values, including daily resets.

3.4.4 Moisture calculation error

To determine the impact of optimization and the ability of the model to predict evaporation, the mean square error was compared for model versus experiment for each level of optimization. The PM equation was first evaluated using standard coefficients from Walter et al., (2005). Goodness of fit was determined by comparing the sum of the squared differences between the measured moisture content and calculated moisture content. Table 4 shows the sum of the least squared differences for the six sets used. The 'long' sets of data, which were all the way around the tracks, were taken twice a day with between 144 and 162 points each in a pattern shown in section 2.2.5. The 'short' runs of 9 points each which were taken as described in section 2.2.5 were separately evaluated. The average least squares difference is given for the optimized data, as a way of quantifying how closely any given point on the calculated moisture curve is to the measured moisture content. The average difference per point is given because the sum increases with additional points, while each additional point may fit as closely as the others. The table also shows the improvement in fit from optimization.

Table 4: Goodness of fit of data to measured moisture content without daily reset. Saratoga and Keeneland 1 and 2 refer to data collected in 2014 and 2015 respectively.

Track	Run	# of sets	Un-optimized least squares difference	Optimized least squares difference	Average least squares difference per-point	Per-point improvement with optimization
Saratoga 1	Long	21	92.0	20.0	0.95	3.43
	Short	120	309.0	180.5	1.50	1.07
Saratoga 2	Long	49	411.7	135.5	2.77	5.64
Santa Anita	Long	18	14.5	9.5	0.53	0.28
	Short	45	45.2	26.0	0.58	0.43
Keeneland 1	Long	50	92.8	60.9	1.22	0.64
	Short	200	276.5	84.0	0.42	0.96
Keeneland 2	Long	27	72.6	16.2	0.60	2.09
Fair Grounds	Long	62	511.6	201.9	3.26	5.00

In all cases, the optimization improves the per-point fit at each track, both with and without use of daily experimental data to correct the model. The optimization of the model decreases the RMS error to 1.5% MWC or less for all but two data sets.

In the second case, the coefficients of the PM equation (X_1, X_2, X_3, and X4) in equations 14 and 15 are optimized by the Nelder-Mead optimization method. Although the coefficients are each optimized to the same type of data, the values are different for each track. The X_2 and X_3 coefficients, used in equation 15, are changed based on track surface conditions. The coefficients X_1 and X_4 are the coefficients used in equation 14 to account for the change in evaporation rate caused by changes in moisture content. The values of the coefficients are shown in

Table 5 and Table 6.

Table 5: Coefficients for PM equation from optimization. Saratoga and Keeneland 1 and 2 refer to data collected in 2014 and 2015 respectively.

Track	X_1	X_2	X_3	X_4
Saratoga 1	8.11	0.05	0.69	3.19
Saratoga 1 Short	12.04	0.10	0.05	10.00
Santa Anita	0.00	0.79	0.05	1.03
Santa Anita Short	0.00	5.00	0.25	1.75
Keeneland 1	7.52	1.37	0.38	10.00
Keeneland 1 Short	4.28	1.58	1.05	10.00
Fair Grounds	12.63	0.05	0.05	10.00
Saratoga 2	10.17	0.27	0.55	10.00
Keeneland 2	9.02	0.72	0.51	10.00

Table 6: Coefficients for PM equation from optimization with reset. Saratoga and Keeneland 1 and 2 refer to data collected in 2014 and 2015 respectively.

Track	X_1	X_2	X_3	X_4
Saratoga 1	0.01	0.05	1.13	1.66
Saratoga 1 Short	11.80	0.05	0.05	10.00
Santa Anita	5.09	5.00	0.05	4.82
Santa Anita Short	0.00	5.00	0.05	2.22
Keeneland 1	7.42	0.73	0.05	3.39
Keeneland 1 Short	0.31	5.00	2.84	10.00
Fair Grounds	12.53	1.08	0.05	10.00
Saratoga 2	9.68	0.24	0.53	10.00
Keeneland 2	9.06	0.33	1.17	10.00

The daily correction further increases the accuracy of the calculations for five of the tracks. Four of the tracks had the accuracy of the calculations decreased, but overall the correction improves the fit of the calculations. Calculations for long data sets from Keeneland during the first period of data collection showed the largest improvement.

Table 7: Table showing goodness of fit with daily reset.

Track	Run	# of sets	Un-optimized least squares difference	Optimized least squares difference	Average least squares difference per-point	Per-point improvement with optimization	Per point improvement with reset
Saratoga 1	Long	21	54.0	20.4	0.97	1.60	-0.02
	Short	120	216.5	144.2	1.20	0.60	0.30
Saratoga 2	Long	49	243.7	150.3	3.07	1.91	-0.30
Santa Anita	Long	18	12.2	11.1	0.62	0.06	-0.09
	Short	45	30.8	19.4	0.43	0.25	0.15
Keeneland 1	Long	50	50.6	32.3	0.65	0.37	0.57
	Short	200	25.6	24.9	0.12	0.00	0.30
Keeneland 2	Long	27	36.1	11.6	0.43	0.91	0.17
Fair Grounds	long	62	346.8	227.7	3.67	1.92	-0.42

4. DISCUSSION AND CONCLUSIONS

The modified PM equation was found to match measured moisture content well at most tracks across several different climates. The PM equation depends on data from weather stations, maintenance personnel, and track moisture measurements. The magnitude of the impact of data from each of the sources on the program output is discussed. The results of the various optimization methods are also discussed.

4.1 Data Collection Discussion

Each of the three sources of data for the PM equation are important to its accurate operation. Weather data is used to determine the rate of evaporation, and the addition of water from rainfall. Maintenance data includes track condition, whether the track is 'open' or 'sealed', as well as water addition from water trucks. TDR measurements were used to optimize and validate the modifications to the PM equation. When the program is implemented at tracks, TDR measurements will serve to reset the calculation whenever they are available.

The energy balance term of the PM equation, equation 2, depends on both solar radiation and ground flux. The value of ground flux calculated from solar radiation does not compare well to direct measurements of ground flux from a flux plate. That poor fit is outweighed by the small magnitude of ground flux compared to solar radiation in the energy balance (Allen et al., 1998). The negative energy balance values at night contribute to dew formation, which is not significant when compared to the other sources of water for the track, such as rain or water trucks. The cost of flux plates or other direct flux measuring techniques, detailed in Appendix J, are on the order of $700 per installation. The solar radiation sensor is already required for the program, and the

calculation of ground flux from solar radiation does not add any cost to the setup. The small impact of the inaccuracy from estimating ground flux does not justify the increase in cost of weather stations.

Maintenance impacts track moisture content both directly with water trucks, and indirectly by changing the surface condition with plates and harrows.

Table 3 shows how Santa Anita, which did not have any rain, spent the highest percentage of the time harrowed, while the other tracks were sealed more.

Variance of TDR measurements could be caused by inconsistency on the track, or measurement error. Some portions of the track could have a higher moisture content due to uneven shadows or clogged drainage on those parts of the track. Dryer parts of the track could have more direct sunlight, or might be missed when the water trucks apply water to the track. Spatial variations in moisture content are outside the scope of this research.

4.2 Program Discussion

The modified PM calculates evaporation from the race track based on weather and track surface condition. Modifications include a moisture content cut-off to simulate track saturation and runoff, as well as a dependence on the current moisture content. The program was also optimized to improve the fit of the output to measured data.

Un-optimized results are shown to demonstrate how much optimization improves the fit of the data. Even when the un-optimized results are reasonably close to the measured data, optimization still improves the fit, as seen in Table 4. After using the

Nelder-Mead optimization method, the calculated moisture content correlated well with the moisture content measured by the TDR probe, as can be seen in Figure 38.

The reset improves results from large sets, and decreases accuracy of results from smaller sets. In the case of tracks with fewer data sets, with fewer than 50 sets, the daily reset tends to have a negative impact on the fit. The larger sets all tend to be improved by the reset. The improvement is likely because the reset decreases the amount of time that it is required to optimize over. More work is required to determine why the reset negatively impacts the performance of the model on some data sets.

The relationship between moisture content and rainfall is shown in Figure 40. The figure shows that the moisture content is increased by both water trucks and rainfall. Due to the impact of water trucks, improved measurements of water application would likely improve the accuracy of the calculations. Additionally, it is possible that improving the way the calculations account for runoff and percolation would improve the response of the calculations to rain that saturates or nearly saturates the track.

The error on day 10 of Figure 41 could be caused in part by inaccurate measurement time entered with the TDR data. The measurement was taken during a rainstorm, and increased the moisture content due to the correction. The moisture content continued to increase immediately after the measurement due to rain, so subsequent calculations were above the measured values. If the measurement had been recorded after the rain had finished, the reset would not have further increased the moisture content, and the subsequent measurements may have been more accurate. A data logger with a timestamp would remove that as a potential problem.

Overall, the moisture content calculated by the model agrees well with the measured moisture content from the TDR probe. Modeling the saturation and subsequent runoff from the track is essential to accurate modelling, otherwise the models calculations would be artificially elevated after a heavy rain. It is also important that the model parameters be optimized separately for each track. Separate optimization is needed because each track has different particle size distributions and different pieces of maintenance equipment. Those differences cause different evaporation rates under different conditions. That is shown by the different coefficients for each track that the optimization produces.

BIBLIOGRAPHY

Allen, R. G., Pereira, L. S., Raes, D., & Smith, M. (1998). Crop evapotranspiration: guidelines fo computing crop water requirements. Irrigation and Drainage Paper 56., 300.

Al-Shayea, N. a. (2001). The combined effect of clay and moisture content on the behavior of remolded unsaturated soils. *Engineering Geology*, *62*(4), 319–342. http://doi.org/10.1016/S0013-7952(01)00032-1

ASTM. (2004). Standard Test Method for Consolidated Undrained Triaxial Compression Test for. *Annual Book of ASTM Standards*, *i*.

ASTM. (2007). Standard Test Methods for Laboratory Compaction Characteristics of Soil Using Standard Effort (12 400 ft-lbf / ft 3 (600 kN-m / m 3)) 1, *3*, 1–13. http://doi.org/10.1520/D0698-12E01.1.3.1

Deloitte Consulting for the American Horse council. (2005). The economic impact of the horse industry in the United States. *The Blood Horse*, 3717.

Evett, S. R. (2007). Soil Water and Monitoring Technology, (30).

Feng, D., Zhang, J., Cao, C., Sun, J., Shao, L., Li, F., … Sun, C. (2014). Soil Salt Accumulation and Crop Yield under Long-Term Irrigation with Saline Water, (2001), 1–7. http://doi.org/10.1061/(ASCE)IR.1943-4774.0000924.

Grubbs, F. . (1969). Profedures for detecting outlying observations in samples. *Technometrics*, *11*(2), 1–21.

Haine, W. (1930). Studies in the physical properties of soil. V. The hysteresis effect in capillary properties, and the modes of moisture distribution associated therewith. *Journal of Acricultural Science*, *20*(1), 97–116.

Hayler, W. (2011). Lingfield Park to act after jockeys warn of danger from kickback. Retrieved October 25, 2015, from http://www.theguardian.com/sport/2011/oct/27/lingfield-jockeys-kickback

Hitchens, P. L., Hill, a. E., & Stover, S. M. (2013). Jockey Falls, Injuries, and Fatalities Associated With Thoroughbred and Quarter Horse Racing in California, 2007-2011. *Orthopaedic Journal of Sports Medicine*, *1*(1), 2007–2011. http://doi.org/10.1177/2325967113492625

Jasechko, S., Sharp, Z. D., Gibson, J. J., Birks, S. J., Yi, Y., & Fawcett, P. J. (2013). Terrestrial water fluxes dominated by transpiration. *Nature*, *496*(7445), 347–350. Retrieved from http://dx.doi.org/10.1038/nature11983

Jocky Club. (n.d.). Equine injury database. Retrieved October 25, 2015, from http://www.jockeyclub.com/default.asp?section=Advocacy&area=10

Kindle, E. M. (1936). Dominant Factor sin the formation of firm and soft sand beaches. *Journal of Sedimentary Petrology*, *6*(1), 16–22.

Mahaffey, C. A. (2012). Surface Variable Effects on the Dynamic Properties of Thoroughbred Horse Racetracks.

Mahaffey, C. A., Peterson, M. L., & McIlwraith, C. W. (2012). archetypes in thoroughbred dirt racetracks regarding track design, clay mineralogy, and climate. *Sports Engineering*, *15*(1), 21–27.

Mahaffey, C. A., Peterson, M. L., & Roepstorff, L. (2013). the effects of varying cushion depth on dynamic loading in shallow sand thoroughbred horse dirt racetracks. *Biosystems Engineering*, *114*(2), 178–186.

Mohammed, H. O., Hill, T., & Lowe, J. (1991). Risk factors associated with injuties in thoroughbred horses. *Equine Veterinary Journal*, *23*(6), 445–448.

National Thoroughbred Racing Asociation. (n.d.). Safety Alliance. Retrieved October 25, 2015, from http://www.ntra.com/en/safety-alliance/

Palmer, L. A., Barber, E. S., & Krynine, D. (1937). Principles of soil mechanics involved in fill constructions. In *proceedings of the seventeenth annual meeting of the highway research board*. Washington D.C.

Peterson, M. L., & McIlwraith, C. W. (2008). Effect of track maintenance on mechanical properties of a dirt racetrack: a preliminary study. *Equine Veterinary Journal*, *40*(6), 602–605. http://doi.org/10.2746/042516408X330347

Peterson, M. L., Reiser, R. F., Kou, P.-H., Radford, D., & McIlwraith, W. C. (2010). The effect of temperature on 6 furlong times on a synthetic racing surface. *Equine Veterinary Journal*, *42*(4), 351–357.

Peterson, M. L., Roepstorff, L., Thomason, J., Mahaffey, C., & McIlwraith, C. W. (2011). Racing Surfaces White Paper.

Pricci, J. (2013). Track Bias unfair to horses, horsemen and bettors alike. Retrieved October 25, 2015, from http://www.horseraceinsider.com/John-Pricci/comments/11052013-track-bias-unfair-to-horses-horsemen-and-bettors-alike/

Ratzlaff, M. H., Hyde, M. L., Hutton, D. V., Rathgeber, R. a., & Balch, O. K. (1997). Interrelationships between moisture content of the track, dynamic properties of the track and the locomotor forces exerted by galloping horses. *Journal of Equine Veterinary Science*, *17*(1), 35–42. http://doi.org/10.1016/S0737-0806(97)80456-X

Walter, I. A., Allen, R. G., Elliott, R., Itenfisu, D., Brown, P., Jensen, M. E., … Wright, J. L. (2005). THE ASCE STANDARDIZED REFERENCE Task Committee on Standardization of Reference Evapotranspiration.

Welsh, C. E., Lewis, T. W., Blott, S. C., Mellor, D. J., Lam, K. H., Stewart, B. D., & Parkin, T. D. H. (2013). Preliminary genetic analyses of important musculoskeletal conditions of Thoroughbred racehorses in Hong Kong. *Veterinary Journal*, *198*(3), 611–615. http://doi.org/10.1016/j.tvjl.2013.05.002

Yamanaka, T., & Yonetani, T. (1999). Dynamics of the evaporation zone in dry sandy soils. *Journal of Hydrology*, *217*(1-2), 135–148. http://doi.org/10.1016/S0022-1694(99)00021-9

Zhang, B., Zhao, Q. G., Horn, R., & Baumgartl, T. (2001). Shear strength of surface soil as affected by soil bulk density and soil water content. *Soil and Tillage Research*, *59*(3-4), 97–106. http://doi.org/10.1016/S0167-1987(01)00163-5

APPENDICES

APPENDIX A CALCULATION OF MASS% FROM VWC

It is necessary to convert from the VWC given by the TDR probe to mass percent (Evett, 2007). The conversion calculates m_p, the mass percent of the water in the soil, with

$$m_P = \theta\left(\frac{\rho_w}{\rho_b}\right) \qquad 16$$

where θ is the volumetric % of the water in the soil, ρ_w is the density of water in the soil, and ρ_b is the bulk density of the soil.

Table 8: Shows bulk density for each track, as well as the conversion factor to calculate mass percent water content from volumetric water content.

Track	Keeneland	Saratoga	Fair Grounds	Santa Anita
Peak Bulk Density(kg/m^3)	1762	1923	1808	1854
Conversion Factor	0.567	0.519	0.552	0.538

It is also important to convert from mm of water to mass percentage, for which the conversion factor is the ratio of the heights of water to dirt multiplied by the ratio of the density of water to dirt. The conversion calculates m_p with

$$m_P = H\left(\frac{1}{H_d}\right)\left(\frac{\rho_w}{\rho_b}\right) * 100 \qquad 17$$

where H is the height of the water in the track in mm, and H_d is the height of the track material in mm. The factor of 100 is included so that the result is a percentage.

Table 9: Shows the conversion factor to calculate mass percent water content from water height. Units are mm^{-1}.

Track	Keeneland	Saratoga	Fair Grounds	Santa Anita
Conversion Factor	0.638	0.511	0.544	0.531

APPENDIX B EVAPORATION PROGRAM

Matlab Code for evaporation program

```
clc
clear all;
close all

tr={'SAR','SAR','SA','SA','KEE','KEE','FG','SAR2','KEE2'};
ru={'long','short','long','short','long','short','long','long','long'};

for q=1:length(tr) %loop through everything to generate all the graphs q=1:1%
    fclose('all');

    track=tr{q}; %'KEE'; %       %KEE, SAR, SA, FG, SAR2, and KEE2 work.
    run=ru{q}; %'long'; %       %Use 'long' full data sets or 'short' for
    %3x3 sets. Fair Grounds only has long data sets

    %This script takes weather inputs and calculates evaporation

    %Deals with TDR data
    [n,basename]=TDR_Vacuum(track,run);           %Pulls tdr data into matlab
    nav=transpose(mean(n));  %Averages the tdr data from each set
    err=transpose(std(n));
    if strcmp(track,'FG')       %FG data is formatted differerntly
        basename(:,1:12)=[];
        basename(:,15:end)=[];
        tdate=datenum(basename,'yyyymmdd_HHMMSS');  %Puts dates into date
numbers
    elseif strcmp(track,'KEE2')||strcmp(track,'SAR2')
        tdate=datenum(basename,'mm/dd/yyyy HH:MM:SS AM');
        basename=datestr(tdate,'mm_dd_yy_HHMM');
    elseif strcmp(track,'SAR')&&strcmp(run,'long')
        basename(:,15:end)=[];
        tdate=datenum(basename,'mm_dd_yy_HHMM');  %Puts dates into date numbers
    else
        basename(:,16:end)=[];
        tdate=datenum(basename,'mm_dd_yy_HHMM');  %Puts dates into date numbers
    end

    %Deals with weather data
    [wdate,avgweather]=Weather_Vacuum(track); %Pulls weather data into matlab
    if strcmp(track,'KEE')||strcmp(track,'SAR')||strcmp(track,'KEE2')...
            ||strcmp(track,'SAR2')
        wdate=flipud(wdate);                      %Reorients data
        avgweather=flipud(avgweather);
    elseif strcmp(track,'SA')||strcmp(track,'FG')%||strcmp(track,'KEE2')
        %Data does not need to be reoriented
    end
    wnum=datenum(wdate,'mm/dd/yyyy HH:MM');   %Puts dates into date numbers

    %Calculates some variables from weather data
    [delta,e_s,e_a,T,U,R_s]=TRH(avgweather);
```

```
    %Calculates net radiation from short wave radiation and weather/date/time
    R_n=Rad(R_s,wdate,e_a,avgweather(:,3),track);

    %Ground flux calculation
    G=Gflux(track,avgweather,R_n);

    %Gets track condition information from file
    [gstatus]=Maint(track,wnum);

    %Creates new figure for optimized graph and prints a label for diff
    track
    run
    optimizer
end


%Tidy up for looping
clear diff totwater E

%This script puts the moisture data into a more useful form, converts all
%data to be in mass% from whatever units it had been in, and optimizes the
%coefficents of the evaporation equation, both with and without the reset.

%Sort tdr data into the same hourly scale as the evaporation data
tdrdat=horzcat(tdate,nav);
tdr=zeros(size(wnum));

%Constant:
lambda=2.45;     %Latent heat of vaporization

%trim out the less usefull parts of maintenance info
tstatus=gstatus;
tstatus(:,1)=[];
tstatus(tstatus(:,1)==0,1)=1;

%Differnet tracks have different sized water trucks. Convert from number of
%times water trucks were used to mm of water added to track
if strcmp(track,'KEE')||strcmp(track,'KEE2')
    tstatus(:,2)=tstatus(:,2)*.7717;
elseif strcmp(track,'SAR')||strcmp(track,'SAR2')
    tstatus(:,2)=tstatus(:,2)*.6173;
elseif strcmp(track,'FG')
    tstatus(:,2)=tstatus(:,2)*.9646;
elseif strcmp(track,'SA')
    tstatus(:,2)=tstatus(:,2)*.6752;
end

%Gross holds the total added water for the period
gross_raw=tstatus(:,2)+avgweather(:,2);

%Converts to mass% of water per unit area.  Rainfall and water truck
%watering is measured in mm, we need mass%
if strcmp(track,'KEE')||strcmp(track,'KEE2')
```

```
    gross=gross_raw*.638;
elseif strcmp(track,'SAR')||strcmp(track,'SAR2')
    gross=gross_raw*.511;
elseif strcmp(track,'FG')
    gross=gross_raw*.544;
elseif strcmp(track,'SA')
    gross=gross_raw*.531;
end

%Pads TDR data with zeros so that it can be compared to totwater
for i=1:length(wnum)-1
    count=0;
    for j=1:length(tdrdat)
        if tdrdat(j,1)>=wnum(i)&&tdrdat(j,1)<wnum(i+1)
            tdr(i,1)=nav(j)+tdr(i,1);
            count=count+1;
        end
    end
    tdr(i,1)=tdr(i,1)/count;
end

tdr_time=datestr(wnum); %look at time of TDR data to decide if you reset
tdr_time(:,[1:12,15:end])=[];

%Converts to mass% of water to soil from VWC% (TDR)
if strcmp(track,'KEE')||strcmp(track,'KEE2')
    tdr=tdr*.567;
    navv=nav*.567;
elseif strcmp(track,'SAR')||strcmp(track,'SAR2')
    tdr=tdr*.519;
    navv=nav*.519;
elseif strcmp(track,'FG')
    tdr=tdr*.552;
    navv=nav*.552;
elseif strcmp(track,'SA')
    tdr=tdr*.538;
    navv=nav*.538;
end

%Initial guess with variables from stock
x=[5,.37,.37,3];

%Unoptimized calculations(No Reset)
[diff(1),totwater(:,1),E(:,1)]=...
    waterO(x,delta,R_n,G,lambda,T,U,e_s,e_a,tdr,track,gross,tstatus,0,tdr_time);

%Optimization(No Reset)
x=fminsearch(@waterO,x,[]...
    ,delta,R_n,G,lambda,T,U,e_s,e_a,tdr,track,gross,tstatus,0,tdr_time);

%Optimized calculations(No Reset)
[diff(2),totwater(:,2),E(:,2)]=...
    waterO(x,delta,R_n,G,lambda,T,U,e_s,e_a,tdr,track,gross,tstatus,0,tdr_time);
fprintf('No Reset \n');
x
```

```
diff %#ok<*NOPTS>


%Reset initial guess
x=[5,.37,.37,3];

%Unoptimized calculations(With Reset)
[diff(3),totwater(:,3),E(:,3)]=...
    waterO(x,delta,R_n,G,lambda,T,U,e_s,e_a,tdr,track,gross,tstatus,1,tdr_time);

%Optimization(With Reset)
x=fminsearch(@waterO,x,[]...
    ,delta,R_n,G,lambda,T,U,e_s,e_a,tdr,track,gross,tstatus,1,tdr_time);

%Optimized calculations(With Reset)
[diff(4),totwater(:,4),E(:,4)]=...
    waterO(x,delta,R_n,G,lambda,T,U,e_s,e_a,tdr,track,gross,tstatus,1,tdr_time);
fprintf('With Reset \n');
x
diff %#ok<*NOPTS>

% %write to an excel sheet for convenince
% xlswrite('output.xlsx',{strcat(track,'_',run)},...
%     'data',strcat('A',num2str((q-1)*6+1)))
% xlswrite('output.xlsx',x','data',strcat('A',num2str((q-1)*6+2)))
% xlswrite('output.xlsx',diff','data',strcat('B',num2str((q-1)*6+2)))
% fclose('all');

%feed all the output to be plotted
Plotstuff_Test(track,tdate,navv,wnum,totwater,run,err);

function Plotstuff_Test(track,tdate,navv,wnum,totwater,run,err)

filetype='png';   %Easy way to change all filetypes, '-deps' to print
plotposition=[100 100 950 550];
margin=[.085 .085 .85 .85];
fontsize=14;
loc='north';
%% Unoptimized figure
figure('Units','pixels','Position',plotposition...
    ,'name',strcat(track,'_',run,'_unopt'))
plot(tdate-min(tdate)+1,navv,'x-',wnum-min(tdate)+1,totwater(:,1));
hold on
if strcmp(run,'long');
    errorbar(tdate-min(tdate)+1,navv,err)
end
hold off
if strcmp(track,'KEE')      %Different scales for different tracks
    set(gca,'YLim',[6 18])
    set(gca,'Ytick',6:2:18)
elseif strcmp(track,'KEE2')      %Different scales for different tracks
    set(gca,'YLim',[4 16])
    set(gca,'Ytick',4:2:16)
elseif strcmp(track,'SAR')  %Different scales for different tracks
    set(gca,'YLim',[10 24])
```

```
    set(gca,'Ytick',10:2:24)
elseif strcmp(track,'SAR2')  %Different scales for different tracks
    set(gca,'YLim',[4 24])
    set(gca,'Ytick',4:2:24)
elseif strcmp(track,'SA')   %Different scales for different tracks
    set(gca,'YLim',[2 12])
    set(gca,'Ytick',2:2:12)
elseif strcmp(track,'FG')   %Different scales for different tracks
    set(gca,'YLim',[6 26])
    set(gca,'Ytick',6:2:26)
end
set(gca,'XLim',[0,ceil(max(tdate-min(tdate)))+2])
set(gca,'XMinorTick','on','YMinorTick','on','FontSize',fontsize,'FontName',...
    'Times New Roman','Position',margin)
xlabel('Day','FontSize',fontsize,'FontName','Times New Roman');
ylabel(gca,'Water content(Mass %)','FontSize',fontsize,'FontName',...
    'Times New Roman');
legend('Measured water content(Mass %)','Calculated water content(Mass %)',...
    'location',loc);
set(gcf,'PaperPositionMode','auto');
saveas(gcf,horzcat(track,'_',run,'_unopt'),filetype);

%% Optimized figure
figure('Units','pixels','Position',plotposition...
    ,'name',strcat(track,'_',run,'_opt'));
plot(tdate-min(tdate)+1,navv,'x-',wnum-min(tdate)+1,totwater(:,2));
hold on
if strcmp(run,'long');
    errorbar(tdate-min(tdate)+1,navv,err)
end
hold off
if strcmp(track,'KEE')      %Different scales for different tracks
    set(gca,'YLim',[6 18])
    set(gca,'Ytick',6:2:18)
elseif strcmp(track,'KEE2')      %Different scales for different tracks
    set(gca,'YLim',[4 16])
    set(gca,'Ytick',4:2:16)
elseif strcmp(track,'SAR')  %Different scales for different tracks
    set(gca,'YLim',[10 24])
    set(gca,'Ytick',10:2:24)
elseif strcmp(track,'SAR2')  %Different scales for different tracks
    set(gca,'YLim',[4 24])
    set(gca,'Ytick',4:2:24)
elseif strcmp(track,'SA')   %Different scales for different tracks
    set(gca,'YLim',[2 12])
    set(gca,'Ytick',2:2:12)
elseif strcmp(track,'FG')   %Different scales for different tracks
    set(gca,'YLim',[6 26])
    set(gca,'Ytick',6:2:26)
end
set(gca,'XLim',[0,ceil(max(tdate-min(tdate)))+2])
set(gca,'XMinorTick','on','YMinorTick','on','FontSize',fontsize,'FontName',...
    'Times New Roman','Position',margin)
xlabel('Day','FontSize',fontsize,'FontName','Times New Roman');
ylabel(gca,'Water content(Mass %)','FontSize',fontsize,'FontName',...
    'Times New Roman');
legend('Measured water content(Mass %)','Calculated water content(Mass %)',...
```

```
    'location',loc);
set(gcf,'PaperPositionMode','auto');
saveas(gcf,horzcat(track,'_',run,'_opt'),filetype);

%% Unoptimized figure with reset
figure('Units','pixels','Position',plotposition...
    ,'name',strcat(track,'_',run,'_unopt_reset'))
plot(tdate-min(tdate)+1,navv,'x-',wnum-min(tdate)+1,totwater(:,3));
hold on
if strcmp(run,'long');
    errorbar(tdate-min(tdate)+1,navv,err)
end
hold off
if strcmp(track,'KEE')      %Different scales for different tracks
    set(gca,'YLim',[6 18])
    set(gca,'Ytick',6:2:18)
elseif strcmp(track,'KEE2')      %Different scales for different tracks
    set(gca,'YLim',[4 16])
    set(gca,'Ytick',4:2:16)
elseif strcmp(track,'SAR')  %Different scales for different tracks
    set(gca,'YLim',[10 24])
    set(gca,'Ytick',10:2:24)
elseif strcmp(track,'SAR2')  %Different scales for different tracks
    set(gca,'YLim',[4 24])
    set(gca,'Ytick',4:2:24)
elseif strcmp(track,'SA')   %Different scales for different tracks
    set(gca,'YLim',[2 12])
    set(gca,'Ytick',2:2:12)
elseif strcmp(track,'FG')   %Different scales for different tracks
    set(gca,'YLim',[6 26])
    set(gca,'Ytick',6:2:26)
end
set(gca,'XLim',[0,ceil(max(tdate-min(tdate)))+2])
set(gca,'XMinorTick','on','YMinorTick','on','FontSize',fontsize,'FontName',...
    'Times New Roman','Position',margin)
xlabel('Day','FontSize',fontsize,'FontName','Times New Roman');
ylabel(gca,'Water content(Mass %)','FontSize',fontsize,'FontName',...
    'Times New Roman');
legend('Measured water content(Mass %)','Calculated water content(Mass %)',...
    'location',loc);
set(gcf,'PaperPositionMode','auto');
saveas(gcf,horzcat(track,'_',run,'_unopt_reset'),filetype);

%% Optimized figure with reset
figure('Units','pixels','Position',plotposition...
    ,'name',strcat(track,'_',run,'_opt_reset'));
plot(tdate-min(tdate)+1,navv,'x-',wnum-min(tdate)+1,totwater(:,4));
hold on
if strcmp(run,'long');
    errorbar(tdate-min(tdate)+1,navv,err)
end
hold off
if strcmp(track,'KEE')      %Different scales for different tracks
    set(gca,'YLim',[6 18])
    set(gca,'Ytick',6:2:18)
elseif strcmp(track,'KEE2')      %Different scales for different tracks
```

```
    set(gca,'YLim',[4 16])
    set(gca,'Ytick',4:2:16)
elseif strcmp(track,'SAR')  %Different scales for different tracks
    set(gca,'YLim',[10 24])
    set(gca,'Ytick',10:2:24)
elseif strcmp(track,'SAR2')  %Different scales for different tracks
    set(gca,'YLim',[4 24])
    set(gca,'Ytick',4:2:24)
elseif strcmp(track,'SA')   %Different scales for different tracks
    set(gca,'YLim',[2 12])
    set(gca,'Ytick',2:2:12)
elseif strcmp(track,'FG')   %Different scales for different tracks
    set(gca,'YLim',[6 26])
    set(gca,'Ytick',6:2:26)
end
set(gca,'XLim',[0,ceil(max(tdate-min(tdate)))+2])
set(gca,'XMinorTick','on','YMinorTick','on','FontSize',fontsize,'FontName',...
    'Times New Roman','Position',margin)
xlabel('Day','FontSize',fontsize,'FontName','Times New Roman');
ylabel(gca,'Water content(Mass %)','FontSize',fontsize,'FontName',...
    'Times New Roman');
legend('Measured water content(Mass %)','Calculated water content(Mass %)',...
    'location',loc);
set(gcf,'PaperPositionMode','auto');
saveas(gcf,horzcat(track,'_',run,'_opt_reset'),filetype);


function [diff,totwater,E]=water0(x,delta,R_n,G,lambda,T,U,e_s,e_a,...
    tdr,track,gross,tstatus,reset,tdr_time)

%Calculates moisture content. Returns diff, totwater, E. diff is sum of
%least squares differeneces for all TDR points.  totwater is the moisture
%content at each point in time, E is the total evaporation for each hour

%Preallocate for speed
E=zeros(length(tdr),1);
totwater=zeros(size(tdr));%Pays attention to amount of water in track

a=[0,1];    %Turns on x(2) or x(3) based on surface condition
b=[1,0];

if strcmp(track,'KEE')  %Different tracks have different initial conditions
    totwater(1,1)=11;
elseif strcmp(track,'SAR')
    totwater(1,1)=15;
elseif strcmp(track,'SA')
    totwater(1,1)=6;
elseif strcmp(track,'FG')
    totwater(1,1)=14;
elseif strcmp(track,'KEE2')
    totwater(1,1)=11;
elseif strcmp(track,'SAR2')
    totwater(1,1)=11;
end
```

```
for i=1:length(tdr)-1
    %               ***REPARAM AND BOUND COULD BE MORE ELEGANT***
    E(i)=(.408.*delta(i)*(R_n(i)-G(i))+lambda*Reparam(totwater(i),x(1),x(4))...
        *2/(T(i)+273).*U(i)*(e_s(i)-e_a(i))./(a(tstatus(i))*(delta(i)+...
        lambda*(1+abs(bound(x(2)))*U(i)))+b(tstatus(i))*(delta(i)+lambda*...
        (1+abs(bound(x(3)))*U(i))));

%After a ceritan amount of rain, the track is saturated and excess rain runs off
    if strcmp(track,'KEE')
        if totwater(i,1)+gross(i)-E(i)>14
            totwater(i,1)=14;   %Saturation
            gross(i)=0;         %Ignore extra water
        end
    elseif strcmp(track,'KEE2')
        if totwater(i,1)+gross(i)-E(i)>13
            totwater(i,1)=13;
            gross(i)=0;
        end
    elseif strcmp(track,'SAR')||strcmp(track,'KEE2')
        if totwater(i,1)+gross(i)-E(i)>20
            totwater(i,1)=20;
            gross(i)=0;
        end
    elseif strcmp(track,'FG')
        if totwater(i,1)+gross(i)-E(i)>18
            totwater(i,1)=18;
            gross(i)=0;
        end
        %There was no rain at SA, so it is unknown at what point it would
        %become saturated
    end

    %Adds water in, subtracts evaporation for new content
    totwater(i+1,1)=totwater(i,1)+gross(i)-E(i);

    %Resets moisture content to what is measured by TDR probe
    %don't want to reset in the afternoon, it's not what the maintenance
    %guys will do, so only reset in morning
    if reset==1&&tdr(i)>0
        if str2num(tdr_time(i,:))<=12
         totwater(i+1,1)=tdr(i);
        end
    end
end

%Sum the squares to find the overall error
diff=sum((tdr(tdr>0)-totwater(tdr>0)).^2);



function [n,basefilename]=TDR_Vacuum(track,run)

%Returns n and basefilename.  n contains all the data from all the TDR data
%sets.  basefilename contains the filename, which includes date and time.
```

```
if strcmp(track,'KEE')
    if strcmp(run,'long')
        datasize=153;
    elseif strcmp(run,'short')
        datasize=9;
    end
elseif strcmp(track,'SAR')
    if strcmp(run,'long')
        datasize=162;
    elseif strcmp(run,'short')
        datasize=9;
    end
elseif strcmp(track,'SA')
    if strcmp(run,'long')
        datasize=144;
    elseif strcmp(run,'short')
        datasize=9;
    end
elseif strcmp(track,'FG')
    datasize=47;
elseif strcmp(track,'KEE2')
    datasize=51;
end

myfolder='data';
if strcmp(track,'FG')
    filePattern=fullfile(myfolder,track,'*.dat');
elseif strcmp(track,'KEE2')
    filePattern=fullfile(myfolder,track,'*.xlsx');
elseif strcmp(track,'SAR2')
    filePattern=fullfile(myfolder,track,'*.xlsx');
else
    filePattern=fullfile(myfolder,track,'*.txt');
    if strcmp(run,'short')
        filePattern=fullfile(myfolder,track,run,'*.txt');
    end
end
Files=dir(filePattern);
g=0;
for k=1:length(Files)       %file names should all be the same length
    basefilename(k,:)=Files(k).name; %#ok<*SAGROW>
    if strcmp(run,'long')
        fullFileName=fullfile(myfolder,track,basefilename(k,:));
    elseif strcmp(run,'short')
        fullFileName=fullfile(myfolder,track,run,basefilename(k,:));
    end
    fileID=fopen(fullFileName);
    fullfilename(k,:)=fullFileName;
    if strcmp(track,'KEE2')%new data from Keeneland is in a different format

[m,dates]=xlsread(fullfile(myfolder,track,'KEE2_dat.xlsx'),'KEE2.dat','B4:AB55')
;
        break %Data has been presorted, so skip the sorting
    elseif strcmp(track,'SAR2')%new data from Saratoga is in a different format

[m,dates]=xlsread(fullfile(myfolder,track,'SAR2_dat.xlsx'),'SAR2_dat','B4:BG19')
;
```

```
        break %Data has been presorted, so skip the sorting
    else
        m=textscan(fileID,'%s %s %s %s %s %s','delimiter',',\t');
    end
  %SAR/FG files are tab delimited, so they dont have the preceding
  %delimieters like the other files
  if strcmp(run,'long')
      if strcmp(track,'SAR')||strcmp(track,'FG')
          G=str2double(m{1,2});
          H=str2double(m{1,1});
      else
          G=str2double(m{1,4});
      end
  elseif strcmp(run,'short')
      G=str2double(m{1,4});
  end
  %FG is all messed up because he doesn't turn the probe off between sets
  if strcmp(track,'FG')
      nums=1:length(G);
      if sum(H==1)>1
          nums=nums(H==1);
          nums(1:end-1)=[];
          G(1:nums-1)=[];
      end
      if length(G)>datasize+4
          G=[];
      end
  end
  g=cat(1,g,0,G);
  g(isnan(g))=[];
end
nol=length(g);
j=1;
full=0;
num=0;
count=0;
k=0;

for i=1:nol
    if g(i)~=0;
        count=count+1;
        num=1;
        N(count,j)=g(i,1);
        if count==datasize
            k=k+1;
            loc(k)=j;
            full(j)=1;      %Keeps track of full data runs
        end
    elseif num==1
        num=0;
        j=j+1;
        count=0;
    end
end

fullnum=sum(full);       %Gives the number of  data sets in the file
```

```
for i=1:fullnum          %Puts data from full runs into n
    n(:,i)=N(:,loc(i));
end

if strcmp(track,'FG')
    basefilename=basefilename(loc,:);   %Saves file names of full files
elseif strcmp(track,'KEE2')||strcmp(track,'SAR2')
    n=m;
    basefilename=dates;
end


function [wdate,avgweather]=Weather_Vacuum(track)

%Returns wdate and avgweather.  wdate is the date and time for the hour
%that the data is averaged from.  avgweather contains all the pertinant
%weather data from the weather stations.  All of the stations were
%configured slightly differently, so the variables in avgweather vary
%depending on the track.

if strcmp(track,'KEE')||strcmp(track,'SAR')||strcmp(track,'SA')||...
        strcmp(track,'FG')||strcmp(track,'KEE2')||strcmp(track,'SAR2')
else
    uiwait(warndlg('Put in the right track identifyer'));
end

path='data';
name=fullfile(path,track,strcat(track,'.csv'));
if strcmp(track,'KEE2')||strcmp(track,'SAR2')
    name=fullfile(path,track,strcat(track,'W.csv'));
end
fileid=fopen(name);
%Format for Campbell Scientific staion
weathercells=textscan(fileid,'%s %f %f %f %f %f %f %f %f %f %f %f %f %f %f'...
    ,'delimiter',',','HeaderLines',1);

wdate=weathercells{1};

%               ***THIS COULD BE WAY BETTER***
if strcmp(track,'KEE')||strcmp(track,'SAR')||strcmp(track,'FG')...
        ||strcmp(track,'KEE2')||strcmp(track,'SAR2')
    wdate=char(datestr(datenum(wdate(1:60:end-60)),'mm/dd/yyyy HH:MM'));
elseif strcmp(track,'SAR2')
    wdate=char(datestr(datenum(wdate(1:60:end-60)),'yyyy-mm-dd HH:MM:00'));
elseif strcmp(track,'SA')
    %Weather data from every 5min, instead of every min
    wdate=char(datestr(datenum(wdate(1:12:end-12)),'mm/dd/yyyy HH:MM'));
end

weathercells{1}=[];
weather=zeros(length(weathercells{:,2}),length(weathercells));
for i=1:length(weathercells)-1
    weather(:,i)=weathercells{:,i+1};
end
```

```
%Averages(solar energy, rain) and sums everything else to be used hourly
if strcmp(track,'KEE')
    avgweather=zeros(floor(length(weather)/60),14);
    for step=1:length(weather)/60
    avgweather(step,1)=mean(weather(60*(step-1)+1:60*(step-1)+61,1));   %baro
    avgweather(step,2)=sum(weather(60*(step-1)+1:60*(step-1)+61,2));    %rain
    avgweather(step,3)=mean(weather(60*(step-1)+1:60*(step-1)+61,3));   %temp
    avgweather(step,4)=mean(weather(60*(step-1)+1:60*(step-1)+61,4));   %RH
    avgweather(step,5)=mean(weather(60*(step-1)+1:60*(step-1)+61,5));   %solar
power
    avgweather(step,6)=sum(weather(60*(step-1)+1:60*(step-1)+61,6));    %solar
enrgy
    avgweather(step,7)=mean(weather(60*(step-1)+1:60*(step-1)+61,7))...
%windspeed
        *4.87/log(67.8*3-5.42); %convert from measured height to 2m
    avgweather(step,8)=mean(weather(60*(step-1)+1:60*(step-1)+61,8));   %winddir
    avgweather(step,9)=mean(weather(60*(step-1)+1:60*(step-1)+61,9));   %vmc
    avgweather(step,10)=mean(weather(60*(step-1)+1:60*(step-1)+61,10)); %ec
    avgweather(step,11)=mean(weather(60*(step-1)+1:60*(step-1)+61,11)); %soil
temp
    avgweather(step,12)=mean(weather(60*(step-1)+1:60*(step-1)+61,12)); %gflux
    avgweather(step,13)=mean(weather(60*(step-1)+1:60*(step-1)+61,13)); %soil
top
    avgweather(step,14)=mean(weather(60*(step-1)+1:60*(step-1)+61,14)); %soil
bot
    end
elseif strcmp(track,'SAR')
    avgweather=zeros(floor(length(weather)/60),11);
    for step=1:length(weather)/60
    avgweather(step,1)=mean(weather(60*(step-1)+1:60*(step-1)+61,1));   %baro
    avgweather(step,2)=sum(weather(60*(step-1)+1:60*(step-1)+61,2));    %rain
    avgweather(step,3)=mean(weather(60*(step-1)+1:60*(step-1)+61,3));   %temp
    avgweather(step,4)=mean(weather(60*(step-1)+1:60*(step-1)+61,4));   %RH
    avgweather(step,5)=mean(weather(60*(step-1)+1:60*(step-1)+61,5));   %solar
power
    avgweather(step,6)=sum(weather(60*(step-1)+1:60*(step-1)+61,6));    %solar
enrgy
    avgweather(step,7)=mean(weather(60*(step-1)+1:60*(step-1)+61,7))...
%windspeed
        *4.87/log(67.8*3-5.42); %convert from measured height to 2m
    avgweather(step,8)=mean(weather(60*(step-1)+1:60*(step-1)+61,8));   %winddir
    avgweather(step,9)=mean(weather(60*(step-1)+1:60*(step-1)+61,9));   %vmc
    avgweather(step,10)=mean(weather(60*(step-1)+1:60*(step-1)+61,10)); %ec
    avgweather(step,11)=mean(weather(60*(step-1)+1:60*(step-1)+61,11)); %soil
temp
    end
elseif strcmp(track,'SA') %SA had fewer sensors than the others
    avgweather=zeros(floor(length(weather)/12),5);
    for step=1:length(weather)/12
    %no rainfall for the period of tdr measurements
    avgweather(step,1)=mean(weather(12*(step-1)+1:12*(step-1)+13,2));   %baro
    avgweather(step,3)=mean(weather(12*(step-1)+1:12*(step-1)+13,1));   %temp
    avgweather(step,4)=mean(weather(12*(step-1)+1:12*(step-1)+13,4));   %RH
    avgweather(step,7)=mean(weather(12*(step-1)+1:12*(step-1)+13,3))...
%windspeed
        *4.87/log(67.8*3-5.42); %convert from measured height to 2m
```

```
    end
elseif strcmp(track,'FG')
    avgweather=zeros(floor(length(weather)/60),14);
    for step=1:length(weather)/60
    avgweather(step,1)=mean(weather(60*(step-1)+1:60*(step-1)+61,1));   %baro
    avgweather(step,2)=sum(weather(60*(step-1)+1:60*(step-1)+61,2));    %rain
    avgweather(step,3)=mean(weather(60*(step-1)+1:60*(step-1)+61,3));   %temp
    avgweather(step,4)=mean(weather(60*(step-1)+1:60*(step-1)+61,4));   %RH
    avgweather(step,5)=mean(weather(60*(step-1)+1:60*(step-1)+61,5));   %solar
power
    avgweather(step,6)=sum(weather(60*(step-1)+1:60*(step-1)+61,6));    %solar
enrgy
    avgweather(step,7)=mean(weather(60*(step-1)+1:60*(step-1)+61,7))...
%windspeed
        *4.87/log(67.8*10-5.42); %convert from measured height to 2m
    avgweather(step,8)=mean(weather(60*(step-1)+1:60*(step-1)+61,8));   %winddir
    avgweather(step,9)=mean(weather(60*(step-1)+1:60*(step-1)+61,9));   %vmc
    avgweather(step,10)=mean(weather(60*(step-1)+1:60*(step-1)+61,10)); %ec
    avgweather(step,11)=mean(weather(60*(step-1)+1:60*(step-1)+61,11)); %soil
temp
    avgweather(step,13)=mean(weather(60*(step-1)+1:60*(step-1)+61,13)); %soil
top
    avgweather(step,14)=mean(weather(60*(step-1)+1:60*(step-1)+61,14)); %soil
bot
    end
elseif strcmp(track,'KEE2')
    avgweather=zeros(floor(length(weather)/60),14);
    for step=1:length(weather)/60
    avgweather(step,1)=mean(weather(60*(step-1)+1:60*(step-1)+61,1));   %baro
    avgweather(step,2)=sum(weather(60*(step-1)+1:60*(step-1)+61,2));    %rain
    avgweather(step,3)=mean(weather(60*(step-1)+1:60*(step-1)+61,3));   %temp
    avgweather(step,4)=mean(weather(60*(step-1)+1:60*(step-1)+61,4));   %RH
    avgweather(step,5)=mean(weather(60*(step-1)+1:60*(step-1)+61,5));   %solar
power
    avgweather(step,6)=sum(weather(60*(step-1)+1:60*(step-1)+61,6));    %solar
enrgy
    avgweather(step,7)=mean(weather(60*(step-1)+1:60*(step-1)+61,7))...
%windspeed
        *4.87/log(67.8*3-5.42); %convert from measured height to 2m
    avgweather(step,8)=mean(weather(60*(step-1)+1:60*(step-1)+61,8));   %winddir
    avgweather(step,9)=mean(weather(60*(step-1)+1:60*(step-1)+61,9));   %vmc
    avgweather(step,10)=mean(weather(60*(step-1)+1:60*(step-1)+61,10)); %ec
    avgweather(step,11)=mean(weather(60*(step-1)+1:60*(step-1)+61,11)); %soil
temp
    avgweather(step,13)=mean(weather(60*(step-1)+1:60*(step-1)+61,13)); %soil
top
    avgweather(step,14)=mean(weather(60*(step-1)+1:60*(step-1)+61,14)); %soil
bot
    end
elseif strcmp(track,'SAR2')
    avgweather=zeros(floor(length(weather)/60),14);
    for step=1:length(weather)/60
    avgweather(step,1)=mean(weather(60*(step-1)+1:60*(step-1)+61,1));   %baro
    avgweather(step,2)=sum(weather(60*(step-1)+1:60*(step-1)+61,2));    %rain
    avgweather(step,3)=mean(weather(60*(step-1)+1:60*(step-1)+61,3));   %temp
    avgweather(step,4)=mean(weather(60*(step-1)+1:60*(step-1)+61,4));   %RH
```

```
    avgweather(step,5)=mean(weather(60*(step-1)+1:60*(step-1)+61,5));   %solar
power
    avgweather(step,6)=sum(weather(60*(step-1)+1:60*(step-1)+61,6));    %solar
enrgy
    avgweather(step,7)=mean(weather(60*(step-1)+1:60*(step-1)+61,7))...
%windspeed
        *4.87/log(67.8*3-5.42); %convert from measured height to 2m
    avgweather(step,8)=mean(weather(60*(step-1)+1:60*(step-1)+61,8));   %winddir
    avgweather(step,9)=mean(weather(60*(step-1)+1:60*(step-1)+61,9));   %vmc
    avgweather(step,10)=mean(weather(60*(step-1)+1:60*(step-1)+61,10)); %ec
    avgweather(step,11)=mean(weather(60*(step-1)+1:60*(step-1)+61,11)); %soil
temp
    avgweather(step,13)=mean(weather(60*(step-1)+1:60*(step-1)+61,13)); %soil
top
    avgweather(step,14)=mean(weather(60*(step-1)+1:60*(step-1)+61,14)); %soil
bot
    end
end


function [delta,e_s,e_a,T,U,R_s]=TRH(avgweather)

%Returns various variables as calculated from weather data

T=avgweather(:,3);
RH=avgweather(:,4);

delta=2503.*exp(17.27.*T./(T+237.3))./(T+237.3).^2;

e_s=.6108.*exp(17.27.*T./(T+237.3));

e_a=RH./100.*.6108.*exp(17.27.*T./(T+237.3));

U=avgweather(:,7);

R_s=avgweather(:,5);


function R_n=Rad(R_s,date,e_a,T_C,track)

% Returns R_n, net solar radiation, from the measured shortwave radiation,
% location, date, and time that the data was collected.
% R_s is just the incoming solar radiation, in MJ/hrm^2
% a is the albedo of dirt
% G_sc solar constant, units of MJ/m^2h
% z;%elevation of each track
% phi;%latitude of the track, in radians
% delta;%solar declination, in radians
% D_M;%day of the month(1-31)
% M;%month of the year(1-12)
% Yr;%number of the year
% t_1;%length of time step, 1 for hr, .5 for 30min
% e_a actual vapor pressure(kPa)
% w;%solar time angle at midpoint of the time period, in radians
```

```
% w_1;%solar time angle at beginning of period, in radians
% w_2;%solar time angle at end of period, in radians
% w_s;%sunset hour angle
% t;%time at the midpoint of the measurement period, in hours. 14:30=14.5
% after correcting for daylight savings time
% L_z;%longitude of center of the local time zone
% L_m;%longitude of the solar radiation measurement site
% S_c;%seasonal correction for solar time, in hours
% d_r;%inverse relative distance factor(squared) from the sun to the earth, no
units
% X is just a big variable that feeds into w_s


%Tracks in different places have different latitude, longitude, elevation,
%and time zone.
if strcmp(track,'KEE')||strcmp(track,'KEE2')
    phi=pi/180*(38.046503);
    L_m=pi/180*(-84.608900);
    z=250;
    L_z=75;
elseif strcmp(track,'SAR')||strcmp(track,'SAR2')
    phi=pi/180*(43.071656);
    L_m=pi/180*(-73.768569);
    z=91;
    L_z=75;
elseif strcmp(track,'SA')
    phi=pi/180*(34.140893);
    L_m=pi/180*(-118.044982);
    z=147;
    L_z=120;
elseif strcmp(track,'FG')
    phi=pi/180*(29.983841);
    L_m=pi/180*(-90.081098);
    z=0;
    L_z=90;
else
    uiwait(errordlg('Please put in a valid track identifyer'));
end

%Parses out date and time info
Yr=str2num(date(:,7:10));
M=str2num(date(:,1:2));
D_M=str2num(date(:,4:5));
Hr=str2num(date(:,12:13));
Mn=str2num(date(:,15:16));

t=Hr+.5;                          %Midpoint of measurements
a=.17;                            %Albedo of dirt
T_K=T_C+273.16;                   %Convert to K from C
G_sc=4.92;                        %Solar constant, units of MJ/m^2h
t_1=1;                            %Time step of 1 hour
J=D_M-32+floor(275*M/9)+2*transpose(floor(3/(M+1)))+floor(M/100-
mod(Yr,4)/4+.975);
d_r=1+.033*cos(2*pi/365*J);
delta=.409*sin(2*pi/365*J-1.39);
b=2*pi*(J-81)/364;
```

```
S_c=.1645*sin(2*b)-.1255*cos(b)-.025*sin(b);
w=pi/12*((t+.06667*(L_z-L_m)+S_c)-12);
w_1=w-pi*t_1/24;
w_2=w+pi*t_1/24;
X=1-(tan(phi)).^2.*(tan(delta)).^2;

if X<=0
    X=.00001;   %Don't want it 0 or negative
end

w_s=pi/2-atan((-tan(phi).*tan(delta))./X.^.5);

if w_1<-w_s
    w_1=-w_s;
elseif w_1>w_s
    w_1=w_s;
elseif w_1>w_2
    w_1=w_2;
end

if w_2<-w_s
    w_2=w_s;
elseif w_2>w_s
    w_2=w_s;
end

R_a=12/pi.*G_sc.*d_r.*((w_2-w_1).*sin(phi).*sin(delta)+cos(phi).*...
    cos(delta).*(sin(w_2)-sin(w_1)));
if strcmp(track,'SA')
    a_s=.25;    %Default values
    b_s=.5;
    n=1;        %SA was sunny all the time
    N=1;
    R_s=(a_s+b_s*n/N)*R_a;  %Solar radiation estimation without measurement
end
for i=1:length(R_a)
if R_a(i)<0
    R_a(i)=0;
end
end
R_so=(.75+2*10^-5*z)*R_a;
f_cd=1.35.*R_s./R_so-.35;
for i=1:length(f_cd)
if f_cd(i)>=0&&f_cd(i)<=1
else
    f_cd(i)=0;
end
end
R_nl=2.042*10^-10.*f_cd.*(.34-.14.*sqrt(e_a)).*T_K.^4;
R_ns=(1-a)*R_s;

R_n=R_ns-R_nl;

R_n(R_n<0)=0;
```

```
function G=Gflux(track,avgweather,R_n)

if strcmp(track,'KEE')  %Keeneland was the only track with flux plate data
    G=avgweather(:,12)./1000000*60;  %gflux is in J/m^2/min, need it in
MJ/m^2/hr

    for j=1:(length(G))%Deals with bad ground flux data   ***COULD VECTORIZE***
        if G(j)==0.47994; %Value of bad data from CS flux sensor
            G(j)=R_n(j)*.1;%replaces bad data with estimate from solar rad
        end
    end
elseif strcmp(track,'FG') %Fair Grounds had thermocouples and conductivity
measurements
    G=(avgweather(:,13)-
avgweather(:,14)).*(349.18*avgweather(:,9)+12.845)*2/6.75/1000;
else%Flux data can be estimated from solar radiation if data is missing
    G=R_n*.1; %Solar rad is already in MJ/m^2/hr
end

end
```

```
function [gstatus]=Maint(track,wnum)

%Determines the track maintenance state and water truck times based on the
%track selected and the maintenance file downloaded from MQS.  1st column i
%s date, 2nd column is track condition(1 for harrowed, 2 for sealed) 3rd
%column is number of water loads that hour

if strcmp(track,'KEE')||strcmp(track,'SAR')||strcmp(track,'SA')...
        ||strcmp(track,'FG')||strcmp(track,'KEE2')||strcmp(track,'SAR2')
else
    uiwait(warndlg('Please use a valid track identifyer'));
end

%Read and sort the maintenance data
path='data';
name=fullfile(path,track,strcat(track,'_maint.csv'));
fileid=fopen(name);
maint=textscan(fileid,'%s %s %s %f','delimiter',',','HeaderLines',1);
mnum=datenum(strcat(maint{1},maint{2}),'mm/dd/yyyyHH:MM:SS');
equip=maint{3};

%Interprets the amount of water the trucks put down
if strcmp(track,'KEE')||strcmp(track,'KEE2')
    water_loads=ceil(maint{4}/8);   %water trucks went in pairs
elseif strcmp(track,'SAR')||strcmp(track,'SAR2')
    water_loads=ceil(maint{4}/4.5);   %water trucks went solo
elseif strcmp(track,'SA')
    water_loads=maint{4};
```

```
elseif strcmp(track,'FG')
    water_loads=ceil(maint{4}/15);
end

water_loads(isnan(water_loads))=0;  %No such thing as NaN water loads
water_loads(water_loads>4)=4;

%Decides if it's open or closed based on equipment
if strcmp(track,'KEE')||strcmp(track,'KEE2')
    state(strcmp(equip,'Conditioner')|strcmp(equip,'Drag Harrow')|strcmp(...
        equip,'Hydraulic Diamond Harrow')|strcmp(equip,...
        'Float_ Back teeth down'))=1;  %Track open
    state(strcmp(equip,'Roller')|strcmp(equip,'Float_ Front teeth down')|...
       strcmp(equip,'Float (no teeth down)')|strcmp(equip,'Grader
w/GPS'))=2;%closed
    state(strcmp(equip,'Water'))=0;                                    %water truck
elseif strcmp(track,'SAR')||strcmp(track,'SAR2')
    state(strcmp(equip,'Harrow_ Double')|strcmp(equip,'Harrow_
Speed')|strcmp(...
        equip,'Harrow_ Three point')|strcmp(equip,...
        'Float_ Back teeth down'))=1;  %Track open
    state(strcmp(equip,'Roller')|strcmp(equip,'Float_ single')|...
        strcmp(equip,'Float_ double')|strcmp(equip,'Grader_ motor')|...
        strcmp(equip,'Grader_ tow behind'))=2;%closed
    state(strcmp(equip,'Water_ boom'))=0;
elseif strcmp(track,'SA')
    state=str2double(equip)';
elseif strcmp(track,'FG')
    state(strcmp(equip,'Harrow'))=1;  %Track open
    state(strcmp(equip,'Roller')|strcmp(equip,'Float')|...
        strcmp(equip,'Grader'))=2;%closed
    state(strcmp(equip,'Water'))=0;
end

%Preallocate for speed
status=horzcat(mnum,transpose(state),water_loads);
gstatus=horzcat(zeros(length(wnum),3),zeros(length(wnum),1));

%Figures out which hour the maintenance happened in, and bins it
for i=1:length(wnum)-1
    for j=1:length(status)
        if status(j,1)>=wnum(i)&&status(j,1)<wnum(i+1)
            if status(j,2)~=0
                gstatus(i,2:3)=gstatus(i,2:3)+status(j,2:3);

                %fancy way to add 1 to the counter, unless its a WT
                gstatus(i,4)=gstatus(i,4)+ceil(status(j,2)/2);
            else
                gstatus(i,2:3)=status(j,2:3);
            end
        end

    end

    %average the equipment that went out over the hour
```

```
    if gstatus(i,4)>0
        gstatus(i,2)=ceil(gstatus(i,2)/gstatus(i,4));
    end

    %fill in track state with previous values if there isnt anything new
    if gstatus(i,2)==0&&i>1
        gstatus(i,2)=gstatus(i-1,2);
    end
end
gstatus(:,1)=wnum;
gstatus(length(gstatus),2)=gstatus(length(gstatus)-1,2);
gstatus(gstatus(:,2)==0,2)=1;

%get rid of the counter, we don't need it anymore
gstatus(:,4)=[];
```

APPENDIX C MOISTURE CONTENT MEASUREMENTS

Time domain reflectometry (TDR) works by sending an electrical pulse through a discontinuity, and measuring the magnitude of the reflection. To measure the moisture content with TDR, the TDR300 probe has two conductive tips of a known alloy, and the electrical pulse is sent between them through the soil. The dielectric conductivity of soil depends highly on the moisture content of the soil, so the magnitude of the reflection of the pulse is proportional to the moisture content of the soil.

The TDR300 probe measures a volume of soil extending out from each of the tips by 3cm, creating a roughly oval cross section that is measured by the probe, shown in Figure 47. The probe measurement area also extends 3cm out from the end of the probe tips, shown in Figure 48.

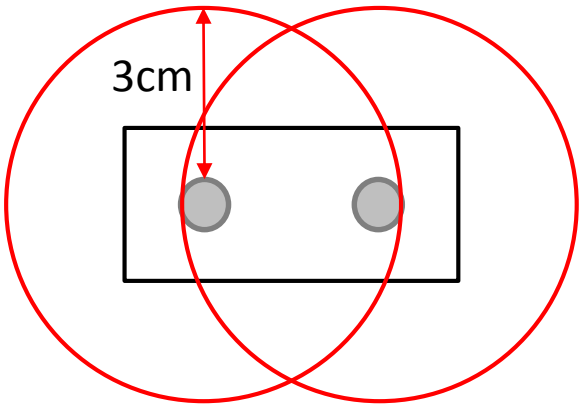

Figure 47: Cross section of TDR measurement

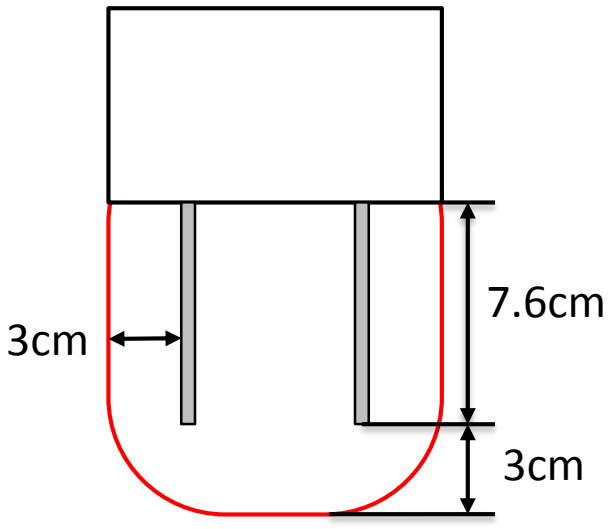

Figure 48: Depth of TDR measurement

APPENDIX D MAINTENANCE QUALITY SYSTEM

The Maintenance Quality System (MQS) is a way for tracks to monitor weather and their use of maintenance equipment, and at the same time make the data available for research. Data from weather stations also feeds into MQS, so it is available to track personnel if they need to know how much rain has fallen or what the temperature is. Information on which pieces of equipment are used on the track at different times is recorded by track personnel, so it is possible to know whether the track is harrowed or sealed at any given time. The times that water trucks go out is also recorded, so the moisture model can account for water added by the water trucks.

Some tracks have GPS tracking units on tractors and water trucks to monitor maintenance without manually inputting the information. Eventually the water trucks will be set up with floats to tell how much water is in the truck at any given time. Knowing how the trucks position changes over time as well as how the water level changes with time provides information on the rate that water is added all the way around the track.

APPENDIX E WEATHER STATION

Table 10: Campbell Scientific Weather Station Sensors

Component Name	Model Number	Maker	Accuracy	Use
Barometric Pressure Sensor	CS100	Setra	±1mb @ 0° to 40°C	Used to calculate the psychrometric constant
Short Wave Solar Radiation Sensor	CS300	Apogee	±5% for daily total	Used in the energy balance(R)
Temperature and Relative Humidity Sensor	CS215	Sensirion	T: ±0.4°C (+5° to +40°C) RH: ±2% (10% to 90% range)	temperature and humidity are used to calculate S, T_{ky} in ρ, and VPD
Ground Flux Plate	HFP01	Huskeflux	-15% to +5%, resolution of .533W/m^2	Used in the energy balance(G)
Burial Thermocouple	105E	CS	.49°C resolution	Used in the energy balance
Soil Moisture Content Probe	CS655	CS	VWC: ±3%, T: ±0.5°C	Used in the energy balance
Wind Speed and Direction Monitor	5103	RM Young	U: ±0.3 m/s (0.6 mph) or 1% of reading, Direction: ±3°	Used for aerodynamic calculations(U)
Datalogger	CR1000	CS	±0.06%, 33µV resolution	Logs the data

Weather station program:

```
'CRBasic script to upload data to FTP server from CR1000

'Declare Variables and Units
Public BattV
Public PTemp_C
Public BP_mmHg
Public Rain_mm
Public TRHData(2)
Public SlrkW
Public SlrMJ
Public WS_ms
```

```
Public WindDir
Public CS65X(3)
Public Gflux
Public GTemp_C(2)

'Declare nicknames for variables
Alias TRHData(1)=AirTC
Alias TRHData(2)=RH
Alias CS65X(1)=VWC
Alias CS65X(2)=EC
Alias CS65X(3)=T
Alias GTemp_C(1)=T_Top
Alias GTemp_C(2)=T_Bot

'Define public variables
Public FTPResult
Public NewFileName As String *50 'holds the time stamped destination filename
Const ServerIP = "8.8.8.8" 'This is the address of the FTP server
Const User = "admin" 'user name needed to login to the FTP server
Const Password = "admin" 'password needed to login to the FTP server
Const DestPath = "/data/WS/" 'directory where file will be saved
Const track = "TRACK1" 'put in track name for output file

Units BattV=Volts
Units PTemp_C=Deg C
Units BP_mmHg=mmHg
Units Rain_mm=mm
Units SlrkW=kW/m^2
Units SlrMJ=MJ/m^2
Units WS_ms=meters/second
Units WindDir=degrees
Units AirTC=Deg C
Units RH=%
Units VWC=m^3/m^3
Units EC=dS/m
Units T=Deg C
Units Gflux=W/m^2
Units T_Top=Deg C
Units T_Bot=Deg C

'Define tables
DataTable(Table1,True,-1)
  DataInterval(0,60,Sec,10)
  Average(1,BP_mmHg,FP2,False)
  Totalize(1,Rain_mm,FP2,False)
  Average(1,AirTC,FP2,False)
  Sample(1,RH,FP2)
  Average(1,SlrkW,FP2,False)
  Totalize(1,SlrMJ,IEEE4,False)
```

```
  Average(1,WS_ms,FP2,False)
  Sample(1,WindDir,FP2)
  Average(1,VWC,FP2,False)
  Average(1,EC,FP2,False)
  Average(1,T,FP2,False)
  Average(1,Gflux,FP2,False)
  Average(1,T_Top,FP2,False)
  Average(1,T_Bot,FP2,False)
EndTable

'Main Program
BeginProg
  Scan(1,Sec,1,0)
    'Default Datalogger Battery Voltage measurement 'BattV'
    Battery(BattV)
    'Default Wiring Panel Temperature measurement 'PTemp_C'
    PanelTemp(PTemp_C,_60Hz)
    'CS100 Barometric Pressure Sensor measurement 'BP_mmHg
    PortSet(1,1)
    VoltSe(BP_mmHg,1,mV2500,1,1,0,_60Hz,0.2,600)
    BP_mmHg=BP_mmHg*0.75006
    'TE525/TE525WS Rain Gauge measurement 'Rain_mm'
    PulseCount(Rain_mm,1,1,2,0,0.254,0)
    'CS215 Temperature & Relative Humidity Sensor measurements 'AirTC' and 'RH'
    SDI12Recorder(TRHData(),7,"0","M!",1,0)
    'CS300 Pyranometer measurements 'SlrMJ' and 'SlrkW'
    VoltSe(SlrkW,1,mV250,3,1,0,_60Hz,1,0)
    If SlrkW<0 Then SlrkW=0
    SlrMJ=SlrkW*2.5E-05
    SlrkW=SlrkW*0.005
    '05103 Wind Speed & Direction Sensor measurements 'WS_ms' and 'WindDir'
    PulseCount(WS_ms,1,2,1,1,0.098,0)
    BrHalf(WindDir,1,mV2500,2,1,1,2500,True,0,_60Hz,355,0)
    If WindDir>=360 OR WindDir<0 Then WindDir=0
    'CS650/655 Water Content Reflectometer measurements 'VWC', 'EC', and 'T'
    SDI12Recorder(CS65X(),5,"0","M!",1,0)
    'hfp01 ground heat flux sensor
    VoltDiff(Gflux,1,mV5000,5,True,0,250,1000/61.9,0)
    'both burial thermocouples
    TCDiff(GTemp_C(),2,mV2_5C,6,TypeE,PTemp_C,True,0,_60Hz,1,0)
    'Call Data Tables and Store Data
    CallTable(Table1)
  NextScan

  SlowSequence 'everything in the slow sequence runs in the background
  Scan (10,sec,3,0)
    NewFileName=Replace(public.timestamp(5,0),"-","") 'generates/formats timestamp
    If (Len(NewFileName)>15) Then 'Check for extra characters and strip them off
      NewFileName=left(NewFileName, 15)
```

```
    EndIf
    NewFileName=DestPath & track & "_" & NewFileName & "_WS.dat" 'generates path
    'Set flag to watch result
    FTPResult=999
    'Call FTP instruction
    FTPResult=FTPClient(ServerIP,User,Password,"Table1",NewFileName,8,0,5,Min,-1008)
  NextScan
  EndSequence
EndProg
```

The CRBasic script above is the program that is used to collect and automatically upload weather data to an FTP server. If there is an interruption in the network connection, the program will send all data that it has collected since the last time it has uploaded when the network connection is restored. FTP login information has been removed.

Sensors are polled for data every second, and those data are averaged or totalled over a minute. Variables like wind speed and temperature are averaged, while variables like rainfall and solar energy are totalled. Resolution of seconds is not needed, and would generate excessively large files which then need to be transmitted by cellular modem. The model currently operates with hourly data, but in the future it could be changed to operate on data with higher resolution, such as 15 or 30 minute intervals.

Data was collected by a CR1000 with a NL120 connected over Ethernet to a RT3G-310-W. The datalogger and modem were connected to a PS100 battery backup which ensures that data collection can continue even if there is a power outage. The CR1000 is the datalogger that records all of the data, and the NL120 adds Ethernet connectivity to the CR1000.

Table 11 and Table 12 show how the sensors are wired into the datalogger for the program above. Wiring by location is useful for new weather station installations, so that wires can be installed sequentially. Wiring by sensor is useful for removing or installing a single sensor.

Table 11: Weather station wiring by location.

Wiring by wire location:		
location	Sensor	Wire
1H	CS100	BLUE
1L	05103	GREEN
G	CS100	CLEAR, YELLOW
	TE525	CLEAR, WHITE
2H	CS300	RED
G	CS215	CLEAR
	CS300	BLACK, CLEAR
	05103	BLACK
	05103	WHITE, CLEAR
VX1	05103	BLUE
P1	TE525	BLACK
P2	05103	RED
5H	HFP01	WHITE
5L	HFP01	GREEN
G	HFP01	BLACK
6H	105TA	PURPLE
6L	105TA	PINK
G	105TA	CLEAR
7H	105TB	PURPLE
7L	105TB	PINK
G	105TB	CLEAR
	CS100	BLACK
	CS215	WHITE, BLACK
	CS650	BLACK, CLEAR
	CS650	ORANGE
12V	CS100	RED
	CS215	RED
	CS650	RED
C1	CS100	GREEN
C5	CS650	GREEN
C7	CS215	GREEN

Table 12: Weather station wiring by sensor.

Wiring by sensor:		
location	Sensor	Wire
CS100	1H	BLUE
	G	CLEAR, YELLOW
	G	BLACK
	12V	RED
	C1	GREEN
05103	1L	GREEN
	G	BLACK
	G	WHITE, CLEAR
	VX1	BLUE
	P2	RED
TE525	G	CLEAR, WHITE
	P1	BLACK
CS300	2H	RED
	G	BLACK, CLEAR
CS215	G	CLEAR
	G	WHITE, BLACK
	12V	RED
	C7	GREEN
HFP01	5H	WHITE
	5L	GREEN
	G	BLACK
105TA	6H	PURPLE
	6L	PINK
	G	CLEAR
105TB	7H	PURPLE
	7L	PINK
	G	CLEAR
CS650	G	BLACK, CLEAR
	G	ORANGE
	12V	RED
	C5	GREEN

APPENDIX F NELDER MEAD OPTIMIZATION

Matlab's built in Nelder-Mead simplex optimization method, fminsearch was used to optimize the evaporation model parameters. The Nelder-Mead method evaluates the function it is optimizing and determines which estimate of the ideal function parameters is furthest from its ideal value. It then moves that furthest point in an attempt to move the point closer to the function minimum. It then re-evaluates which estimate is furthest from the minimum, and continues until it has reached the required tolerance.

The Nelder-Mead method, like most optimization methods can be susceptible to local minima, where the optimizer is trapped and unable to get to the absolute minimum. The results can also be effected by the initial guess for the function. The initial guess is not as likely to have a negative impact on the outcome of the optimization of the function if the initial guess is known to be close to the minimum of the function, so the program uses the standard values from the PM equation as an initial guess.

APPENDIX G MODEM SETUP

Setup procedure for RT3G series cellular modems

Hardware Setup:

- Attach antennae as shown in Figure 49

Figure 49: Dual SIM cellular modem for data collection.

  - Center antenna is only for modems with Wi-Fi
- Plug in with supplied power supply
- Connect Ethernet cable to your computer
  - For 300, 300-W, 320, and 320-W, there is only one active Ethernet port, labeled ETH
  - 310(-W) and 311(-W) have two or three active Ethernet ports respectively, ETH and PORT1 for the 310(-W) or ETH, PORT1 and PORT2 for the 311(-W)

Software Configuration:

- Disable Wi-Fi connections on your computer, then open a browser and type in 192.168.1.1
- The default username and password is root/root
- Go to Change Password under Administration, and change the password

Basic Setup:

- For both SIM cards under Mobile WAN, set APN as ‘broadband’, set carriers as generic UMTS

- Enable connection testing, and set test IP to 8.8.8.8 and test interval to 10s.
- Check the box to enable the modem to switch to other SIM card when connection fails.
- Set the initial timeout to 5 min, and the subsequent timeout to 5 min as well with no additive constant.
- Save changes
- Select reboot, and click the reboot at the bottom of the screen. It will take 20 seconds to reboot.

Wi-Fi Setup:

For if the modem has Wi-Fi

- Go under user modules
- Select Wi-Fi
- Check the box to Enable Wi-Fi AP
- Set the SSID as the name you want the network name to be
- Set HW Mode to IEEE 802.11b+g+n
- Pick authentication type (probably WPA2-PSK) and encryption (typically AES) and passphrase
- Set the WPA PSK type
- Choose a password and type it in the WPA PSK box
- Save changes and return to the main page
- Select reboot, and click the reboot at the bottom of the screen. It will take 20 seconds to reboot

Document modem IMEI, MAC Address, Username, Password, SSID, and Wi-Fi PSK.

APPENDIX H RAINWISE STATION SETUP AND TROUBLESHOOTING

Initial Setup:

To begin, you need SN and MAC Address from IP100

- Go to the rainwise.net weather page for a station on the account (such as www.rainwise.net/weather/EMD)
- Click on settings
- Enter credentials
- Mouse over settings and click 'add station'
- Fill in all the info, and set the URL as the track identifier (AQU, EMD, BEL, SAR…)

You should now be able to get to the station at www.rainwise.net/weather/*track-identifier*

Troubleshooting:

If status is 'Offline', there is a problem with the connection between the IP100 and the internet. Check that the Ethernet cable it is plugged into actually has a connection. Also make sure it is powered.

If status is 'No Radio Signal', there is a problem with the connection between the weather station and the IP100. Make sure the weather station is switched on, and has a charged battery. Try moving the station closer, to somewhere that has a direct line of sight to the IP100 to test if the problem is with the weather station, or with how far apart the IP100/station are. There is a light on the IP100 that will blink when it is connected.

APPENDIX I GEOTAB SETUP AND TROUBLESHOOTING

Add new device to a Geotab database:
Go to the Vehicles tab, then Add at the top of the page, click Add vehicle. Put in the serial number and a quick description.

Set up new computer with RF downloader:
Log in to www.my.geotab.com/*database-name*

Click "Administration" then proceed to:
>system>keys and RF>PC and USB

Download the checkmate app (Chrome won't work, use Internet Explorer)

You will need to login to the checkmate app with the database credentials

Enable "GO Radio" or "Key on this PC" (you may need to tab down to the continue button, and then press enter)

Click "Administration" then proceed to:
>system>keys and RF>Radio Downloaders

At the top of the page, Click Add, and enter the serial number in 'Name' under settings, and in Serial number under Advanced

Troubleshooting:

- Ensure system time and date are correct
- Update Microsoft .net (issue might be 3.5.1, update to 4.5.1)
- Delete C:\Users*username*\AppData(which is hidden by default)\Local\Apps\2.0
- Try installing from different browser
- Call Reseller for additional support

To unhide AppData, go into folder options, go into the view tab and select 'show hidden files'

APPENDIX J THERMAL CONDUCTIVITY MEASUREMENT

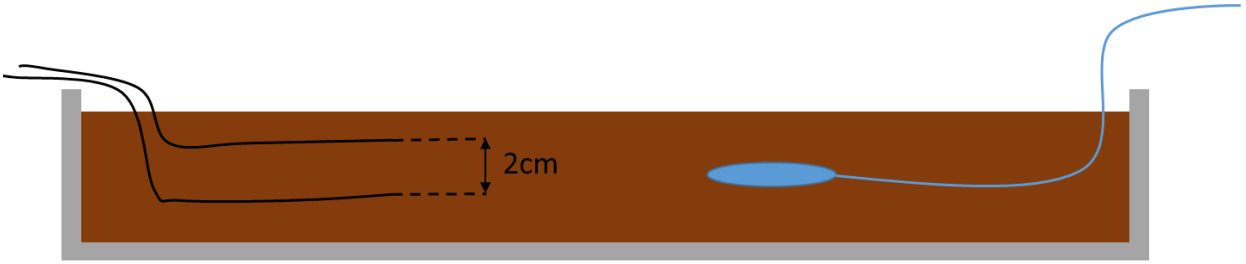

Figure 50: Thermal conductivity test bed.

Figure 50 shows two thermocouples 2cm apart, and a flux plate in a pan of dirt. Moisture content of the dirt greatly impacts the thermal conductivity of the dirt, so the sample is totally dried before being brought up to 8, 10, 12, and 14% moisture content by mass. The range of moisture contents for which the thermal conductivity is known allows reliable calculation of flux for all conditions that the track is likely to experience. The pan with all the sensors is placed on top of an oven that is always on to take advantage of the heat.

Fourier's law is that the thermal gradient is proportional to the flux across the gradient, shown in equation 18

$$q = -k\frac{dT}{dz} \qquad 18$$

Where q is the heat flux density in W/m^2
k is the thermal conductivity in W/mK
dT is the change in temperature over the gradient in K
dz is the change in height over the gradient in m

The thermal conductivity can be calculated by solving Fourier's law for k, shown in equation 19

$$k = -q\frac{dz}{dT} \qquad 19$$

The weather station at Fair Grounds does not have a flux plate, but it does have thermocouples and a moisture sensor. It is possible to use the temperature gradient from the thermocouples, along with the thermal conductivity calculated from the moisture

content to accurately calculate the ground flux, without the need for expensive flux plates.

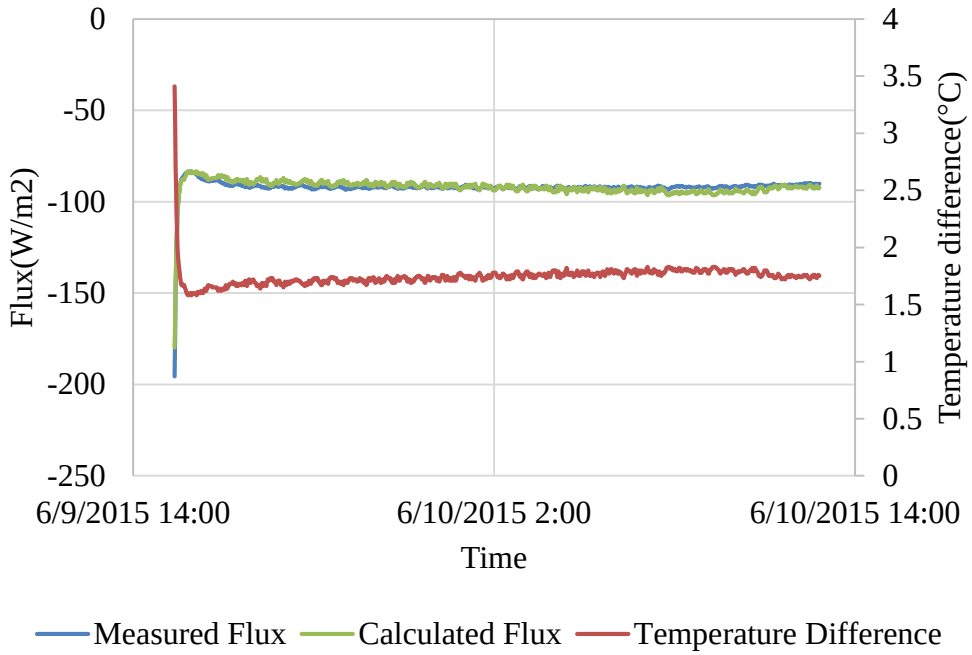

Figure 51: Calculated and measured flux with temperature gradients at 12% VWC.

Flux data collected from a Fair Grounds sample is plotted in Figure 51. It shows the relationship between thermocouple buried as shown in Figure 50, as well as the relationship between measured and calculated flux.

The thermal conductivity test bed uses the CR1000 and flux plate described in Table 10, but the type E thermocouples were replaced with type J thermocouples, shown in Table 13.

Table 13: Thermocouple used for thermal conductivity measurements.

Component Name	Model Number	Maker	Accuracy	Use
Thermocouple	Type J	Omega	Resolution of .66°C	Used to measure temperature gradient

APPENDIX K SOLAR RADIATION CALCULATIONS

For equation 7, the net short wave radiation, R_{ns}, is calculated using

$$R_{ns} = (1 - a)R_s \tag{20}$$

where a is the emissivity of dirt, and R_s is the measured short wave radiation.
If there is no data for short wave radiation, it can be calculated as

$$R_s = \left(a_s + b_s * \frac{n}{N}\right) * R_a \tag{21}$$

where a_s and b_s are the angstrom values typically, .25 and .5 respectively, R_a is the total solar radiation that would be getting to the location if there were no atmosphere, and n/N is the ratio of actual hours of sunshine to the possible number hours of sunshine.

R_a can be calculated as

$$R_a = \left(\frac{12}{pi}\right) G_{sc} d_r ((\omega_2 - \omega_1)\sin(lat)\sin(\delta) + \cos(lat)\cos(\delta)\,(\sin(\omega_2) - \sin(\omega_1)) \tag{22}$$

where G_{sc} is the solar constant, 4.92MJ/m^{2}hr, d_r is squared inverse relative distance factor for the sun to the earth, lat is the latitude of the solar radiation measurement site, δ is the solar declination, ω_1 is the solar time angle at the beginning of the time step, and ω_2 is the solar time angle at the end of the time step.

The squared inverse relative distance factor for the sun to the earth, d_r, is calculated with

$$d_r = 1 + .033cos\left(\frac{2\pi J}{365}\right) \tag{23}$$

where J, the days of the year, are sequenced in a variable.

J is calculated from

$$J = D_M - 32 + floor\left(\frac{275M}{9}\right) + 2floor\left(\frac{3}{M+1}\right) + floor\left(\frac{M}{100} - \frac{mod(Yr,4)}{4} + .975\right) \quad (24)$$

where D_M is the day of the month, M is the number of the month, Yr is the number of the year, the 'floor' function rounds down to the nearest integer, and the 'mod' function finds the modulus, in this case of Yr after dividing by 4.

The solar declination, δ, is calculated from

$$\delta = .409sin\left(\frac{2\pi J}{365} - 1.39\right) \quad (25)$$

ω_1, the solar time angle at the beginning of the time step, is calculated as

$$\omega_1 = \omega - \frac{\pi t_n}{24} \quad (26)$$

where ω is the solar time angle at the angle of the midpoint of the period, and t_n is the number of hours in the time step.

ω_2 is the solar time angle at the end of the time step, calculated as

$$\omega_2 = \omega + \frac{\pi t_n}{24} \quad (27)$$

The solar time angle, ω, is calculated as

$$\omega = \left(\frac{\pi}{12}\right)\left((t + .06667(L_z - L_m) + S_c) - 12\right) \quad (28)$$

where t is the time at the midpoint of the period, in hours, L_z is the longitude of the center of the local time zone, in deg, L_m is the longitude of the solar radiation measurement site, in deg, and S_c is the seasonal correction for solar time, in hours.

S_c is calculated from

$$S_c = .1645\sin(2b) - .1255\cos(b) - .025\sin(b) \quad (29)$$

where b is a term to simplify the equation.

b is calculated with

$$b = \frac{2\pi(J - 81)}{364} \quad (30)$$

R_{nl} is difficult to measure accurately (Walter et al., 2005), so it is commonly calculated as

$$R_{nl} = \sigma f_{cd}\left(.34 - .14e_a^{\frac{1}{2}}\right)T_{kavg}^4 \quad (31)$$

where σ is the Stefan Boltzmann constant, r_{cd} is the dimensionless cloudiness factor, e_a is the actual vapor pressure for the time step , T_{Kavg} is the average temperature at ~2m in K.

The dimensionless cloudiness factor, f_{cd} can be calculated from

$$f_{cd} = 1.35\left(\frac{R_s}{R_{so}}\right) - .35 \quad (32)$$

where R_{so} is the clear sky radiation.

R_{so} is calculated by

$$R_{so} = (.75 + 2 \times 10^{-5}Z)R_a \quad (33)$$

where Z is elevation above sea level.

If $\omega_1 < -\omega_s$ then $\omega_1 = -\omega_s$
If $\omega_2 < -\omega_s$ then $\omega_2 = -\omega_s$
If $\omega_1 > \omega_s$ then $\omega_1 = \omega_s$
If $\omega_2 > \omega_s$ then $\omega_2 = \omega_s$
If $\omega_1 > \omega_2$ then $\omega_1 = \omega_2$

$$\omega_s = arcos(-\tan(lat)\tan(\delta)) \quad 34$$

where ω_s is the sunset hour angle.

arccos is unavailable in some programming languages, so in the code ω_s is calculated as

$$\omega_s = \frac{\pi}{t} - arctan\left(-\frac{\tan(lat)\tan(\delta)}{X^{.5}}\right) \quad 35$$

where

$$X = 1 - (\tan(\varphi))^2(\tan(\delta))^2 \quad 36$$

and X is constrained so that it is never below .00001.

APPENDIX L ADDITIONAL RESULTS

Figure 52 shows the measured moisture content and the calculated moisture content from Santa Anita long data sets. Between day 1 and day 3, the calculated moisture content was 1.5% MWC below the measured value. Between day 3 and day 5, the calculated moisture content was within .25% MWC of the measured value. After day 6, the calculated moisture content was 1% MWC below the measured values.

Figure 53 shows the measured moisture content and the calculated moisture content from Saratoga long data sets. Between day 1 and day 2, the calculated moisture contents were within .25% MWC of the measured value. Between day 5 and day 7, the moisture content was overestimated by 1% MWC. After the rain on day 7, the calculations overestimated the moisture content between day 10 and day 11 by 1% MWC.

Figure 54 shows the measured moisture content and the calculated moisture content from Saratoga long data sets from the second period of measurements. Between day 13 and day 17, the calculated moisture content was within 1% MWC of the measured value. After the rain on day 21, the calculated moisture content was 11%MWC below the measured value.

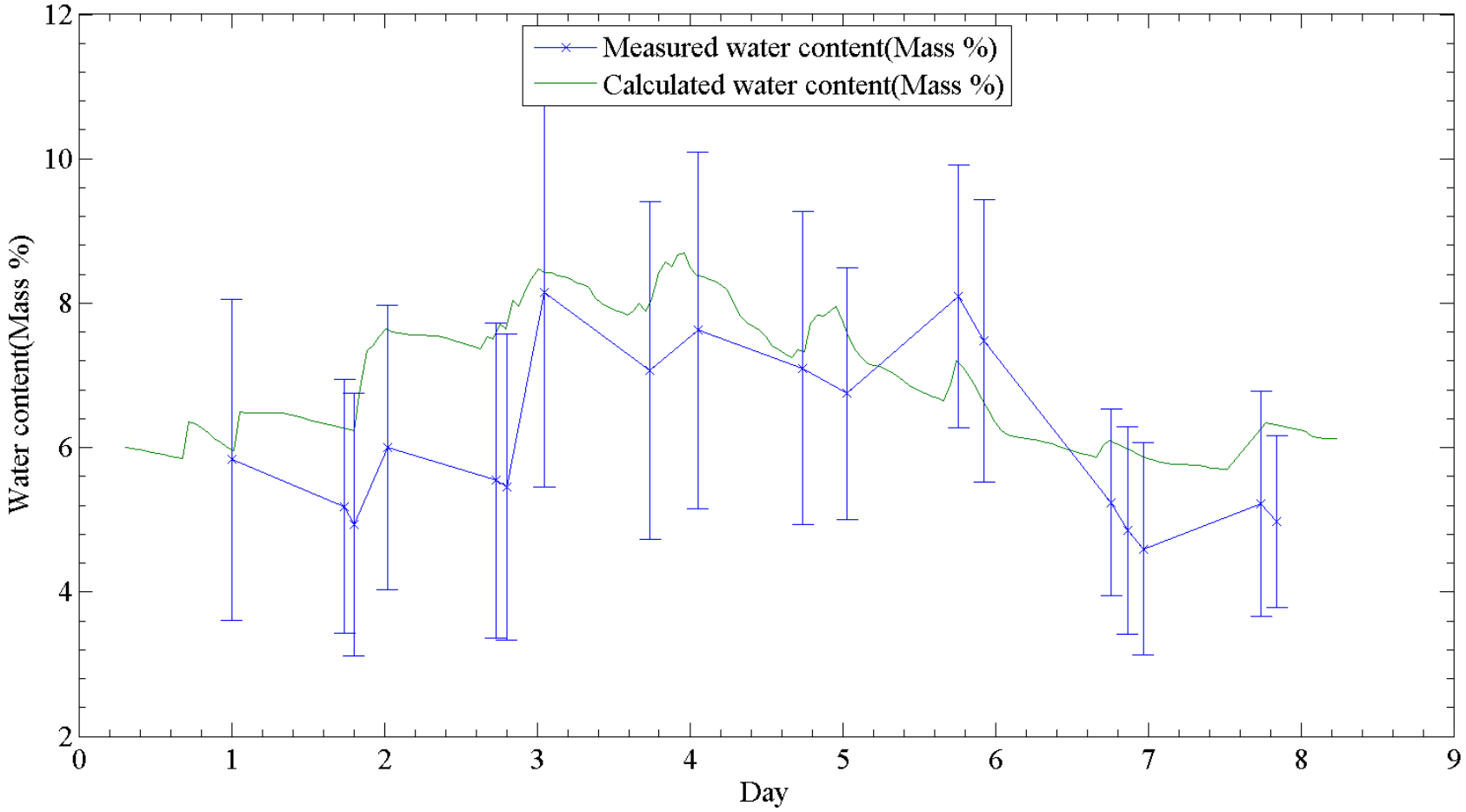

Figure 52: Un-optimized calculations with measured values from Santa Anita.

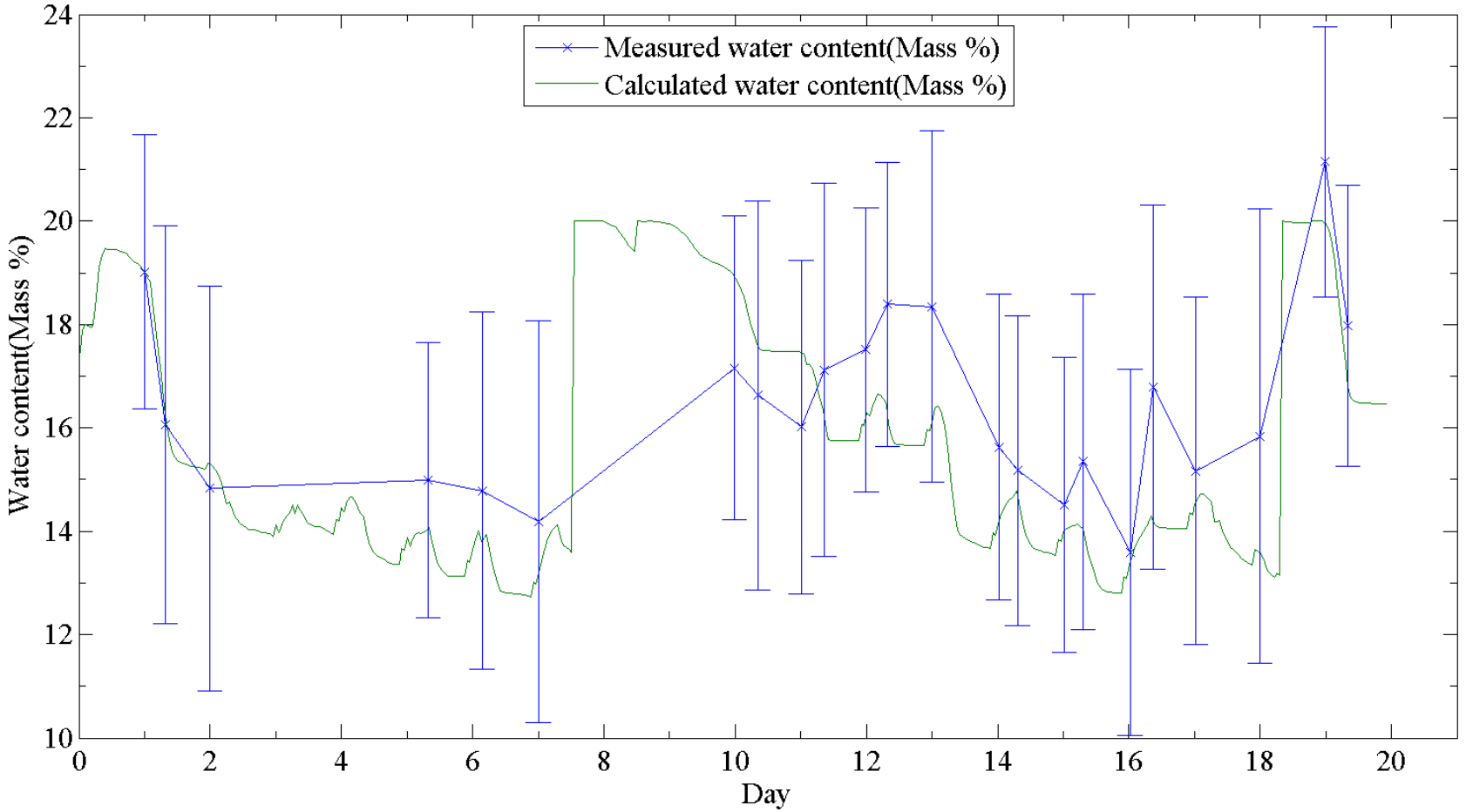

Figure 53: Un-optimized calculations with measured values from Saratoga during the first period of measurements.

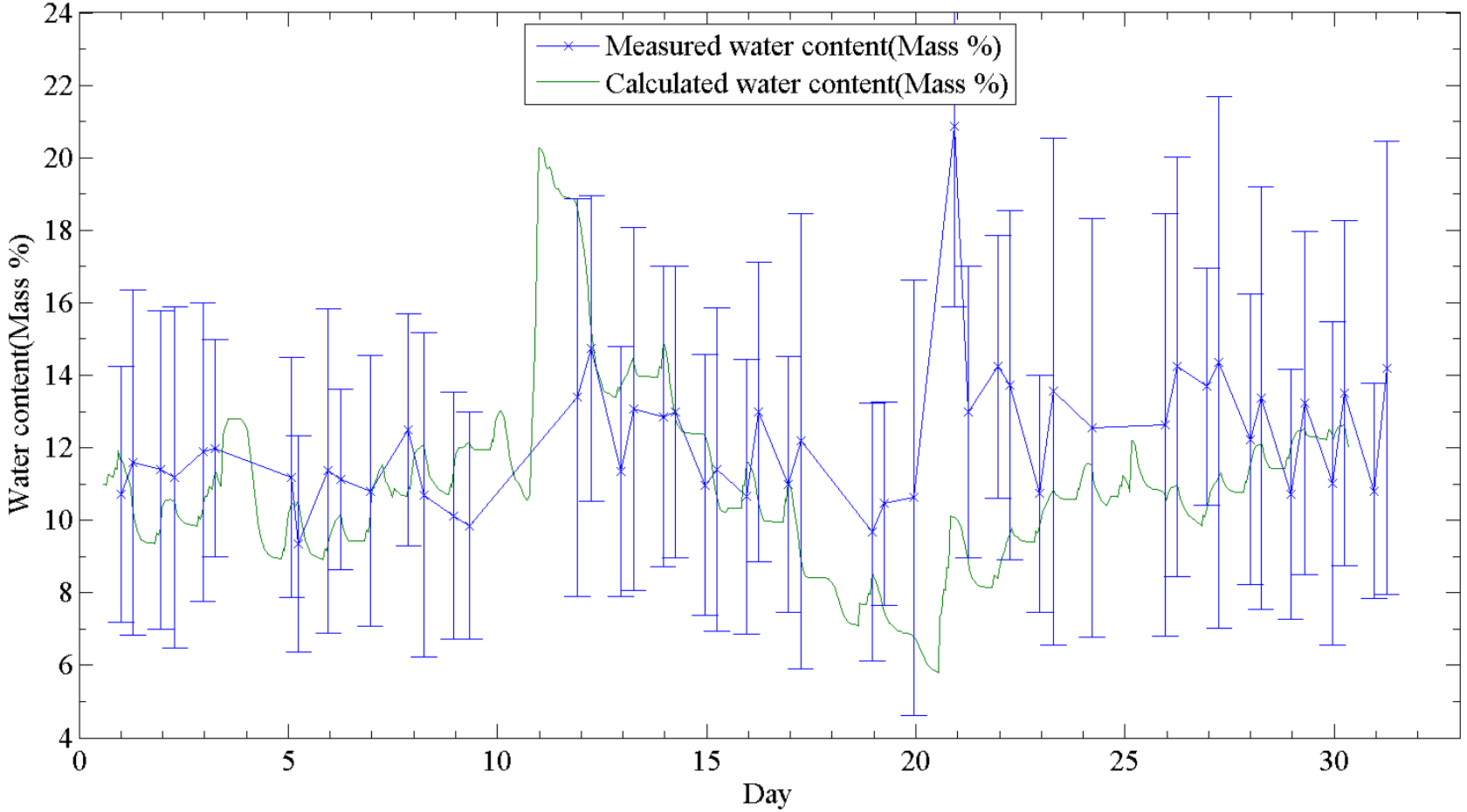

Figure 54: Un-optimized calculations with measured values from Saratoga during the second period of measurements.

Figure 55 shows the measured moisture content and the optimized calculated moisture content from Saratoga long data sets. Between day 1 and day 8, the calculated moisture content was within .5% MWC of the measured value. Between day 9 and day 11, the calculated moisture content was 1.5% MWC below the measured value. Between day 10 and day 16, the calculated moisture content was within .5% MWC of the measured values.

Figure 56 shows the measured moisture content and the optimized calculated moisture content from Santa Anita long data sets. Between day 2 and day 3, the calculated moisture content was 1% MWC above the measured moisture content. Between day 3 and day 5, the calculated moisture content was within .25% MWC of the measured values.

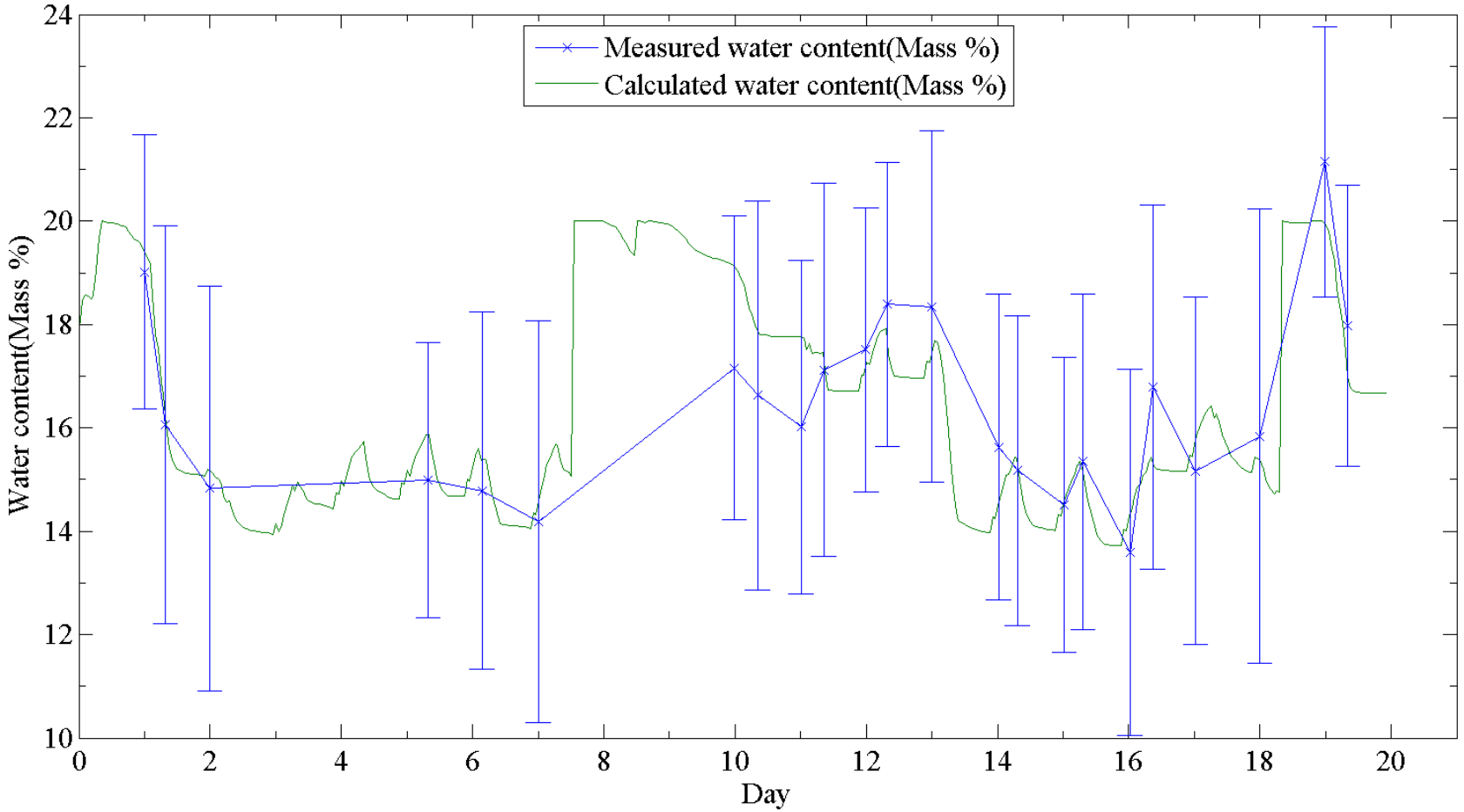

Figure 55: Optimized calculations with measured values from Saratoga.

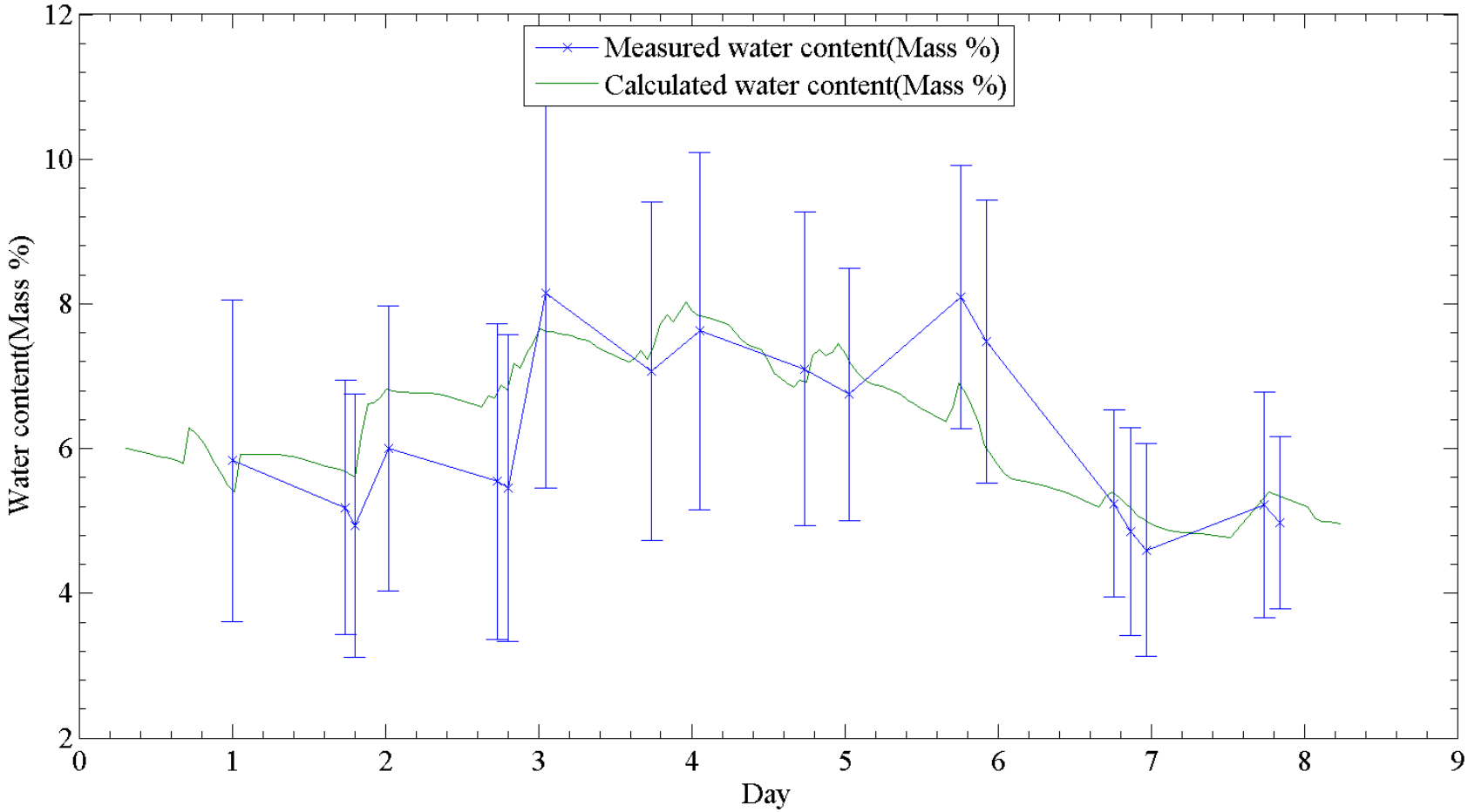

Figure 56: Optimized calculations with measured values from Santa Anita.

BIOGRAPHY OF THE AUTHOR

Nicholas Lawson was born in Media, PA in March 1992. He graduated high school in Sudbury, MA, and earned a B.S. in Mechanical Engineering from the University of Maine in May 2014. He is a candidate for the Master of Science degree in Mechanical Engineering from the University of Maine in May 2016.